Estimation of Diffusion Restrictions in Cardiomyocytes Using Kinetic Measurements

MERVI SEPP

TUT
PRESS

TALLINN UNIVERSITY OF TECHNOLOGY
Institute of Cybernetics
Laboratory of Systems Biology

This dissertation was accepted for the defense of the degree of Doctor of Philosophy (Engineering Physics) on 9 May 2013.

Supervisor: Marko Vendelin, PhD
Laboratory of Systems Biology, Institute of Cybernetics,
Tallinn University of Technology, Tallinn, Estonia

Opponents: Jeroen Jeneson, PhD
BioModeling and Bioinformatics, Department of Biomedical Engineering,
Eindhoven University of Technology, Eindhoven, The Netherlands

Agu Laisk, DSc, Prof
Institute of Molecular and Cell Biology, Chair of Biophysics and Plant Physiology,
Faculty of Science and Technology, University of Tartu

Defense of the thesis: 22 August 2013

Declaration:
I hereby declare that this doctoral thesis, submitted for the doctoral degree at Tallinn University of Technology, is my original investigation and achievement and has not been submitted for the defense of any academic degree elsewhere.

_____
Mervi Sepp

Difusioonitakistuste hindamine kardiomüotsüütides kasutades kineetilisi mõõtmisi

MERVI SEPP

CONTENTS

SUMMARY

THE AIM OF THIS DISSERTATION is to study diffusion restrictions in the energetic pathways of heart muscle cells. For that interdisciplinary approach that combines experimental measurements and mathematical modeling, was used. Specifically, kinetic analysis is applied to rat heart cells whereas experimental data is systematically collected from relaxed cardiomyocytes at cell population level. The results confirm significant diffusion restrictions on mitochondrial outer membrane and demonstrate the existence of diffusion obstacles in cytosolic compartment. The conclusion that diffusion restrictions indeed have intracellular origin, is in accordance with single cell kinetics studies leading to stronger evidence against theories explaining these results with probable experimental artifacts.

The work revealed existence of coupling between a fraction of ATPases and endogenous pyruvate kinase (PKend). This finding evoked a new course in the research project – the renewed target was to establish which of the cellular ATPases are linked to endogenous PK. The role of two membrane ATPases – sarcoplasmic reticulum Ca^{2+} ATPase (SERCA) and sarcolemma Na^+/K^+ ATPase (NKA), was investigated. The results showed minor role of SERCA in our preparation. NKA however, evidenced to makes up to about 45 % of the total ATPase activity in our conditions, was shown to be strongly coupled to glycolysis via pyruvate kinase (PK).

The developed kinetic approach was applied on different animal models. Mathematical models were used to compare the compartmentalization of cellular energetics in wild-type mice and in transgenic mice lacking the GAMT enzyme that produces creatine. The analysis showed no difference in energetic compartmentalization and mitochondrial functioning between GAMT-deficient and wild-type mice. No major structural adaptations were identified in mice with effectively inactive CK system. This is contrary to wide acknowledgment of the importance of CK shuttle in energy transfer.

This thesis demonstrates intracellular compartmentation in rat cardiomyocytes revealing that in this strongly compartmentalized environment a fraction of ATPases have preference over energy production routes – glycolysis or oxydative phosphorylation. Thus proving the importance of glycolysis even in highly oxydative tissue such as heart muscle. The main result of this dissertation is an interdisciplinary method and its application to unravel intracellular compartmentation in heart that widens our understanding in energy transfer of this organ.

KOKKUVÕTE

Käesoleva väitekirja eesmärk on difusioonitakistuste hindamine südamelihasraku, kasutades kineetilisi mõõtmisi. Töö käsitleb raku bioenergeetikaga seonduvat isoleeritud permeabiliseeritud kardiomüotsüüdis. Et uurida energeetiliselt oluliste metaboliitide uurides ATP ning uurides ADP rakusisest liikumist, kasutati interdistsiplinaarset lähenemist, mis kombineerib matemaatilist modelleerimist erinevate eksperimentaalsete meetoditega. Koostati raku protsesse erineva struktuurse keerukusega kirjeldavad matemaatilised mudelid, teostati kineetilised mõõtmised rahuolekus kardiomüotsüütidel ning analüüsiti saadud katseandmeid loodud matemaatiliste mudelitega. Selle tulemusena avastati, et kasutatavas rakupreparaadis on säilinud arvestatav endogeense püruvaatkinaasi (PKend) aktiivsus ja et teatav osa rakusisestest ATPaasidest on sellega funktsionaalselt seostatud. Selle leiu tulemusena sai uueks eesmärgiks teha kindlaks, millised südameraku ATPaasidest selles seostatuses osalevad. Erinevate ATPaaside rolli hindamiseks uuriti kahe erineva ATPaasi rolli südamelihasraku energeetikas: sarkoplasmaatilisel retiikulumil asetseva kaltsiumi ATPaasi (SERCA) ning rakumembraanil asetseva Na+/K + ATPaasi (NKA). Leiti, et rahuolekus rakkudes onuurides SERCA osakaal üldises energeetikas minimaalne ning vaadeldavas olukorras ta rolli ei mängi. Seevastu, uurides NKA rolli, leiti, et tema osakaal üldises ATPaaside töös antud tingimustel on *ca* 45%, ning täiendavalt teostati kogu kineetiliste mõõtmiste katseseeria ja analüüsiti andmeid matemaatiliste mudelitega. Tulemusena leiti, et uurides NKA on seotud endogeense püruvaatkinaasi kaudu glükolüüsiga.

Loodud matemaatilised mudelid kirjeldavad protsesse ühes nn näidisrakus, samas katsed sooritatakse rakupopulatsioonil. Uurimaks, kas populatsioonikatsete tulemused võib üle kanda ühele rakule, hinnati ADP kineetikat ühe raku tasandil, kasutades mitokondriaalse autofluorestsentsi mõõtmisi. Analüüsides tulemusi matemaatilise mudeli kaasabil, näidati, et difusioonitakistused on tõepoolest rakusisene nähtus ning pole põhjustatud rakukogumi preparaadipõhistest iseärasustest.

Lisaks roti südameraku uurimisele on antud töö raames uuritud südameraku energeetikat ka hiirtes. Kasutades väljatöötatud matemaatilisi mudeleid, võrreldi kineetikat metsiktüüpi loomades ning transgeensetes uurides GAMT-puudulikkusega loomades, kellel puudub südamelihasraku energeetika jaoks olulise metaboliidi — kreatiini tootmist katalüseeriv ensüüm. Tulemusena selgus, et vastupidiselt seni kreatiinkinaasi ülekande olulisust rõhutanud seisukohale ei erine rakuenergeetika

rahuolekus rakkude puhul metsiktüüpi loomades ning neis, kellel kreatiinkinaasi süsteem on pärsitud.

Töö tulemusena leiti, et tugevalt kompartmentaliseeritud keskkonnas eelistavad teatud osa ATPaase glükolüütiliselt toodetud ATP-d oksüdatiivse fosforüleerimise tulemusena saadud ATP-le, mis näitab, et glükolüüs mängib olulist rolli ka oksüdatiivses lihases.

Doktoritöö põhitulemus on interdistsiplinaarne meetod rakusisese kompartmentatsiooni uurmiseks, mille rakendamine annab lisateavet elutähtsa organi — südame energeetiliste protsesside kohta.

LIST OF PUBLICATIONS

I Sepp M, Vendelin M, Vija H, Birkedal R; **ADP Compartmentation Analysis Reveals Coupling between Pyruvate Kinase and ATPases in Heart Muscle**. *Biophysical Journal*, Volume 98, 2785-2793, June 2010

II Jepihhina N, Beraud N, Sepp M, Birkedal R, Vendelin M; **Permeabilized rat cardiomyocyte response demonstrates intracellular origin of diffusion obstacles**. *Biophysical Journal*, Volume 101, 2112-2121, November 2011

III Illaste A, Kalda M, Schryer DW, Sepp M ; **Life of mice - development of cardiac energetics**. *Journal of Physiology*, 588(23), 4617-9, December 2010

IV Branovets J, Sepp M, Kotlyarova S, Jepihhina N, Sokolova N, Aksentijevic D, Lygate C. A, Neubauer S, Vendelin M, Birkedal R; **Creatine deficient GAMT-/- mice show no adaptational changes in mitochondrial organization or compartmentation in permeabilized cardiomyocytes**. *AJP–Heart and Circulatory Physiology*, *in press*, 2013

V Sepp M, Kotlyarova S, Sokolova N, Vendelin M; **Glycolysis-coupled Na^+/K^+ ATPase has high activity in permeabilized rat cardiomyocytes**. *submitted*, 2013

Summary of author's contributions

I In Publication I the author participated in the cardiomyocyte isolation process, carried out the oxygraphic measurements, prepared the samples for HPLC experiments, determined the protein concentrations in the cell suspensions, wrote software to analyze the raw data from various measurements, and performed the data analysis. She composed and programmed the mathematical models. The author also participated in writing the manuscript and prepared all tables and the figures contained within it.

II In Publication II, the author isolated the cardiomyocytes together with the first author, performed part of the data analysis, wrote the code to solve the compartmentalized model of cardiomyocyte energetics (Fig.5 in Publication II) and participated in writing the manuscript.

III In Publication III, the author participated in the discussions, wrote parts of the manuscript and prepared the main figure.

IV In Publication IV, the author wrote computer code to analyze the raw data, performed part of the data analysis, and wrote additional code to perform the mathematical modeling.

V In Publication V the author is responsible for planning and performing the majority of the experimental work, including isolating the cardiomyocytes, all oxygraphic measurements and a subset of the spectrophotometric measurements. She analyzed the raw data and modified the mathematical models presented in Publication I to perform numerical simulations using the new data set. In addition, she prepared the figures and tables for the publication and drafted the manuscript.

LIST OF CONFERENCE PRESENTATIONS

I Sepp M, Käämbre T, Sikk P, Vendelin M, Birkedal R. **Kinetic studies of intracellular compartmentalization in permeabilized rat cardiomyocytes**; 36th International Congress of Physiological Sciences (IUPS2009), Kyoto, Japan, July 27-August 1, 2009

II Sepp M, Käämbre T, Sikk P, Vendelin M, Birkedal R; **Kinetic studies of intracellular compartmentalization in permeabilized rat cardiomyocytes**; Biophysical Meeting, Boston, Massachusetts, February 28 - March 4, 2009

III Sepp M, Vendelin M, Vija H, Birkedal R; **Analysis of intracellular ADP compartmentation reveals functional coupling between Pyruvate Kinase and ATPases in rat cardiomyocytes**; Biophysical Meeting, San Francisco, California, USA, February 20 - 24, 2010

IV Sepp M, Branovets J, Sokolova N, Kotlyarova S, Birkedal R, Vendelin M; **Influence of SERCA and actomyosin ATPase on respiration kinetics in permeabilized rat cardiomyocytes**; Biophysical Meeting, Baltimore, Maryland, USA, March 5 - 9, 2011

V Sepp M, Kotlyarova S, Vendelin M; **Na/K ATPase affects respiration kinetics and provides evidence for intracellular diffusion restrictions in permeabilized rat cardiomyocyes**; Biophysical Meeting, Philadelphia, Pennsylvania, USA, February 2 - 6, 2013

PREFACE

THIS DISSERTATION INTRODUCES my doctoral work, presents the main procedures, and highlighting the main results. The main focus is to investigate compartmentation in cardiac energetics, quantify the extent of intracellular diffusion restrictions, and determine the location in subsarcolemmal space using indirect kinetic measurements together with mathematical modeling.

Upon entering the field of cardiac bioenergetics I was a novice to experimental biology being previously involved in the theoretical world of solitons in my bachelor and master studies, with practically no exposure to experimental work. My first steps into the realm of experimental biology was supervised by Dr. Rikke Birkedal and I was introduced to the world of animal research at the bioenergetics laboratory within the National Institute of Chemical Physics under the guidance of Prof.Tuuli Käämbre. Her lab members, Dr. Kersti Tepp and Dr. Natalja Timohhina, supervised my first experiments.

The first stage of experiments was promised to be quite straight forward - repeating the experiments previously performed on skinned fibers on isolated cardiomyocytes. However the results of this study were quite intriguing proving that interesting new knowledge can come from places thought to be quite thoroughly investigated when experimental results are analysed with mathematical models. Results of this project are presented in Publication I.

As the experimental prowess of our newly formed lab widened, it became evident that we cannot efficiently accomplish our research goals without our own basic laboratory facilities. To breach that gap a project was initiated to obtain funding from an EU Regional Development Fund administered by the Archimedes Foundation to set up a laboratory to perform basic biochemical experiments on cells harvested from animals. Because my work largely depends on experimental studies, I was tasked with filling out the necessary paperwork to obtain funding and appropriate licenses. Performing administrative duties, procuring the new lab equipment, and developing procedures for its operation were performed with minimal delay and disruption to the ongoing experimental schedules in the first laboratory at KBFI. Although not directly academic, participating in building a laboratory from scratch is a valuable experience.

The cardiomyocytes used in Publication II and Publication IV were isolated in our new lab.

Acknowledgments

ACRONYMS

ADP	adenosine diphosphate
ANT	adenine nucleotide translocase
ATP	adenosine triphosphate
CK	creatine kinase
Cr	creatine
FP	flavoprotein
GAMT	guanidinoacetate methyltransferase
IMS	mitochondrial intermembrane space
MoM	mitochondrial outer membrane
NADH	nicotinamide adenine dinucleotide
NKA	sarcolemma Na^+/K^+ ATPase
Ox Phos	oxydative phosphorylation
PEP	phosphoenolpyruvate
PK	pyruvate kinase
PKend	endogenous pyruvate kinase
SERCA	sarcoplasmic reticulum Ca^{2+} ATPase
SR	sarcoplasmic reticulum
TG	thapsigargin

THESIS

1

INTRODUCTION

THIS DOCTORAL WORK FOCUSES on the subject of energy metabolism in cardiac cells and how the utilization and regeneration of phosphorylated metabolites is influenced by intracellular compartmentalization and diffusion restrictions. The concentrations of phosphorylated metabolites that participate in intracellular energy metabolism can be used as an indicator of mortality in patients with dilated cardiomyopathy [Neubauer, 2007]. Understanding the coupling of these metabolic functions and how the heart adapts its energetics to outside stimuli has direct clinically relevant implications in designing targeted metabolic interventions [Taegtmeyer, 2000; Taegtmeyer et al., 2005]. Thus understanding the layout of energetic processes could possibly translate into creating physiologically important medical solutions.

The heart can recycle phosphorylated metabolites using various metabolic pathways, both aerobically and anaerobically. These pathways oxidize fatty acids, glucose, lactate, and other substrates [Taegtmeyer, 2000]. The key task of the cells studied in this doctoral work are to match the production of phosphorylated metabolites with their consumption using a minimal reserve pool for metabolite storage. This task is further complicated by spatial separation of the main production site — mitochondria — from the main consumption site — contractile fibrils.

Cardiomyocyte architecture is highly structured. In addition to morphologically evident subcellular organization, the processes of energy metabolism also exhibit compartmentalization. Compartmentalization organizes the production and consumption processes in the heart into energetic units to optimize signaling and feedback while minimizing the effects of a sudden changes in energetic requirements in a way that ensures the long-term sustainability of energy production [Neubauer, 2007]. Cardiac and skeletal muscles contain a specialized creatine kinase (CK) energy transfer system that can mediate the transfer of energy in the form of phosphoryl groups between mitochondria and myofibrils [Saks et al., 2006; Wallimann et al., 1992]. The transfer of phosphorylated metabolites in heart cells is a combination of many different processes, the interplay of which remains largely unknown. This functional compartmentalization of the processes requires dynamic monitor-

ing of many concurrent events that are spatially separated, and thus requires different methods of analyzing these changes. While it is possible to study the molecular components individually, it becomes increasingly difficult to apply this approach to study the interactions of a dynamic system with concurrent and coupled processes while extracting meaningful and unambiguous insight. The methods of systems biology are being increasingly applied to study the myriad of coupled processes in biological systems through a process of mathematically formulating the processes and combining them into a broad descriptive system that can be used to gain quantitative insight.

Strong functional interplay between mitochondria and surrounding ATPases has been demonstrated in mammalian heart cardiomyocytes [Hoerter et al., 1991; Kaasik et al., 2001; Saks et al., 2001; Seppet et al., 2001b] and in morphologically very different ectothermic vertebrates [Birkedal and Gesser, 2004; Sokolova et al., 2009]. Some aspects of this functional interplay is made possible by the existence of localized diffusion restrictions [Saks et al., 2003; Vendelin et al., 2004a]. The apparent magnitude of these diffusion restrictions depends on various physiological and pathological conditions including the stage of development, workload, and metabolic state. Cultured cardiomyocytes, that do not contract against workload and depend more on glycolytic than on aerobic metabolism, have been identified that have no diffusion restrictions [Anmann et al., 2006] suggesting that the magnitude of diffusion restrictions is closely related to cardiac mechanical performance and aerobic capacity.

The first indications of diffusion restrictions came from studies comparing affinity of oxydative phosphorylation (Ox Phos) to adenosine diphosphate (ADP) in skinned fibers or cells and in isolated mitochondria [Kummel, 1988; Veksler et al., 1987]. It was found that the sensitivity of Ox Phos to ADP was an order of magnitude higher in mitochondria than in skinned fibers, indicating that the cytoskeleton must restrict the diffusion of ADP to mitochondria. Additional proof of obstructions in the path of ADP came when PK and phosphoenolpyruvate (PEP) system, that draws away ADP otherwise available for mitochondria, was found to be much less active than would be predicted on the basis of mitochondrial and PK+PEP activities and kinetics [Saks et al., 2001; Seppet et al., 2001a]. Functional linking between mitochondria and enzymes catalysing adenosine triphosphate (ATP) decomposition (ATPase) on sarcoplasmic reticulum (SR) that is caused by diffusion restrictions was also reported by Kaasik et al. [2001].

Diffusion restrictions were shown to be present without any structural candidate to impose such an obstruction [Kaasik et al., 2001; Saks et al., 2003; Seppet et al., 2004; Vendelin et al., 2004b]. It is counter intuitive that restricting the movement of phosphorylated metabolites could be beneficial for the cardiac cell, however, the importance of this compartmentalization is suggested by the observation that a

reduction in diffusion restrictions occurs under pathological conditions and in ischemic cells [Kay et al., 1997a,c]. The physiological role of diffusion restrictions in heart muscle cells is not clear, however the research summarized above implies that they play an important role in cellular energy transfer regulation.

The general aim of this doctoral work is to gain insight into the role that diffusion restrictions play in the cardiac cell using kinetic measurements. A combination of mathematical modeling and experimental work is applied to quantify diffusion restrictions indirectly via measurements of cellular respiration and various ATPase activities. A complete set of kinetic measurements was performed on cells in a resting state in cases where cellular metabolism is unmodified and when it is altered by inhibition of ATPase's. Several mathematical models were constructed, each with a different possible arrangement of intracellular compartmentalization. These models were used to analyze experimental data obtained from rat, wild type mouse cardiomyocytes, and transgenic mouse cardiomyocytes. In addition, the modeling process revealed that the origin of diffusion restrictions is indeed intracellular and is not caused by experimental artifacts such as the clumping of cells that increases diffusion distances.

When designing the mathematical models, we started with the established compartmentation of intracellular environment in the heart muscle. That model was continuously compared with experimental findings and modified to fit new hypotheses. In the end seven different models were used: four main models with different morphology, plus modifications of three of these with different kinetic parameters. The desing of both mathematical and experimental work is described in Chapter 2. In the remaining chapters of this dissertation the results of the work are summarized in Chapter 3 and the main conclusions are drawn in Chapter 4.

<div align="right">

2

</div>

OVERALL DESIGN

To study the distribution of diffusion restrictions in a heart cell a combination of experimental and theoretical approaches were used. Indications about the existence of diffusion restrictions originated from studies on skinned fibers rather than isolated cells: [Kummel, 1988; Saks et al., 2001, 1993; Veksler et al., 1987]. Combination of kinetic studies on permeabilized heart muscle fibers with their analysis by mathematical models is a promising approach that demonstrated existence of intracellular diffusion restrictions grouping ATPase's and mitochondria [Saks et al., 1998a, 2003, 2000; Vendelin et al., 2004b]. Here, the same approach has been developed further by applying it to much more homogeneous preparation - isolated cardiomyocytes - and designing a set of experiments that probe different aspects of intracellular compartmentalization. Although various experiments had been performed on isolated muscle cells [Kay et al., 1997b; Saks et al., 1998b], a complete experimental study that combines measurements of ADP and ATP kinetics and how the processes are affected by PK+PEP together with the buildup of metabolites in solution, had not been completed prior to this work. The aim of this doctoral project was gather this complete set of data and analyze it using mathematical models.

2.1 EXPERIMENTS

A set of kinetic experiments was designed to systematically study the intracellular compartmentalization. The goal was to obtain a complete view of cellular energy transfer by monitoring ATP production via cellular respiration and ATP consumption via cytosolic enzymatic activity and to use this body of data as an input to mathematical models. The considered processes in the cell are depicted in Fig.1. ATP is generated in mitochondria and consumed by ATPase's, ADP generated either by ATPase's or added exogenously enters mitochondria to be rephosphorylated to ATP. In addition to mitochondrial Ox Phos, ADP is also used in PKend and PK reactions. The experimental setup consisted of the following experiments:
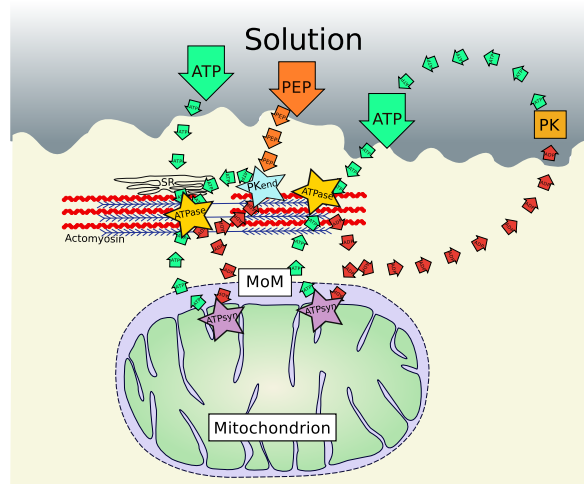
Figure 1 – Schematic representation of mathematical model describing intracellular metabolite kinetics in permeabilized rat cardiomyocytes.

1. Dependence of mitochondrial respiration on stepwise increase in ATP concentration,

2. Dependence of mitochondrial respiration on stepwise increase in ADP concentration,

3. Effect of ADP regeneration by PKend: respiration initiated by 2mM ATP and consecutive inhibition by 5mM PEP and 20IU PK,

4. Spectrophotometric measurement of ATPase activity in the absence of mitochondrial respiration,

5. Spectrophotometric measurement of endogenous PK activity.

For the control case we quantified the buildup of ADP in the solution over time using high-performance liquid chromatography in the presence and absence of mitochondrial respiration. A detailed description of the experimental protocols used are given in Publication I. The solution volumes in the models were taken from the experimental setup, and vary between different experiment types listed. The experiments reflect the behavior of cell populations. In the models, we describe the distribution of metabolites in one representative cell.

The models developed in this work calculate the rate at which products are created from substrates during the regeneration and transfer of phosphorylated metabolites within cardiac cells. Specifically, we focus on the reactions involving ATP and ADP generation and consumption. The purpose was to develop a set of model equations that mimic the reactions involving these two metabolites that also correspond to the experiments introduced above. Note that the models developed are unable to differentiate between the various ATPases, and do not take into account the geometry of organelles. These models provide general insight about the distribution of the diffusion restrictions and energetic properties of the cell before tackling these problems in 3D, which is a more tedious process [Ramay and Vendelin, 2009].

Four different models of varying intracellular complexity are used to reproduce the experimental data. The models are described briefly below, for detailed information see Supporting Material of Publication I. In each of the models, the cellular space was divided into three compartments: cytosol, solution, and mitochondrial intermembrane space (IMS), in models 3 and 4 a fourth compartment C4 was added into the cytosol. It should be noted that the fourth compartment is a phenomenological inclusion to group functionally coupled processes and does not correspond directly to an organelle. The volume of mitochondrial matrix was assumed to be 33% of the cell volume, IMS was 1% of the cell volume, with the volume of cytosolic compartment occupying the rest.

All compartments are separated from each other by diffusion restrictions including the connection between solution and cytosolic compartment. The model solutions were obtained in the form of average concentration within the different compartments in the cell. The concentrations and the rates of reactions are determined by relative activities of the enzymes and extent of diffusion restrictions.

Each model provides an estimation of the overall diffusion restriction between the intracellular environment and extracellular solution, as well as restrictions between ATPases and mitochondria according to the model architecture. It is assumed that the diffusion restrictions imposed on ADP and ATP are the same.

2.2.1 *Model 1-2*

In the mathematical modeling setup, scheme shown in Fig.2, the intracellular space was divided into three major compartments according to where the reactions (noted by curved arrows) occur: IMS - ATP synthase (note that this is phenomenological description of the generation omitting the detailed view of matrix respiratory chain reactions); and cytosol - ATPases. The solution surrounding the cell was defined as

an additional compartment where PK reaction occurs and through which metabolites ATP and ADP are introduced. The movement of ATP and ADP between these compartments and how they affect the diffusion was estimated.
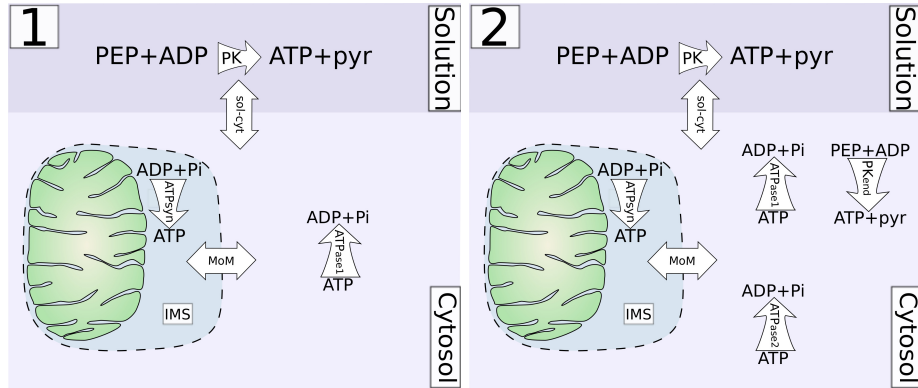
Figure 2 – Schemes of models 1 and 2.

For model 1 and 2 the fluxes of metabolites induced by diffusion between those compartments are

$$
\begin{aligned}
J_{ATP} &= C_{sol-cyt}(ATP_{sol} - ATP_{cyto}) \\
J_{2ATP} &= C_{MoM}(ATP_{cyto} - ATP_{IMS}) \\
J_{ADP} &= C_{sol-cyt}(ADP_{sol} - ADP_{cyto}) \\
J_{2ADP} &= C_{MoM}(ADP_{cyto} - ADP_{IMS}),
\end{aligned}
\tag{2.1}
$$

where $C_{sol-cyt}$ is the exchange coefficients between the solution and cytosol, and C_{MoM} is the exchange coefficient between the cytosol and IMS, noted by double headed arrows in Fig.2.

In addition to diffusion across compartments the reactions in model 1, also shown by curved arrows, are: ATP synthesis in mitochondria by Ox Phos (rate: V_{ATPsyn}), ATP consumption by ATPases in the cytosol (rate: $V_{ATPase1}$); and the synthesis of ATP by the PK reaction in solution (rate: V_{PK}).

For simplicity, the rates of reactions occurring in different compartments are given using a phenomenological description. The rate at which ATP is produced by mitochondria:

$$
V_{ATPsyn} = \frac{V_{maxATPsyn} \cdot ADP_{IMS}}{ADP_{IMS} + K_{mATPsyn}},
\tag{2.2}
$$

where the $K_{mATPsyn}$ was taken equal to 0.015 mM [Saks et al., 1994] in all models. In the cytosol ATP consumption by ATPases is assumed to be competitively inhibited by ADP:

$$V_{ATPase1} = \frac{V_{maxATPase1} \cdot ATP_{cyto}}{ATP_{cyto} + K_{mATPase1}\left(1 + \frac{ADP_{cyto}}{K_{iATPase1}}\right)}. \tag{2.3}$$

The exogenous PK reaction is assumed to depend only on the concentration of ADP:

$$V_{PK} = \frac{V_{maxPK} \cdot ADP_{sol}}{ADP_{sol} + K_{PK}}. \tag{2.4}$$

Here, a dependence of the PK rate on PEP is not taken into account explicitly because the PEP level is assumed to be same in all compartments. Because the PEP concentration used in all experiments (5 mM) is considerably larger than the concentration of ADP, the influence of PEP concentration gradients on the kinetics is assumed to be inconsequential. The apparent kinetic constant K_{PK} was taken to be 0.3 mM in all models.

Model 2 is based on model 1 with ATPase activity split into two fractions (ATPase$_1$ and ATPase$_2$) with different apparent kinetic constants defined analogously to Eq. 2.3 and endogenous PK activity (PKend) is added in the cytosolic compartment. The activity of PKend is defined as Eq.2.4 except the consumed ADP is cytosolic not from solution compartment.

The kinetic equations for the concentrations of each metabolite in each compartment are as follows for model 1:

$$
\begin{aligned}
dATP_{sol}/dt &= (-J_{ATP} + V_{PK})/W_{sol} \\
dADP_{sol}/dt &= (-J_{ADP} - V_{PK})/W_{sol} \\
dATP_{cyto}/dt &= (-V_{ATPase1} + J_{ATP} - J_{2ATP})/W_{cyto} \\
dADP_{cyto}/dt &= (V_{ATPase1} + J_{ADP} - J_{2ADP})/W_{cyto} \\
dATP_{IMS}/dt &= (J_{2ATP} + V_{ATPsyn})/W_{IMS} \\
dADP_{IMS}/dt &= (J_{2ADP} - V_{ATPsyn})/W_{IMS},
\end{aligned}
\tag{2.5}
$$

where W_{sol} is the volume of solution, W_{cyto} is the volume of the cytosol, and W_{IMS} is the volume of IMS. For model 2, the kinetic equations for the metabolites

are the same as for model 1 given in Eq.2.5 except the ones describing ATP and ATP in cytosolic compartment:

$$
\begin{aligned}
\mathrm{dATP_{cyto}}/\mathrm{dt} =& \\
& (-V_{\mathrm{ATPase1}} - V_{\mathrm{ATPase_2}} + J_{\mathrm{ATP}} - J_{2\,\mathrm{ATP}} + V_{\mathrm{PKend1}})/W_{\mathrm{cyto}} \\
\mathrm{dADP_{cyto}}/\mathrm{dt} =& \\
& (V_{\mathrm{ATPase1}} + V_{\mathrm{ATPase_2}} + J_{\mathrm{ADP}} - J_{2\,\mathrm{ADP}} - V_{\mathrm{PKend1}})/W_{\mathrm{cyto}}.
\end{aligned} \tag{2.6}
$$

2.2.2 *Model 3-4*

In models 3 and 4 show in Fig.3, an additional intracellular compartment (compartment 4, C4) with a volume (W_{C4}) equal to 10% of cytosolic volume, is introduced to test whether some of ATPases are coupled to endogenous PK. Part of the PKend and ATPase activities are located in C4. In model 3, C4 is connected to the cytosol and
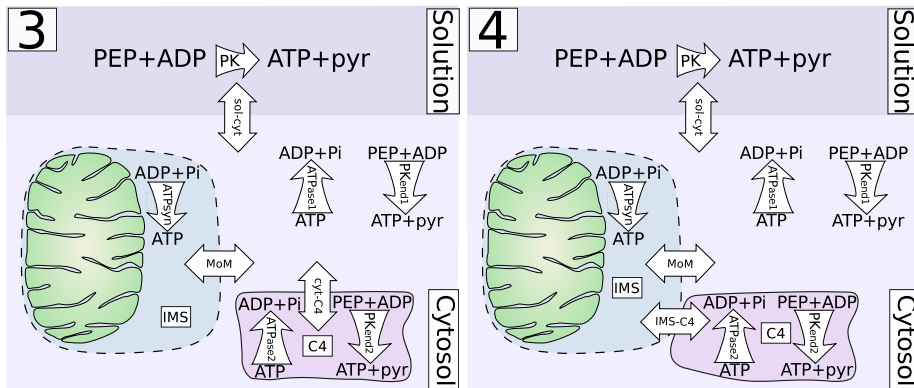

Figure 3 – Schemes of model 3 and 4.

in model 4 directly to IMS. The fluxes of metabolites and the kinetic equations are constructed similarly to models 1 and 2. For detailed description of these models, see Supporting material in Publication I.

3

RESULTS

Tʜɪs ᴅɪssᴇʀᴛᴀᴛɪᴏɴ ᴇxᴀᴍɪɴᴇs the cardiac energetic system using methods from systems biology in combination with experiments designed to study cellular metabolism. The experimental procedures employed are by no means novel, they have been in use to study cellular metabolism for decades. Indeed, the first indications of the existence of diffusion restrictions came from work using the experimental protocols adopted in this work. However, many of these experiments were not performed on isolated permeabilized myocytes, but on skinned fibers — a less elegant preparation than isolated cells due to the inhomogeneous nature of the sample and the fact that grouping of fiber bundles might have undesirable effects [Kongas et al., 2002]. Also, the data from various different experiments have never been analyzed together using mathematical models to reveal the system properties of energetic pathways.

A combination of experiments was designed to study the intracellular compartmentalization. See Fig.4 for representative traces from one kinetic measurement (**A, B, C, D** top) and corresponding final data together with the calculated model solution fits (**A, B, C, D** bottom). In addition to shown experiments, we measured the extent of respiration inhibition when introduction of PK+PEP into the system makes less ADP available for mitochondria. We started off with repeating the experimental protocol originally used on fibers for similar study [Saks et al., 2003] with PEP already in the solution (see Fig.5 left graph). We found however that the 2mM ATP induced respiration rate was much lower than was measured from the ATP titration experiment. We then changed the experimental protocol recording the effect of PEP addition separately (see Fig.5 right graph). PEP inhibited respiration even before addition of PK proving the presence of endogenous PK. That discovery prompted the addition of these two experiments together with spectrophotometric measurement of endogenous PK activity into the list of experiments through which compartmentalization is studied.

A data set was gathered in this work to study rat cardiac myocytes in a resting state. By assessing this experimental data with a set of mathematical models, a subset of these was able to characterize many aspects of cellular function. In
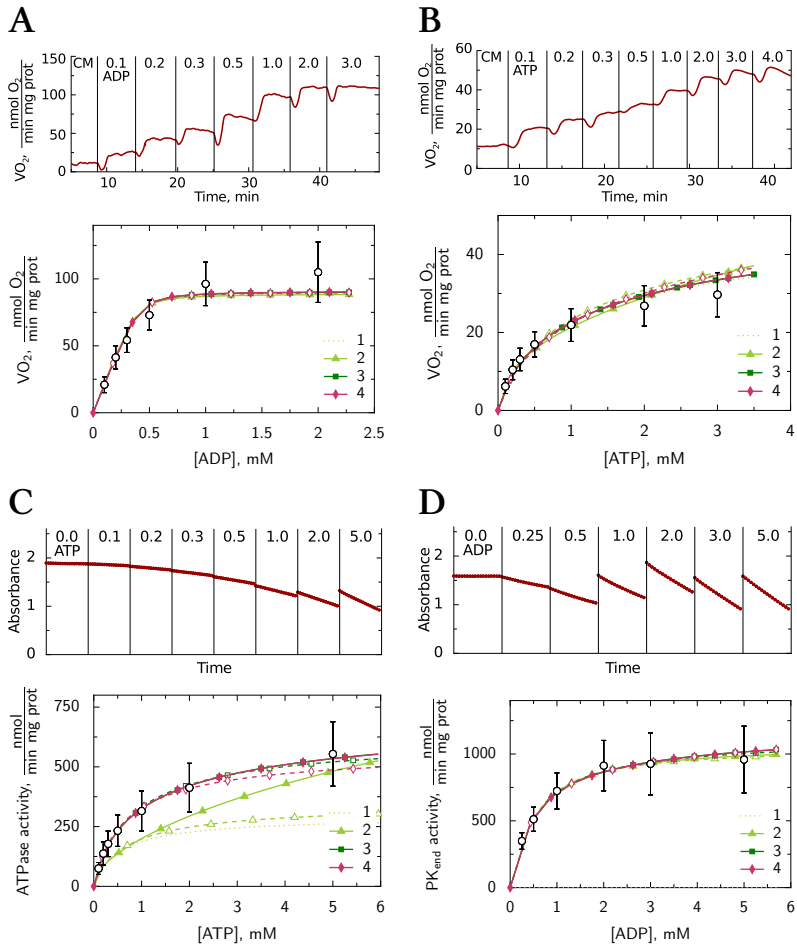
Figure 4 – Experiments and modeling. Representative examples of one experimental measurement trace: respiration dependence on ADP (**A**), respiration dependence on ATP (**B**); spectrophotometric ATPase activity measurement (**C**), and PKend measurement (**D**). Averaged data gathered from a series of experiments (empty circles ± STD) directly below each individual representative trace and fits calculated with different mathematical models.
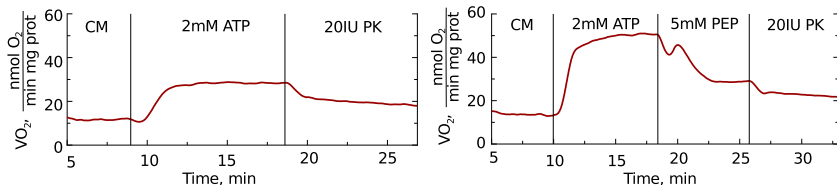
Figure 5 – Representative experimental traces showing the presence of endogenous PK. Respiration stimulated by 2mM ATP with PEP in the solution followed by PK addition (left), and with separate additions of PEP and PK.

permeabilized cardiomycotyes it was found that a fraction of ATPases exist that are functionally coupled to endogenous PK. The additonal compartment C4 acts as phenomenological entity for grouping ATPases and endogenous PK. This study also confirmed the existence of diffusion restriction caused by the outer mitochondrial membrane and showed that additional diffusion restrictions exist in the cytosol as well.

In this work, the preparation under investigation is a population of cells and analyzed using models that describe processes that occur in a single cell. It is assumed that the cell suspension is homogeneous which was additionally verified by quantifying the quality of the preparation prior to all measurements.

However, under the measurement conditions, homogeneity may be compromised and the cells could form clusters by clumping together resulting in an altered assessment of diffusion distances which could possibly affect the results. Mitochondrial autofluorescence was measured to gain insight into the operation of the energetic processes that occur on the single cell level in rat cardiomyocytes. To check whether permeabilized rat cardiomyocytes exhibit low ADP-affinity at the single cell level, in Publication II nicotinamide adenine dinucleotide (NADH) and flavoprotein (FP) response to exogenous ADP and ATP in permeabilized rat cardiomyocyte was followed using fluorescence microscopy. The autofluorescence of reduced and oxidized FPs reflect the redox state of the cell [Chance et al., 1979; Chance and Williams, 1955] and have been used extensively to characterize the state of the respiratory chain in numerous studies [Chance and Baltscheffsky, 1958; Chance et al., 1979; Chance and Williams, 1955; Huang et al., 2002; Kuznetsov et al., 1998; Mayevsky and Barbiro-Michaely, 2009; Sedlic et al., 2010; Winkler et al., 1995]. This investigation was undertaken to test the hypothesis proposed by Kongas et al. [2002] that the apparent affinity of endogenous ATP to Ox Phos could be increased by formation of micro aggregates and unstirred water layers. Because the microscope flow chamber has a simple geometry, the flow profile around the cell was calculated which allowed the separation of the contribution of diffusion gradients in the solution surrounding the cell from those of intracellular origin. Comparing the data to model solutions indicates that intracellular structures impose significant diffusion obstacles in rat cardiomyocytes.

Mathematical models are useful in studying integrated systems and they can be used to test different hypotheses. Moreover, they can aid in elucidating insight from data and avoid mistakes that can come from misinterpretations as was pointed out in Publication III, which is a critique of work published by established researchers. In the original study by [Piquereau et al., 2010] the authors analyze a vast array of experimental work looking at the changes in energetic organization during maturation in mice. They conclude that energetic micro-domains form very early in postnatal development, however, the role of CK as an energetic mediator in devel-

oping organisms is potentially exaggerated resuling from possible misinterpretation of increase in K_{mADP} ratio to K_{Cr} in during maturation [Piquereau et al., 2010] as was pointed out by us in Publication III.

The importance of CK in energy transfer has been strongly emphasized by various research groups. Disruption of the CK system in hearts of CK-deficient mice leads to changes in intracellular morphology and regulation of mitochondrial respiration [Kaasik et al., 2001; Nahrendorf et al., 2006]. Creatine deficiency inhibits the CK system. It may occur due to deficiency in three enzymes that synthesize creatine. A mouse model deficient in one of these enzymes, namely guanidinoacetate methyltransferase (GAMT), has been studied extensively. Publication IV concerns the compartmentalization in GAMT-deficient mice versus wild-type. The main conclusions of this work are that GAMT-deficiency is not associated with any changes in cardiomyocyte mitochondrial organization, stimulated respiration or its regulation by exogenous and endogenous ADP supply. Mathematical models were used to analyze kinetic data gathered on both wild-type and GAMT knockout mice and the results show that there is no change in intracellular compartmentalization, when cells are in a relaxed state.

After the discovery of Publication I that some ATPases are functionally coupled to PKend, our focus turned to investigating the role of different ATPases and establishing their possible connection with PKend. First, we studied the role of SERCA, a pump responsible for getting free Ca^{2+} back to SR after contraction, by inhibiting it with thapsigargin (TG). It was found that in the relaxed cell, SERCA inhibition did not have a significant effect on either cellular respiration or on ATPase activity, thus its coupling with PKend cannot be assessed in our conditions.

Next we turned to investigating the role of sarcolemmal NKA, an enzyme responsible for the maintenance of the cellular sodium and potassium balance and through these it also influences cellular Ca^{2+} management. We found that in permeabilized cardiomyocytes the total ATPase activity is reduced after the addition of ouabain by ∼45%. Respiration rates, however were unaltered after NKA inhibition. This showes that no coupling exists between NKA and *Ox Phos* and that the pump is coupled to PKend. This conclusion was confirmed by performing a kinetic measurements of NKA-inhibited cells and analyzing the measurements with the set of mathematical models developed in this work. Fig.6 summarizes the findings of Publication IV together with cellular architecture and the organization of energy transfer.

For the future – interaction of various processes depicted in this picture are to be investigated further: which of the different ATPases are coupled to Ox Phos and which to glycolysis through PK and which structures are responsible for diffusion restrictions.
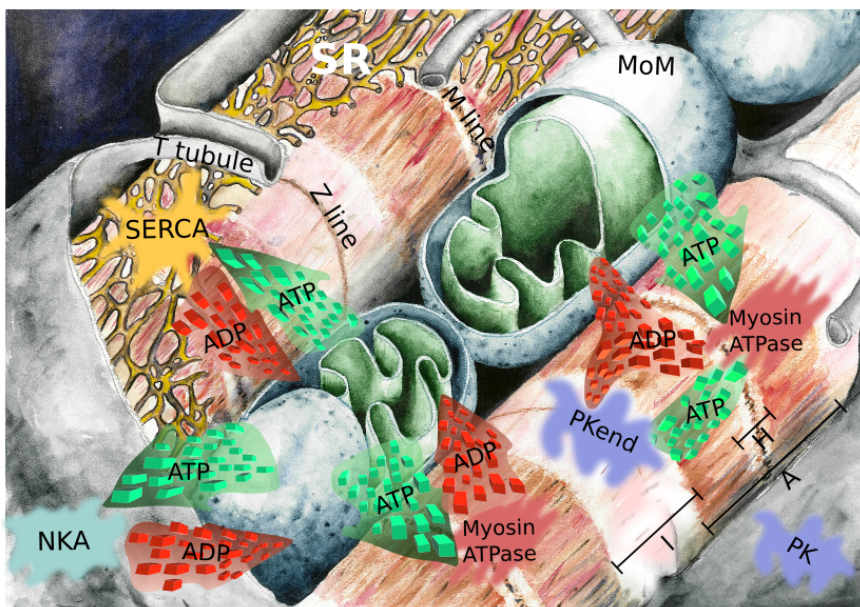
Figure 6 – Illustrative schemes of the processes of ATP production and consumption in cardiomyocyte by different ATPases : SERCA, NKA and myosin ATPase; and PK and PKend competing with mitochondria for ADP.

4

CONCLUSIONS

THE FINDINGS OF THIS THESIS widen the understanding of cellular compartmentation in both healthy cardiomyocytes and in cardiomyocytes with compromised energetic operations. The main conclusions of this work are listed below:

a) A complete and uniform set of kinetic data on relaxed rat cardiomyocytes was gathered to study intracellular compartmentation using systems biology tools.

b) The presence of significant diffusion restrictions caused by the mitochondrial outer membrane (MoM) was confirmed along with the existence of cytosolic diffusion restrictions.

c) By analyzing the data with mathematical models it was found that tight functional coupling exists between glycolysis and a fraction of ATPases.

d) The experimental data shows that after permeabilization, a considerable amount of PK activity remains in rat cardiomyocytes.

e) By analyzing the data with mathematical models it was found that tight functional coupling exists between mitochondria and a fraction of ATPases.

f) By comparing cell population studies and single cell studies it was demonstrated that intracellular structures impose significant diffusion obstacles and are not caused by a large effective diffusion distance.

g) Analyzing compartmentation in GAMT-deficient mice showed that inhibition of the CK-system does not alter the mitochondrial kinetics and intracellular compartmentation in relaxed cardiomyocytes.

h) While investigating the role of SR Ca^{2+} ATPase in cellular energetics it was found that SERCA plays a minor role in relaxed permeabilized rat cardiomyocytes, and a connection of PKend to this ATPase could not be established.

i) Even after permeabilization, inhibition the sarcolemma NKA affects the total ATPase activity.

j) NKA was found to be coupled to glycolysis via PK

BIBLIOGRAPHY

BIBLIOGRAPHY

Anmann, T., Guzun, R., Beraud, N., Pelloux, S., Kuznetsov, A. V., Kogerman, L., Kaambre, T., Sikk, P., Paju, K., Peet, N., Seppet, E., Ojeda, C., Tourneur, Y., and Saks, V. (2006). Different kinetics of the regulation of respiration in permeabilized cardiomyocytes and in hl-1 cardiac cells. importance of cell structure/organization for respiration regulation. *Biochim. Biophys. Acta*, 1757(12):1597–1606.

Birkedal, R. and Gesser, H. (2004). Effects of hibernation on mitochondrial regulation and metabolic capcities in the myocardium of painted turtle (chrysemys picta). *Comp. Biochem. Physiology A*, 139(3):285–291.

Chance, B. and Baltscheffsky, M. (1958). Spectroscopic effects of adenosine diphosphate upon the respiratory pigments of rat-heart-muscle sarcosomes. *Biochem. J.*, 68(2):283–295.

Chance, B., Schoener, B., Oshino, R., Itshak, F., and Nakase, Y. (1979). Oxidation-reduction ratio studies of mitochondria in freeze-trapped samples. nadh and flavoprotein fluorescence signals. *J. Biol. Chem.*, 254(11):4764–4771.

Chance, B. and Williams, G. R. (1955). Respiratory enzymes in oxidative phosphorylation. iii. the steady state. *J. Biol. Chem.*, 217(1):409–427.

Hoerter, J. A., Kuznetsov, A., and Ventura-Clapier, R. (1991). Functional development of the creatine kinase system in perinatal rabbit heart. *Circ. Res.*, 69(3):665–676.

Huang, S., Heikal, A., and Webb, W. (2002). Two-photon fluorescence spectroscopy and microscopy of nad(p)h and flavoprotein. *Biophys. J.*, 82(5):2811–2825.

Kaasik, A., Veksler, V., Boehm, E., Novotova, M., Minajeva, A., and Ventura-Clapier, R. (2001). Energetic crosstalk between organelles: architectural integration of energy production and utilization. *Circ. Res.*, 89(2):153–159.

Kay, L., Daneshrad, Z., Saks, V. A., and Rossi, A. (1997a). Alteration in the control of mitochondrial respiration by outer mitochondrial membrane and creatine during heart preservation. *Cardiovasc. Res.*, 34(3):547–556.

Bibliography

Kay, L., Li, Z., Mericskay, M., Olivares, J., Tranqui, L., Fontaine, E., Tiivel, T., Sikk, P., Kaambre, T., Samuel, J. L., and Others, . (1997b). Study of regulation of mitochondrial respiration in vivo: An analysis of influence of adp diffusion and possible role of cytoskeleton. *Biochimica et Biophysica Acta (BBA)-Bioenergetics*, 1322(1):41–59.

Kay, L., Saks, V. A., and Rossi, A. (1997c). Early alteration of the control of mitochondrial function in myocardial ischemia. *J. Mol. Cell. Cardiol.*, 29(12):3399–3411.

Kongas, O., Yuen, T., Wagner, M., Beek, J., and Krab, K. (2002). High k(m) of oxidative phosphorylation for adp in skinned muscle fibers: where does it stem from? *Am. J. Physiol. Cell. Physiol.*, 283(3):C743–C751.

Kummel, L. (1988). Ca, mg-atpase activity of permeabilised rat heart cells and its functional coupling to oxidative phosphorylation of the cells. *Cardiovasc. Res.*, 22(5):359–367.

Kuznetsov, A. V., Mayboroda, O., Kunz, D., Winkler, K., Schubert, W., and Kunz, W. S. (1998). Functional imaging of mitochondria in saponin-permeabilized mice muscle fibers. *J. Cell Biol.*, 140(5):1091–1099.

Mayevsky, A. and Barbiro-Michaely, E. (2009). Use of nadh fluorescence to determine mitochondrial function in vivo. *Int. J. Biochem. Cell Biol.*, 41(10):1977–1988.

Nahrendorf, M., Streif, J., Hiller, K., Hu, K., Nordbeck, P., Ritter, O., Sosnovik, D., Bauer, L., Neubauer, S., Jakob, P., Ertl, G., Spindler, M., and Bauer, W. (2006). Multimodal functional cardiac mri in creatine kinase-deficient mice reveals subtle abnormalities in myocardial perfusion and mechanics. *Am. J. Physiol. Heart Circ. Physiol.*, 290(6):H2516 –H2521.

Neubauer, S. (2007). The failing heart–an engine out of fuel. *N. Engl. J. Med.*, 356(11):1140–1151.

Piquereau, J., Novotova, M., Fortin, D., Garnier, A., Ventura-Clapier, R., Veksler, V., and Joubert, F. (2010). Postnatal development of mouse heart: formation of energetic microdomains. *J. Physiol. (Lond.)*, 588(Pt 13):2443–2454.

Ramay, H. R. and Vendelin, M. (2009). Diffusion restrictions surrounding mitochondria: A mathematical model of heart muscle fibers. *Biophys. J.*, 97(2):443–52.

Saks, V., Aliev, M., Santos, P. D., Vendelin, M., and Kongas, O. (1998a). Mathematical model of energy transfer in hearts with inhibited or ablated creatine kinase system. *MAGMA*, 6(2-3):124–125.

Saks, V., Dzeja, P., Schlattner, U., Vendelin, M., Terzic, A., and Wallimann, T. (2006). Cardiac system bioenergetics: metabolic basis of the frank-starling law. *J Physiol*, 571(Pt 2):253–273.

Saks, V., Kuznetsov, A., Andrienko, T., Usson, Y., Appaix, F., Guerrero, K., Kaambre, T., Sikk, P., Lemba, M., and Vendelin, M. (2003). Heterogeneity of adp diffusion and regulation of respiration in cardiac cells. *Biophys. J.*, 84(5):3436–3456.

Saks, V. A., Kaambre, T., Sikk, P., Eimre, M., Orlova, E., Paju, K., Piirsoo, A., Appaix, F., Kay, L., Regitz-Zagrosek, V., Fleck, E., and Seppet, E. (2001). Intracellular energetic units in red muscle cells. *Biochem. J.*, 356(Pt 2):643–657.

Saks, V. A., Khuchua, Z. A., Vasilyeva, E. V., Belikova, O. Y., and Kuznetsov, A. V. (1994). Metabolic compartmentation and substrate channelling in muscle cells. role of coupled creatine kinases in in vivo regulation of cellular respiration–a synthesis. *Mol. Cell. Biochem.*, 133-134:155–192.

Saks, V. A., Kongas, O., Vendelin, M., and Kay, L. (2000). Role of the creatine/phosphocreatine system in the regulation of mitochondrial respiration. *Acta Physiol. Scand.*, 168(4):635–641.

Saks, V. A., Vasil'eva, E., Belikova, Y. O., Kuznetsov, A. V., Lyapina, S., Petrova, L., and Perov, N. A. (1993). Retarded diffusion of adp in cardiomyocytes: possible role of mitochondrial outer membrane and creatine kinase in cellular regulation of oxidative phosphorylation. *Biochim. Biophys. Acta*, 1144(2):134–148.

Saks, V. A., Veksler, V. I., Kuznetsov, A. V., Kay, L., Sikk, P., Tiivel, T., Tranqui, L., Olivares, J., Winkler, K., Wiedemann, F., and Kunz, W. S. (1998b). Permeabilized cell and skinned fiber techniques in studies of mitochondrial function in vivo. *Mol. Cell. Biochem.*, 184(1-2):81–100.

Sedlic, F., Pravdic, D., Hirata, N., Mio, Y., Sepac, A., Camara, A., Wakatsuki, T., Bosnjak, Z., and Bienengraeber, M. (2010). Monitoring mitochondrial electron fluxes using nad(p)h-flavoprotein fluorometry reveals complex action of isoflurane on cardiomyocytes. *Biochim. Biophys. Acta*, 1797(10):1749–1758.

Seppet, E., Kaambre, T., Sikk, P., Tiivel, T., Vija, H., Tonkonogi, M., Sahlin, K., Kay, L., Appaix, F., Braun, U., Eimre, M., and Saks, V. (2001a). Functional complexes of mitochondria with ca,mgatpases of myofibrils and sarcoplasmic reticulum in muscle cells. *Biochim. Biophys. Acta (BBA)-Bioenergetics*, 1504(2-3):379–395.

Seppet, E. K., Eimre, M., Andrienko, T., Kaambre, T., Sikk, P., Kuznetsov, A. V., and Saks, V. (2004). Studies of mitochondrial respiration in muscle cells in situ:

use and misuse of experimental evidence in mathematical modelling. *Mol. Cell. Biochem.*, 256(1):219–227.

Seppet, E. K., Kaambre, T., Sikk, P., Tiivel, T., Vija, H., Tonkonogi, M., Sahlin, K., Kay, L., Appaix, F., Braun, U., Eimre, M., and Saks, V. A. (2001b). Functional complexes of mitochondria with ca,mgatpases of myofibrils and sarcoplasmic reticulum in muscle cells. *Biochim. Biophys. Acta*, 1504(2-3):379–395.

Sokolova, N., Vendelin, M., and Birkedal, R. (2009). Intracellular diffusion restrictions in isolated cardiomyocytes from rainbow trout. *BMC Cell Biol.*, 10(1):90.

Taegtmeyer, H. (2000). Metabolism–the lost child of cardiology. *J. Am. Coll. Cardiol.*, 36(4):1386.

Taegtmeyer, H., Wilson, C. R., Razeghi, P., and Sharma, S. (2005). Metabolic energetics and genetics in the heart. *Ann. N. Y. Acad. Sci.*, 1047:208–218.

Veksler, V. I., Kuznetsov, A. V., Sharov, V. G., Kapelko, V. I., and Saks, V. A. (1987). Mitochondrial respiratory parameters in cardiac tissue: a novel method of assessment by using saponin-skinned fibers. *Biochim. Biophys. Acta*, 892(2):191–196.

Vendelin, M., Eimre, M., Seppet, E., Peet, N., Andrienko, T., Lemba, M., Engelbrecht, J., Seppet, E., and Saks, V. (2004a). Intracellular diffusion of adenosine phosphates is locally restricted in cardiac muscle. *Mol. Cell. Biochem.*, 256-257(1):229–241.

Vendelin, M., Eimre, M., Seppet, E., Peet, N., Andrienko, T., Lemba, M., Engelbrecht, J., Seppet, E., and Saks, V. (2004b). Intracellular diffusion of adenosine phosphates is locally restricted in cardiac muscle. *Mol. Cell. Biochem.*, 256/257(1/2):229–241.

Wallimann, T., Wyss, M., Brdiczka, D., Nicolay, K., and Eppenberger, H. (1992). Intracellular compartmentation, structure and function of creatine kinase isoenzymes in tissues with high and fluctuating energy demands: the 'phosphocreatine circuit' for cellular energy homeostasis. *Biochem. J.*, 281:21–40.

Winkler, K., Kuznetsov, A. V., Lins, H., Kirches, E., Bossanyi, P. v., Dietzmann, K., Frank, B., Feistner, H., and Kunz, W. S. (1995). Laser-excited fluorescence studies of mitochondrial function in saponin-skinned skeletal muscle fibers of patients with chronic progressive external ophthalmoplegia. *Biochim. Biophys. Acta*, 1272(3):181–184.

CURRICULUM VITAE

Curriculum Vitae

Mervi Sepp

Personal information

Date of Birth	February 4, 1980	
Contact	Sõpruse pst 230-25, 13412	Tallinn, Estonia
	✉ mervi@sysbio.ioc.ee ☎ +372 5661 9917	

Education

2006 — 2013	**Tallinn University of Technology (TUT)**	Tallinn, Estonia
Subject	**PhD, Engineering Physics**	
Thesis	Estimation of diffusion restrictions in cardiomyocytes using kinetic measurements	
Supervisor	**Dr. Marko Vendelin**, markov@sysbio.ioc.ee, +372 620 4169	
	Head of Laboratory of Systems Biology, Institute of Cybernetics at TUT (IoC)	

2003 — 2006	**Tallinn University of Technology**	Tallinn, Estonia
Subject	**MSc**, *de facto cum laude*, **Engineering Physics**	
Thesis	Propagation characteristics of nonstationary coherent optical waves in a stratified medium with Kerr nonlinearity	
Supervisors	**Prof. Yasuo Tomita**, ytomita@tmtv.ne.jp	
	Department of Electronics Engineering, University of Electro-Communications	Tokyo, Japan
	Dr. Pearu Peterson, pearu@cens.ioc.ee	
	Senior Researcher at IoC	Tallinn, Estonia

1998 — 2003	**Tallinn University of Technology**	Tallinn, Estonia
Subject	**BSc, Engineering Physics**	
Thesis	Influence of higher-order nonlinear effects on soliton formation	
Supervisor	Prof. Andrus Salupere, salupere@ioc.ee	
	Senior Researcher at IoC, Professor of Applied Mechanics, TUT	

Research experience

2007 — Present	**Institute of Cybernetics at TUT**	Tallinn, Estonia
	Laboratory of Systems Biology	
Supervisor	**Dr. Marko Vendelin**	

Isolation of cardiomyocytes, oxygraphic and spectrophotometric measurements, experimental investigation of various ATPases, mathematical modeling of ATP production and consumption processes. Programming data analysis tools.

2008 — 2010	**National Institute of Chemical Physics and Biophysics (NICPB)**	Tallinn, Estonia
	Bioenergetics Laboratory	
Supervisor	**Prof. Tuuli Käämbre**, tuuli.kaambre@kbfi.ee	

Curriculum Vitae

Using the laboratory of prof. Valdur Saks' Bioenergetics group to learn the experimental techniques of cardiomyocyte isolation, animal models and methods of biological experiment setup. Oxygraphic, spectrophotometric and HPLC measurements.

2003 — 2007	**Institute of Cybernetics at TUT**	Tallinn, Estonia
	Center of Excellence for Nonlinear Studies	
SUPERVISORS	**Prof. Andrus Salupere, Dr. Pearu Peterson**	

Numerical analysis of Korteweg de Vries equation using Matlab during BSc studies. Numerical simulations describing optical waves in grated material using Matlab and Phyton programming during MSc studies.

2004 — 2005	**University of Electro-Communications**	Tokyo, Japan
	Optics and Photonics Laboratory	
SUPERVISOR	**Prof. Yasuo Tomita**	

Numerical simulations of light propagation in optically induced photonic crystal grating. MSc project.

WORK EXPERIENCE

2007 — Present	**Institute of Cybernetics at TUT**	Tallinn, Estonia
	Laboratory of Systems Biology	
POSITION	**Researcher/PhD student**	

Coordinating the setup of new experimental laboratory facilities, preparing documentation for funding, paperwork to get licenses for performing animal experiments and permits for buying psychotropic drugs, writing grant proposals

2005 — 2007	**Swedbank**	Tallinn, Estonia
	Analysis and Sales Department	
POSITION	**Analyst**	

Distribution, analysing and reporting monthly costs to department heads, reporting weekly sales by different product groups, analysis and reporting of the private banking and private wealth management clients

2004 — 2005	**Chofu City Government**	Tokyo, Japan
POSITION	**English teacher**	

2003 — 2007	**Institute of Cybernetics at TUT**	Tallinn, Estonia
POSITION	**Engineer/MSc student**	

1999 — 2004	**Tere Dairy Company**	Tallinn, Estonia
	Sales Department	
POSITION	**Billing specialist**	

<div align="center">

Curriculum Vitae

</div>

SKILLS

Operating Systems	UNIX/Linux, Mac OS, Windows
Programming	Routine use of Python (scipy, numpy packages), experience with Matlab, Visual Basic, Maple
Tools	Emacs, Python visualisation(Matplotlib, PyX), LaTeX, Excel, version control tools
Certificates	Federation of Laboratory Animal Science Associations (FELASA) C-category competence certificate

EXPERIMENTAL EXPERIENCE

- Isolation of rat cardiomyocytes - Langerdorff perfusion system

- Oxygraphy - Oroboros Instruments, Srathkelvin Instruments

- Spectrophotometry - kinetic measurements and protein quantification

- Basic experience with fluorescence and confocal microscopy

SCHOLARSHIPS AND AWARDS

- Award for the best scientific publication of a young scientist at the Institute of Cybernetics at TUT for **ADP Compartmentation analysis reveals coupling between pyruvate kinase and ATPases in heart muscle**. Mervi Sepp, Heiki Vija, Marko Vendelin, Rikke Birkedal *Biophysical Journal*, 2010, **98**, 2785 - 2793

- Archimedes/DoRa travel grants for presenting at international conferences 2009, 2010, 2013

- TUT Development Fund, Tiina Mõis Scholarship, 2010

- Association of International Education Japan scholarship to participate in exchange program Japanese University Studies in Science and Technology at The University of Electro-Communications, 2004

PUBLICATIONS

- Jepihhina, Natalja; Beraud, Nathalie; Sepp, Mervi; Birkedal, Rikke; Vendelin, Marko (2011). **Permeabilized rat cardiomyocyte response demonstrates intracellular origin of diffusion obstacles.** *Biophysical Journal*, **101**, 2112 - 2121.

- Illaste, Ardo; Kalda, Mari; Schryer, David W.; Sepp, Mervi (2010). **Life of mice - development of cardiac energetics.** *The Journal of Physiology*, **588**, 4617 - 4619.

- Sepp, Mervi; Vendelin, Marko; Vija, Heiki; Birkedal, Rikke (2010). **ADP Compartmentation analysis reveals coupling between pyruvate kinase and ATPases in heart muscle.** *Biophysical Journal*, 98, 2785 - 2793.

Curriculum Vitae

2009	**53rd Biophysical Annual Meeting**	Boston, USA
Poster	Sepp M, Käämbre T, Sikk P, Vendelin M, Birkedal R.	
	Kinetic studies of intracellular compartmentalization in permeabilized rat cardiomyocytes	
2009	**36th International Congress of Physiological Sciences (IUPS2009)**	
		Kyoto, Japan
Poster	Sepp M, Käämbre T, Sikk P, Vendelin M, Birkedal R.	
	Kinetic studies of intracellular compartmentalization in permeabilized rat cardiomyocytes	
2010	**54th Biophysical Annual Meeting**	San Francisco, USA
Poster	Sepp M, Vendelin M, Vija H, Birkedal R	
	Analysis of intracellular ADP compartmentation reveals functional coupling between Pyruvate Kinase and ATPases In rat cardiomyocytes	
2011	**55th Biophysical Annual Meeting**	Baltimore, USA
Poster	Sepp M, Branovets J, Sokolova N, Kotlyarova S, Birkedal R, Vendelin M	
	Influence of SERCA and actomyosin ATPase on respiration kinetics in permeabilized rat cardiomyocytes	
2013	**57th Biophysical Annual Meeting**	Philadelphia, USA
Poster	Sepp M, Kotlyarova S, Vendelin M	
	Na/K ATPase affects respiration kinetics and provides evidence for intracellular diffusion restrictions in permeabilized rat cardiomyocyes	

Teaching

• Supervised Aleksander Klepinin's Bachelor thesis "Comparative analysis of inhibition of endogenous ADP stimulated respiration by pyruvate kinase (PK) and phosphoenolpyruvate (PEP) system in rat and rainbow trout cardiomyocytes", 2011

• Seminars for starting PhD students on basics of biochemistry, bioenergetics and biophysics, 2007-2010

• Giving training for starting PhD, MSc and BSc students on cell isolation and oxygraphic measurements

Extras

Languages	Estonian (mother tongue), English (C2), Finnish (C1), Portuguese (B2), French (B2), Japanese (A1), (CEFR levels)
Activities	Member of the Board of European Students of Technology Alumni (BEST). **Participated in the following BEST courses**:
2003	Valladolid, Spain, winter course: "Nonlinear effects and solitons in optical communications"
2003	Lisbon, Portugal, summer course : "Euro 2004 - Get into the challenge" **Organised BEST events**:
2004	Tallinn, Estonia, International BEST Symposium about the future of engineering education in Europe
2005	Tallinn, Estonia summer course:"For Greener Grass" about environmental assessment and ecotoxicology
Licenses	category B driver's license, boat driving license
Interests	calligraphy, ballet, painting, travelling

Elulookirjeldus

MERVI SEPP

ISIKUANDMED

SÜNNIAEG	4. veebruar, 1980
SÜNNIKOHT	Tallinn
KODAKONDSUS	Eesti
KONTAKT	✉ mervi@sysbio.ioc.ee

HARIDUSKÄIK

2006 — 2013   **Tallinna Tehnikaülikool**
ERIALA   **PhD, Tehniline füüsika**
LÕPUTÖÖ TEEMA   Difusioonitakistuste hindamine kardiomüotsüütides kasutades kineetilisi mõõtmisi
JUHENDAJA   **Dr. Marko Vendelin**, markov@sysbio.ioc.ee, +372 620 4169
Süsteemibioloogia labori juht, TTÜ Küberneetika Instituut (KübI)

2003 — 2006   **Tallinna Tehnikaülikool**
ERIALA   **MSc, Tehniline füüsika**
LÕPUTÖÖ TEEMA   Mittestatsionaarsete koherentsete optiliste lainete levi karakteristikud Kerri mittelineaarsusega kihilises keskkonnas.
JUHENDAJAD   **Prof. Yasuo Tomita**, ytomita@tmtv.ne.jp
Elektroenergeetika osakond, Elektro-kommunikatsiooni Ülikool
Tokyo, Jaapan
Dr. Pearu Peterson, pearu@cens.ioc.ee
KübI Vanemteadur

1998 — 2003   **Tallinna Tehnikaülikool**
ERIALA   **BSc, Tehniline füüsika**
LÕPUTÖÖ TEEMA   Kõrgemat järku mittelineaarsete efektide mõju solitonide formeerumisele
JUHENDAJA   Prof. Andrus Salupere, salupere@ioc.ee
KübI vanemteadur, Rakendusmatemaatika professor, TTÜ

TÄIENDUSÕPE

2003	Valladolid, Hispaania, talvekursus: "Nonlinear effects and solitons in optical communications"
2003	Lissabon, Portugal, suvekursus : "Euro 2004 - Get into the challenge"
2004	Tallinn, Eesti, Rahvusvaheline BEST sümpoosium Euroopa insenerihariduse tulevikust
2004-2005	Vahetusüliõpilane Elektro-kommunikatsiooni Ülikoolis Jaapanis
2005	Tallinn, Eesti suvekursus:"For Greener Grass" about environmental assessment and ecotoxicology

Elulookirjeldus

Eesti keel	emakeel	Inglise keel	kõrgtase
Soome keel	kesktase	Portugali keel	kesktase
Prantsuse keel	kesktase	Jaapani keel	baastase

TEADUSTÖÖ KOGEMUS

2007 — ... **TTÜ Küberneetika Instituut**
Süsteemibioloogia laboratoorium
JUHENDAJA **Dr. Marko Vendelin**

Kardiomüotsüütide isoleerimine, oksügraafilised ning spektromeetrilised mõõtmised, ATPaaside eksperimentaalne uurimine, ATP tootmis- ning tarbimisprotsesside matemaatiline modelleerimine, andmete analüüsi tarkvara programmeerimine.

2008 — 2010 **Keemilise ja bioloogilise füüsika instituut**
Bioenergeetika laboratoorium
JUHENDAJA **Prof. Tuuli Käämbre**, tuuli.kaambre@kbfi.ee

Katseloomatehnika aluste, bioloogiliste eksperimentaalmeetodite ning kardiomüotsüütide isoleerimise õppimine.

2003 — 2007 **TTÜ Küberneetika Instituut**
Mittelineaarsete uuringute teaduse tippkeskus
JUHENDAJAD **Prof. Andrus Salupere, Dr. Pearu Peterson**

Korteweg de Vries võrrandi numbriline lahendamine kasutades Matlabi bakalaureusetöö raames. Optilisi laineid kihilises keskonnas kirjeldavate võrrandite numbriline lahendamine kasutades Matlabi ning Pythonit magistritöö raames.

2004 — 2005 **Elektro-kommunikatsiooni Ülikool, Tokyo, Jaapan**
Optika ja fotoonika laboratoorium
JUHENDAJA **Prof. Yasuo Tomita**

Lainelevi optiliselt indutseeritud footonkristallides numbrilised simulatsioonid. Magistritöö projekt.

OSKUSED

Operatsioonisüsteemid	UNIX/Linux, Mac OS, Windows
Programmeerimine	Python (scipy, numpy paketid),
	Matlab, Visual Basic, Maple
	Emacs, Python graafika(Matplotlib, PyX), LaTeX, Excel,
Sertifikaadid	Federation of Laboratory Animal Science Associations (FELASA)
	C-kategooria kompetents

Elulookirjeldus

STIPENDIUMID JA AUTASUD

- TTÜ Küberneetika Instituudi aasta parim teaduspublikatsioon noorte kategoorias **ADP Compartmentation analysis reveals coupling between pyruvate kinase and ATPases in heart muscle**. Mervi Sepp, Heiki Vija, Marko Vendelin, Rikke Birkedal *Biophysical Journal*, 2010, **98**, 2785 - 2793

- Archimedes/DoRa stipendiumid rahvusvahelistel konverentsidel osalemiseks 2009, 2010, 2013

- TTÜ Arengufond, Tiina Mõisa Stipendium, 2010

- Jaapani valitsuse stipendium programmis Japanese University Studies in Science and Technology (JUSST) osalemiseks Elektro-kommunikatsiooni ülikoolis, Tokyos, Jaapanis, 2004

PUBLIKATSIOONID

- Jepihhina, Natalja; Beraud, Nathalie; Sepp, Mervi; Birkedal, Rikke; Vendelin, Marko (2011). **Permeabilized rat cardiomyocyte response demonstrates intracellular origin of diffusion obstacles.** *Biophysical Journal*, **101**, 2112 - 2121.

- Illaste, Ardo; Kalda, Mari; Schryer, David W.; Sepp, Mervi (2010). **Life of mice - development of cardiac energetics.** *The Journal of Physiology*, **588**, 4617 - 4619.

- Sepp, Mervi; Vendelin, Marko; Vija, Heiki; Birkedal, Rikke (2010). **ADP Compartmentation analysis reveals coupling between pyruvate kinase and ATPases in heart muscle.** *Biophysical Journal*, 98, 2785 - 2793.

ETTEKANDED RAHVUSVAHELISTEL KONVERENTSIDEL

2009	**53rd Biophysical Annual Meeting**	Boston, USA
POSTER	Sepp M, Käämbre T, Sikk P, Vendelin M, Birkedal R.	
	Kinetic studies of intracellular compartmentalization in permeabilized rat cardiomyocytes	
2009	**36th International Congress of Physiological Sciences (IUPS2009)**	
		Kyoto, Jaapan
POSTER	Sepp M, Käämbre T, Sikk P, Vendelin M, Birkedal R.	
	Kinetic studies of intracellular compartmentalization in permeabilized rat cardiomyocytes	
2010	**54th Biophysical Annual Meeting**	San Francisco, USA
POSTER	Sepp M, Vendelin M, Vija H, Birkedal R	
	Analysis of intracellular ADP compartmentation reveals functional coupling between Pyruvate Kinase and ATPases In rat cardiomyocytes	
2011	**55th Biophysical Annual Meeting**	Baltimore, USA
POSTER	Sepp M, Branovets J, Sokolova N, Kotlyarova S, Birkedal R, Vendelin M	
	Influence of SERCA and actomyosin ATPase on respiration kinetics in permeabilized rat cardiomyocytes	
2013	**57th Biophysical Annual Meeting**	Philadelphia, USA
POSTER	Sepp M, Kotlyarova S, Vendelin M	
	Na/K ATPase affects respiration kinetics and provides evidence for intracellular diffusion restrictions in permeabilized rat cardiomyocyes	

<h1 style="text-align:center">Elulookirjeldus</h1>

- Aleksander Klepinin'i bakalaureusetöö kaasjuhendaja. "Comparative analysis of inhibition of endogenous ADP stimulated respiration by pyruvate kinase (PK) and phosphoenolpyruvate (PEP) system in rat and rainbow trout cardiomyocytes", 2011

- Alustavate doktorantide baaskursused biokeemias, bioenergeetikas ja biofüüsikas, 2007-2010

- Doktorantide, magistrantide ning bakalaureusetudengite koolitamine rakkude isoleerimises ning oksügraafiliste mõõtmiste sooritamises

TEENISTUSKÄIK

2007 — ...	**TTÜ Küberneetika Instituut**
	Süsteemibioloogia laboratoorium
AMETIKOHT	**Teadur/doktorant**

Bioloogiliste eksperimentide teostamiseks vajaliku baaslabori käimalükkamine koos labori sisseseade ning mõõteriistade hankimise, finantseerimisaruandluse ning loomkatsete teostamiseks vajalike eetikakomisjoni lubade ning psühhotroopsete medikamentide ostuõiguste vormistamisega.

2005 — 2007	**Swedbank**
	Müügi- ja analüüsiosakond
AMETIKOHT	**Analüütik**

Distributsioonianalüüs, igakuine kuluaruannete koostamine osakondade lõikes, nädala müüginumbrite analüüs ning raporteerimine, privaatpanganduse ning varahalduse kliendiaruanded.

2004 — 2005	**Chofu linnavalitsus, Tokyo, Jaapan**
AMETIKOHT	**Inglise keele õpetaja**

2003 — 2007	**TTÜ Küberneetika Instituut**
AMETIKOHT	**Insener/magistrant**

1999 — 2004	**Tere AS**
	Müügiosakond
AMETIKOHT	**Arvete koostaja**

APPENDIX

Sepp M, Vendelin M, Vija H, Birkedal R

ADP Compartmentation Analysis Reveals Coupling between Pyruvate Kinase and ATPases in Heart Muscle.

ADP Compartmentation Analysis Reveals Coupling between Pyruvate Kinase and ATPases in Heart Muscle

Mervi Sepp,[†] Marko Vendelin,[†]* Heiki Vija,[‡] and Rikke Birkedal[†]*

[†]Laboratory of Systems Biology, Institute of Cybernetics, Tallinn University of Technology, Tallinn, Estonia; and [‡]Laboratory of Bioorganic Chemistry, National Institute of Chemical Physics and Biophysics, Tallinn, Estonia

ABSTRACT   Cardiomyocytes have intracellular diffusion restrictions, which spatially compartmentalize ADP and ATP. However, the models that predict diffusion restrictions have used data sets generated in rat heart permeabilized fibers, where diffusion distances may be heterogeneous. This is avoided by using isolated, permeabilized cardiomyocytes. The aim of this work was to analyze the intracellular diffusion of ATP and ADP in rat permeabilized cardiomyocytes. To do this, we measured respiration rate, ATPase rate, and ADP concentration in the surrounding solution. The data were analyzed using mathematical models that reflect different levels of cell compartmentalization. In agreement with previous studies, we found significant diffusion restriction by the mitochondrial outer membrane and confirmed a functional coupling between mitochondria and a fraction of ATPases in the cell. In addition, our experimental data show that considerable activity of endogenous pyruvate kinase (PK) remains in the cardiomyocytes after permeabilization. A fraction of ATPases were inactive without ATP feedback by this endogenous PK. When analyzing the data, we were able to reproduce the measurements only with the mathematical models that include a tight coupling between the fraction of endogenous PK and ATPases. To our knowledge, this is the first time such a strong coupling of PK to ATPases has been demonstrated in permeabilized cardiomyocytes.

INTRODUCTION

The viewpoint that the cell is a well mixed reactor is being replaced by the understanding that metabolic regulation depends not only on enzyme kinetics, but also on the location and colocalization of enzymes and substrates. Thus, metabolism can be considered as a network of metabolic modules, which are spatially compartmentalized to optimize energetic communication between energy-producing and energy-consuming parts of the cell (1). It has been suggested that compartmentalization of adenosine nucleotides (ADP and ATP) by intracellular diffusion restrictions plays a vital role in regulation of heart energetics (2). In rat heart, the apparent magnitude of diffusion restrictions increases during ontogeny (3) and is diminished by ischemia-reperfusion damage of the tissue (4). Similar diffusion restrictions have been identified in cardiomyocytes of ectothermic vertebrates (5) and have been found to depend on acclimation conditions in turtles (6). In comparison, cultured cardiomyocytes, which do not contract against a workload and depend more on glycolytic than aerobic metabolism, have almost no diffusion restrictions (7). Taken together, this suggests that the magnitude of diffusion restrictions is closely related to cardiac mechanical performance and aerobic capacity.

Permeabilized heart muscle fibers or permeabilized isolated cardiomyocytes have been extensively used to study the diffusion restrictions that compartmentalize the intracellular environment (8–12). In those studies, several approaches have indicated that the diffusion of ATP and ADP from the solution surrounding the cells to the adenine nucleotide translocase in the inner mitochondrial membrane is restricted by the mitochondrial outer membrane as well as in the cytosol. According to our models, the cytosolic diffusion restrictions leading to intracellular compartmentalization and functional coupling between ATP-consuming and ATP-producing organelles are most probably localized in certain areas of the cell (12,13). The high level of diffusion restrictions indicates that they are formed by cytoskeleton proteins (14), leading, together with the intracellular organization of mitochondria and sarcoplasmic reticulum (SR), to anisotropic diffusion of molecules (15).

Most of the studies pointing to diffusion restrictions between solution and intracellular environment have been made on permeabilized heart muscle fibers (10,11,16). The results from these studies have also been used as input for mathematical models (12–14). However, fiber preparations can be heterogeneous in terms of diffusion distance, as compared to a suspension of permeabilized cardiomyocytes. As a result, the use of cardiomyocytes to study intracellular energy transfer has increased recently (5,17,18). However, a systematic study of intracellular diffusion patterns is needed for input into mathematical models. This study was undertaken to fill the void of data on intracellular energy transfer recorded on permeabilized cardiomyocytes and to use this data set for analysis with a simple mathematical model.

The aim of this work was to analyze the intracellular diffusion of ATP and ADP in rat cardiomyocytes. To do this, we refined the method used previously to isolate rat cardiomyocytes to obtain a high yield of Ca^{2+}-tolerant cells that would contract upon electrical field stimulation. Intracellular energetic communication between mitochondria and ATPases was approached from several angles, including determination of respiration rate, ADP concentration in media, and ATPase rate under several conditions. The data were analyzed using mathematical models that reflect different levels of compartmentalization of the cell.

MATERIALS AND METHODS

Experimental procedures

Adult outbred Wistar rats of both sexes weighing 300–500 g were used in the experiments. Animal procedures were approved by the Estonian National Committee for Ethics in Animal Experimentation (Estonian Ministry of Agriculture).

Experiments

Isolation of cardiomyocytes is described in the Supporting Material. All recordings on permeabilized cardiomyocytes were performed in Mitomed solution (see composition below) at 25°C. The oxygen solubility factor for the solution was calculated as described previously (19). Respiration was recorded in a high-resolution respirometer (Oroboros Oxygraph, Paar KG, Innsbruck, Austria). For ADP and ATP kinetics, the concentrations of ADP and ATP, respectively, were increased in a stepwise manner. The effect of activating a competitive ADP trap consisting of pyruvate kinase (PK) and phosphoenolpyruvate (PEP) was assessed in two ways: first, as has been done earlier (12), with PEP in the solution from the beginning of the experiments (see Fig. 2 C), and second, with PEP and exogenous PK added consecutively after stimulation with 2 mM ATP (see Fig. 2 D). ATPase activity was assessed spectrophotometrically (Evolution 600, Thermo Scientific, Waltham, MA) using a coupled enzyme system (13) with 0.3 mM nicotinamide adenine dinucleotide (NADH), 5 mM PEP, 7.2 U/ml lactate dehydrogenase (LDH) and 20 U/ml PK added to the Mitomed solution. These experiments were performed with 5 mM NaCN and 10 μM oligomycin to inhibit mitochondrial respiration and ATP synthase. Endogenous PK activity was recorded in a similar manner, in the presence of NaCN and oligomycin, and with 5 mM PEP, 0.3 mM NADH, and 7.2 U/ml LDH added to the Mitomed solution. To assess the activity of ATPases and their interaction with mitochondria in the absence of PK, the release of ADP into the surrounding medium after stimulation of ATPases with a single dose of 2 mM ATP was analyzed as a function of time using the high-performance liquid chromatography method described in Sikk et al. (20). This was done with and without oxidative phosphorylation inhibited by 5 mM NaCN and 10 μM oligomycin. Samples were taken out 0, 1, 2, 4, 6, 10, and 18 min after stimulation of ATPases with 2 mM ATP.

For each cell suspension, protein concentration was determined with the Pierce BCA Assay Kit (Thermo Scientific) according to the manufacturer's instructions. Knowing the volume of cell suspension added to each experiment allowed us to normalize the rates to milligrams of protein.

Solutions

Solutions used in this work are listed in the Supporting Material.

Statistics

The raw data were analyzed using homemade software. All results are shown as mean ± SD.

Biophysical Journal 98(12) 2785–2793

Mathematical model

We used four different model versions to reproduce the experimental data (Fig. 1). In all models, several compartments were considered. In the simpler versions, models 1 and 2 (Fig. 1, *schemes 1* and *2*), three compartments were included: solution, cytosol, and intermembrane space (IMS). In models 3 and 4, an additional compartment (compartment 4 (C4)) was added to fit the measurements more effectively (Fig. 1, *schemes 3* and *4*). Diffusion between two compartments was assumed to be proportional to the difference in concentrations in those compartments multiplied by the exchange coefficient (*C*). In this work, diffusion between the following compartments (Fig. 1, *double-headed arrows*) was considered: solution and cytosol (Fig. 1, *schemes 1–4*, *sol-cyt*); IMS and cytosol (Fig. 1, *schemes 1–4*, *MoM*); cytosol and C4 (Fig. 1, *scheme 3*, *cyt-C4*); IMS and C4 (Fig. 1, *scheme 4*, *IMS-C4*). The reactions included in the models were ATP synthesis by mitochondrial oxidative phosphorylation (ATPsyn), ATP consumption by ATPases (depending on the model, ATPase, ATPase1, or ATPase2), ATP synthesis by endogenous PK (PKend, PKend1, or PKend2), and ATP synthesis by exogenously added PK (PK). Reactions are indicated by single-headed arrows in Fig. 1 and localized in their corresponding compartments. The reactions were described by simplified Michaelis-Menten kinetics with the apparent kinetic constants V_{max} and K_m. ATPases were considered to be inhibited competitively by ADP (apparent inhibition constant denoted by $K_{iATPase}$).

As shown in Fig. 1, *scheme 1*, model 1 is the simplest of the models and includes only ATPsyn, ATPase, and exogenous PK. This model is similar to those used previously to describe intracellular fluxes in permeabilized cardiac muscle fiber (12,13). Model 2 is based on model 1, with ATPase activity split into two fractions with the different apparent kinetic constants and addition of endogenous PK activity (Fig. 1, *scheme 2*). Models 3 and 4 are based on model 2, but with the addition of C4, which contains part of ATPase and endogenous PK activity (Fig. 1, *schemes 3* and *4*). The only difference between models 3 and 4 is that the connection of C4 to the rest of the cell is via cytosol in model 3 and via IMS in model 4.

Such modifications of the base model (model 1) were based on the comparison of model solution with the experimental data. Justification of these modifications is given below, together with the description of the modeling results.

Detailed description of the models, fitting procedures, numerical methods, and statistical analysis of the model fits is presented in the Supporting Material.

RESULTS

Experimental results

The experiments were set up in a manner similar to that of earlier studies of intracellular diffusion restrictions (12,13), the main difference being that these experiments were conducted on isolated permeabilized cardiomyocytes instead of fibers.

We recorded the mitochondrial respiration rate at different concentrations of ADP and ATP (representative traces shown in Fig. 2, *A* and *B*). The respiration rate after addition of substrates and before addition of ADP or ATP (V_0) was 12.1 ± 1.5 and 10.8 ± 1.6 nmol O_2/(min mg prot), respectively. Addition of 2 mM ADP or ATP increased respiration to 105 ± 23 and 27 ± 5 nmol O_2/(min mg prot), respectively, above V_0. Thus, respiration rates recorded with 2 mM ADP (V_{2mMADP}) or ATP were 117 ± 27 and 37.6 ± 6.1 nmol O_2/(min mg prot), respectively. The dependence of the increase is shown in Fig. 3, *A* and *B* (*open circles*). The acceptor control ratio, defined here as V_{2mMADP}/V_0, was 9.7.
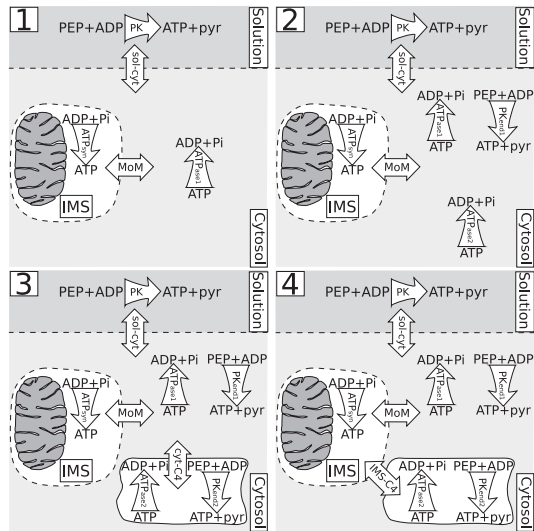
FIGURE 1 Models of permeabilized cardiomyocytes considered in this work. In the schemes, reactions are shown by curved arrows; exchange between compartments is indicated by straight arrows. The level of complexity increases from model 1 to models 3 and 4. All models have compartments representing solution, cytosol, and mitochondrial IMS. In models 3 and 4, an additional compartment was added (*C4*). The reactions considered in this work are ATP synthesis by mitochondria (*ATPsyn*), ATP consumption by ATPases (*ATPase, ATPase1, ATPase2*), and ATP synthesis by endogenous PK (*PKend, PKend1, PKend2*) and by exogenously added PK (*PK*). Compartment exchanges occurred between solution and cytosol (*sol-cyt*); IMS and cytosol through mitochondrial outer membrane (*MoM*); cytosol and C4 (*cyt-C4*); and IMS and C4 (*IMS-C4*).

In addition to the respiration kinetics, we recorded how mitochondrial respiration stimulated by endogenous ADP produced by ATPases upon addition of 2 mM ATP was affected by addition of an ADP trapping system consisting of PK and PEP. In the beginning, the experiments were performed in a manner similar to that used in an earlier study on fibers (12), where the cells were added to Mitomed solution that already contained 5 mM PEP. A typical trace is shown in Fig. 2 *C*. However, we were surprised to find that stimulation of respiration by addition of 2 mM ATP increased respiration rate by only 16.7 ± 5.3 nmol O_2/(min mg prot) ($n = 11$). Addition of 20 U/ml PK decreased the respiration rate to 7.4 ± 1.9 nmol O_2/(min mg prot) above V_0, leaving $45.6 \pm 9.8\%$ of the respiration rate. This is similar to the inhibition ratio reported earlier in fibers (12). However, with PEP already present in the Mitomed solution, the extent of stimulation of respiration by addition of 2 mM ATP was considerably smaller than that obtained by ATP titration, indicating the presence of endogenous PK competing for endogenously produced ADP. Indeed, when PEP was not present in Mitomed at the beginning of the experiments (Fig. 2 *D*), stimulation of respiration with 2 mM ATP increased respiration rate by 32.2 ± 3.6 nmol O_2/(min mg

prot) ($n = 11$), similar to stimulation during ATP titration. The addition of PEP alone brought respiration down to 10.2 ± 2.1 nmol O_2/(min mg prot) above V_0, and subsequent addition of 20 U/ml PK brought it down further, to 5.3 ± 1.9 nmol O_2/(min mg prot) above V_0. These rates in the presence of PEP and PK are slightly lower than when PEP was already present in the medium due to a time-dependent decrease in ATP-stimulated respiration (see representative traces in Fig. 2, *C* and *D*). Thus, when taking the effect of endogenous PK into account, it is possible to reduce ATP-stimulated respiration by ~80% through addition of PEP and exogenous PK.

The activity of endogenous PK was assessed spectrophotometrically (Fig. 2 *E*) and was found to be relatively high, with average kinetics shown in Fig. 3 *D* (*open circles*).

The activity of ATPases was measured spectrophotometrically to complement the recordings of respiration rate stimulated by ATP. In these experiments, mitochondrial respiration was inhibited. A representative example is shown in Fig. 2 *F*. The average kinetics is shown in Fig. 3 *C* (*open circles*). Note that the activity of ATPases reached 413 ± 102 nmol/(min mg prot) after addition of 2 mM ATP. Assuming an ATP/O_2 ratio equal to 6, that should correspond to a respiration rate of ~69 nmol O_2/(min mg prot), i.e., much higher than the rate recorded in the oxygraph (Fig. 3 *B*). This suggests that some of the ATPases in our preparation were active only in the presence of an active PK system (see below for analysis).

To get additional information for the further analysis, we used high-performance liquid chromatography to measure ADP concentration in solution after addition of 2 mM ATP in the presence and absence of oxidative phosphorylation (OxPhos) (Fig. 3, *E* and *F*, *open circles*). Due to a small fraction of ADP in the injected ATP, the concentration of ADP was 0.031 ± 0.018 mM at the beginning of the experiment. This concentration increased, and if the OxPhos was not inhibited, it reached 0.063 ± 0.022 mM after 18 min. The increase was much more profound if OxPhos was inhibited, leading to ADP concentrations in solution reaching 0.193 ± 0.053 mM after 18 min.

In the analysis of the measurements presented below, the contribution of adenylate kinase (AK) has been ignored. To estimate the contribution of AK, we performed a series of experiments in which respiration rate in permeabilized cells was stimulated by exogenous ADP (as in Fig. 2 *A*). Experiments were performed in parallel with and without inhibition of AK by 0.01 mM diadenosine pentaphosphate (Ap5A). As a result, we observed that the increase of respiration rate above V_0 was 1.09 ± 0.09 times higher when AK was inhibited compared to the control case ($n = 5$ experiments, significantly different from 1, with $p < 0.001$). Here, the increases in rate observed at all concentrations used were averaged. More specifically, such a difference was observed at all concentrations of ADP >0.2 mM (0.2–3.0 mM, with the increase in respiration rate varying from 1.05 to 1.09).
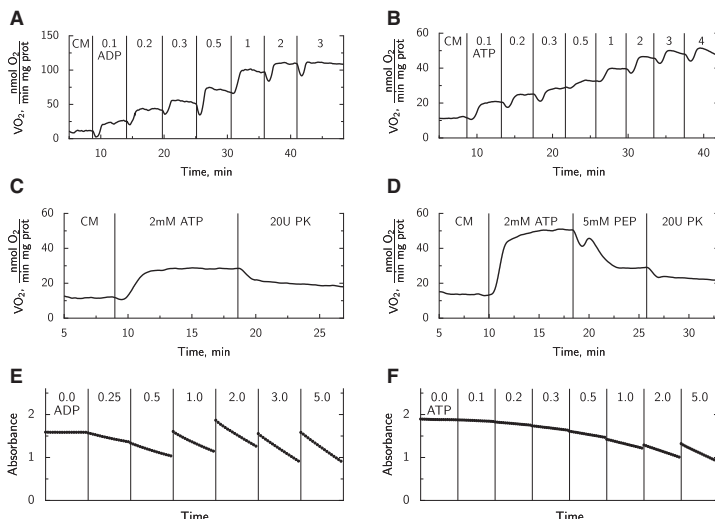
FIGURE 2 Representative examples of individual experiments performed in this work. Vertical lines indicate the time moment when solution was changed by injecting ATP, ADP, PK, or PEP. (*A* and *B*) Respiration rates recorded during titration with ADP (*A*) and ATP (*B*). First, cardiomyocytes (*CM*) were added (moment of addition not shown) and then successive additions of ADP or ATP were performed to reach the concentrations indicated. (*C* and *D*) Inhibition by PK+PEP system. In *C*, 5 mM PEP was in solution before the experiment began. In *D*, the effects of addition of 5 mM PEP and 20 U/ml PK are demonstrated. (*E* and *F*) Mitochondrial respiration was inhibited by cyanide and oligomycin, as shown by ADP dependency of endogenous PK assessed spectrophotometrically (*E*) and ATPase activity of cardiomyocytes assessed by titration with ATP (*F*). In these experiments, NADH was sometimes replenished, leading to an increase in absorbance.

When measured at an ADP concentration equal to 0.1 mM, the increase was somewhat higher (1.19 ± 0.17, $n = 5$, not significantly different from 1, with $p = 0.07$). From those measurements, we conclude that by not incorporating AK into the models, we ignore ~10% of the flux.

Analysis by mathematical models

In this work, we considered four models with different levels of complexity and tried to fit the experimental data with them. In all models, the studied system was viewed as consisting of different compartments. For simplicity, diffusion within each of the compartments was assumed to be fast. This allowed us to describe the intracellular diffusion restrictions only through exchange between compartments. The extent of the diffusion restriction was given in the exchange coefficient: the smaller the exchange coefficient, the larger the diffusion restriction between compartments.

We started our analysis with the simplest possible scheme (Fig. 1, *scheme 1*), which would correspond to models considered previously that describe intracellular fluxes in cardiac muscle fibers (12,13). As is clear from the fitting results (Fig. 3 and Table 1), there are several problems with this scheme. For instance, there is no consideration of endogenous PK, and as a result, neither kinetics of endogenous PK (Fig. 3 *D*; model 1 solution is zero) nor inhibition of respiration via endogenous PK (Table 1) can be fitted. In addition, the calculated ATPase activity measured with OxPhos inhibited is considerably lower than that measured experimentally (Fig. 3 *C*).

To improve the fit, we considered a more complicated model (Fig. 1, *scheme 2*). First, we added an endogenous PK reaction into the system. Second, we split the ATPase activity into two reactions with different kinetics. The exis-

tence of two different ATPases was suggested on the basis of the differences in ATPase activity depending on whether ATP was regenerated intracellularly by OxPhos or by PK. Indeed, model 2 is able to fit the data much better. The main problem with the model 2 fit is that there is no difference in inhibition of OxPhos by simple addition of PEP or PEP together with PK (Table 1). The simulations performed using this model lead to relatively low values of ATPase activity when measured in the presence of PK+PEP (Fig. 3 *C*) and relatively high ATPase activity when measured in the presence of OxPhos (Fig. 3 *B*). Thus, the model is not able to reproduce the differences in those measurements very well. In addition, the kinetics of endogenous PK is fitted relatively poorly, due to the small apparent K_m(ADP) value of endogenous PK found by the model (Table 2).

For further improvement of the fit, an additional compartment was introduced (C4) and connected via exchange either with cytosol (model 3) or mitochondrial IMS (model 4). The motivation for such a modification was that the experimental data suggested functional coupling between PK and ATPases. The schemes corresponding to models 3 and 4 are shown in Fig. 1. As is clear from the results shown in Fig. 3 and Table 1, both of these models are able to reproduce all the experimental results quite well. The best fit was obtained by almost isolating C4 from the rest of the solution (see the corresponding exchange coefficients in Table 2). Thus, ATPases in C4 were activated only in the case where local ATP was supplied by PK in the same compartment. Note that, as discussed below, the parameter values found for ATPases in C4 should be considered phenomenological only and suggest a tight functional coupling between some ATPases and endogenous PK in permeabilized rat cardiomyocytes.
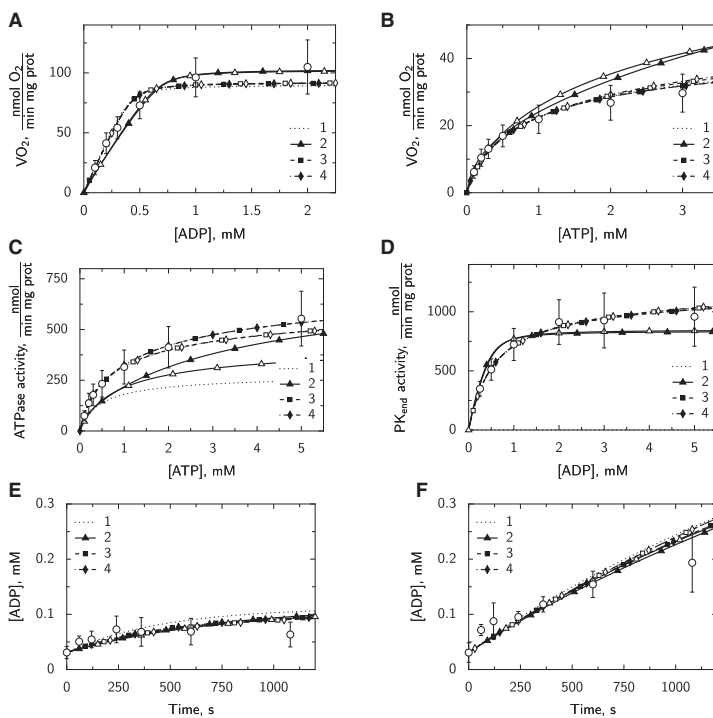
FIGURE 3 Experimental data (*open circles*, mean ± SD) are compared to the solutions using models 1 (*dotted line*) and 2–4 (*lines with solid symbols*). The fits obtained using the simplified versions of the models are indicated by the lines with the corresponding open symbols. The fitted experimental data were respiration rate recorded during titration with ADP (*A*; $n = 10$) or ATP (*B*; $n = 8$); endogenous ATPase (*C*; $n = 9$) and PK activities (*D*; $n = 7$) measured spectrophotometrically; and ADP concentration dependence on time in the presence (*E*; $n = 5$) or absence (*F*; $n = 5$) of oxidative phosphorylation. Note that in all cases, the lines corresponding to models 3 and 4 are very close to each other, leading to the formation of a single dashed line. In addition, since there is no endogenous PK activity in model 1, the rate of PK_{end} calculated by model 1 is zero in *D*.

In models 2–4, we used two sets of apparent affinities for two ATPase fractions (ATPase 1 and 2). To see whether one set of affinities would be sufficient to fit the data, we repeated the simulations using the simplified versions of models 2–4. In those simulations, apparent affinities of ATPases 1 and 2 were either the same (simplified versions of models 3 and 4) or only one ATPase was considered (simplification of model 2). The results of the fitting by the simplified models are shown in Tables 1 and 2 and in Fig. 3, with the simplified models denoted as 2s, 3s, and 4s. As is clear from the simulation results, the fits using the simplified model versions were similar to those using the corresponding full models (see below for statistical analysis).

As expected, the best fits were obtained using the most complicated models. This could be due to the larger degrees of freedom in those models compared to the simpler ones. To test whether the simpler model was correct and the larger deviation was induced by chance, an F-test of nested models can be used in which the fits of two models are compared.

Here, the models are considered nested if the simpler version of the model can be obtained from the more complicated model by selecting particular values of model parameters. Thus, models 3 and 3s cannot be compared with 4 and 4s, since those models are not nested into each other. The results of the test are shown in Table 3. Each model (*rows*) is compared with the more complicated version (columns) and the *p*-value calculated by the F-test is shown. For *p*-values <0.05, we conclude that the fit obtained by the more complicated model was significantly better than that obtained by the simpler model, and there is sufficient evidence to reject the simpler version of the model. According to our analysis, the addition of C4 was necessary, and it improved the fit significantly. From the comparison of the fits produced by models 2–4, we conclude that the models without C4 can be rejected, since the probability is very small ($p < 0.001$) that model 2 is correct and the differences in fit can be explained by random scatter in the data. According to our analysis, models 3s and 4s give the best results.

TABLE 1 Respiration rate stimulated by endogenous ATPases and inhibited by PK

	Experimental	1	2s	2	3s	3	4s	4
VO₂(PEP), nmol/min mg prot	16.7 ± 5.3	28.89	8.11	8.37	15.08	15.12	14.80	15.12
VO₂(PEP+PK), nmol/min mg prot	7.4 ± 1.9	6.51	7.16	7.48	7.70	7.60	7.69	7.60

Respiration rate was stimulated by endogenous ATPases and inhibited by endogenous PK (VO₂(PEP)) only or together with exogenously added 20 U/ml PK (VO₂(PEP+PK)). The experimental data are compared with the simulation results obtained by the full models 1, 2, 3, 4 and their corresponding simplified versions (2s, 3s, and 4s). Endogenous ATPases were stimulated by 2 mM ATP and PK was activated by 5 mM PEP added to solution.

TABLE 2   Model parameters found by fitting the experimental data

Parameter	Model 1	2s	2	3s	3	4s	4
$V_{maxATPsyn}\left(\frac{nmol}{min \cdot mg\ prot}\right)$	540	614	618	554	552	554	552
	154–1317	291–1133	262–1263	349–844	338–861	348–846	338–861
$c_{sol-cyt}\left(\frac{1}{mM}\frac{nmol}{min \cdot mg\ prot}\right)$	7385	1540	1542	3799	4213	3689	4215
	1031–>10^6	727–3551	634–4468	1473–18984	1519–28658	1430–18399	1520–28631
$c_{MoM}\left(\frac{1}{mM}\frac{nmol}{min \cdot mg\ prot}\right)$	1651	2109	1915	1893	1833	1913	1833
	574–5516	1099–4137	936–3835	1187–3125	1135–3038	1190–3194	1135–3038
$c_{IMS-C4}\left(\frac{1}{mM}\frac{nmol}{min \cdot mg\ prot}\right)$						15	0.087
						0.015–66	0.006–65
$c_{cyto-C4}\left(\frac{1}{mM}\frac{nmol}{min \cdot mg\ prot}\right)$				9.63	0.108		
				0.013–57	0.007–79		
$V_{maxATPase1}\left(\frac{nmol}{min \cdot mg\ prot}\right)$	276	506	2632	239	268	233	268
	141–434	354–679	1283–4331	183–298	205–337	176–293	205–337
$K_{mATPase1}$ (mM)	0.349	0.793	10	0.381	0.346	0.378	0.346
	0.099–1.29	0.493–1.36	5.89–>10	0.233–0.628	0.199–0.611	0.231–0.625	0.199–0.611
$K_{iATPase1}$ (mM)	0.051	0.05	0.05	0.069	0.05	0.066	0.05
	<0.05–>10	<0.05–0.1	<0.05–0.112	<0.05–0.247	<0.05–0.169	<0.05–0.22	<0.05–0.168
$V_{maxATPase2}\left(\frac{nmol}{min \cdot mg\ prot}\right)$			68	483	447	452	447
			7.73–130	109–2051	102–912	112–1498	101–914
$K_{mATPase2}$ (mM)			0.056		1.05		0.95
			<0.05–2.63		0.323–8.45		0.29–7.69
$K_{iATPase2}$ (mM)			0.05		0.051		0.051
			<0.05–>10		<0.05–>10		<0.05–>10
$V_{maxPKend1}\left(\frac{nmol}{min \cdot mg\ prot}\right)$		849	838	796	771	780	771
		513–1298	471–1346	477–1139	456–1111	460–1124	456–1111
K_{mPKend} (mM)		0.053	0.047	0.396	0.33	0.385	0.33
		<0.01–0.178	<0.01–0.2	0.191–0.839	0.123–0.844	0.181–0.832	0.123–0.843
$V_{maxPKend2}\left(\frac{nmol}{min \cdot mg\ prot}\right)$				471	2268	528	2246
				108–1836	96–>7200	115–2585	98–>7200

The parameter values found by fitting are shown above the confidence interval for each model parameter.

Indeed, all models that are simpler than those models lead to a significantly worse fit. However, the addition of further degrees of freedom is not justified on the basis of our data ($p > 0.05$). Thus, there is no sufficient evidence for using different apparent kinetic constants of ATPases in C4 and cytosol (the difference between models 3 and 4 and their simplified versions 3s and 4s).

A similar conclusion was reached if corrected Akaike information criteria (AICc) and Bayesian information criteria (BIC) were calculated for the models (Table 3). According to those criteria, the best models (with the smallest values of AICc and BIC) are 3s and 4s.

To check the sensitivity of the model fits to the changes of model parameters, the confidence intervals were estimated (see Supporting Material). The confidence intervals are shown in Table 2 as a range, below the optimal value for each model parameter. As is clear from Table 2, some model parameters do not influence the model solution significantly. For example, ATPase apparent inhibition constants ($K_{iATPase}$) can be changed in a wide range.

DISCUSSION

The experimental results presented in this work cover multiple aspects of energy transfer in isolated permeabilized rat cardiomyocytes. From the analysis of the experimental data, we were able to identify compartmentalization of ATPases and the exchange coefficients for movement of

TABLE 3   Statistical analysis of model fits. See text for description

Model	AIC	AICc	BIC	F test 2s	2	3s	3	4s	4
1	74.30	76.70	207.54	<0.001	<0.001	<0.001	<0.001	<0.001	<0.001
2s	15.31	19.68	71.22		0.333	<0.001	<0.001	<0.001	<0.001
2	16.77	25.57	78.20				<0.001		<0.001
3s	−16.73	−7.93	57.82				0.272		
3	−16.50	−3.50	63.86						
4s	−16.10	−7.30	58.07						0.218
4	−16.51	−3.51	63.85						

ATP and ADP between the compartments. In addition, the obtained results point to strong coupling between endogenous pyruvate kinase and ATPases in cardiac muscle cells. This conclusion was reached on the basis of statistical analysis of the fits by models with different levels of complexity. To our knowledge, this is the first time such a coupling has been identified in permeabilized cardiomyocytes.

The experimental results obtained in this work are in agreement with earlier studies. As has been shown earlier, diffusion restrictions between solution surrounding the permeabilized cardiomyocytes and adenine nucleotide translocase lead to an apparent Km(ADP) of OxPhos that is much higher than that for isolated mitochondria (9). A similar conclusion was obtained for permeabilized fibers. In fibers, oxidative phosphorylation was inhibited by 40–60% upon addition of exogenous PK (10,11). In this work, when PEP was present in solution at the beginning of the experiment (Fig. 2 C), a similar inhibition was obtained. Stimulation of respiration by endogenous ATPases upon addition of 2 mM ATP was also similar to that reported by others for permeabilized rat cardiomyocytes (17). In the presence of OxPhos, the concentration of ADP in solution (Fig. 3 E) was similar to values recorded in experiments on permeabilized fibers from rat (10) and ectothermic vertebrates (8) and somewhat higher than values reported for rat by Seppet et al. (11). Finally, PK activity recorded in this work is the same as that recorded by Monge et al. (18). At an ADP concentration of 1.2 mM, activity of 637 ± 69 nmol/(min mg prot) was reported (18), similar to our measurements (Fig. 3 D). Thus, our results for permeabilized cardiomyocytes are similar to those of others.

Cardiomyocytes are an excellent preparation for studying intracellular compartmentalization due to the homogeneous nature of the preparation. Fibers may bundle together and, due to the variation in diameter, the diffusion distance between solution and mitochondria may vary. However, it is intriguing that in permeabilized rat cardiomyocytes, the increase in respiration rate above V_0 by addition of 2 mM ATP was only 30% of that obtained by stimulating with 2 mM ADP. In contrast, in permeabilized rat fibers, the increase of respiration rate above V_0 after addition of 2 mM ATP was ~75% of the maximal respiration rate obtained by stimulation with ADP (12). It remains uncertain what causes this discrepancy between fibers and cardiomyocytes. The preparation of cardiomyocytes is a relatively complicated process and requires a large amount of tuning to obtain large populations of rod-shaped and calcium-tolerant cells (>75% of the total population in this work). It is possible that something happens to cardiomyocytes during the isolation procedure that affects the ATPases, but further studies and variations of the cardiomyocyte isolation protocol are required to understand this phenomenon.

The main difference between results reported previously and those presented in this work is that we found a significant effect of endogenous PK on ATPases. Namely, we found that some of the ATPases are not activated unless ATP is provided via PK. As we argue below, this indicates functional coupling between those ATPases and PK. In addition, we have shown that endogenous PK is an effective OxPhos competitor for endogenously produced ADP. This finding was possible because of a change in the procedure that allowed us to account for endogenous PK. Indeed, endogenous PK alone (activated upon addition of PEP) is able to inhibit OxPhos stimulated by exogenous ATP by 50–70% (Fig. 2 D and Table 1). Such effects of endogenous PK have not been reported previously in studies of energy transfer in permeabilized cardiomyocytes or muscle fibers.

The analysis of our experimental data clearly shows the existence of a fraction of ATPases that are activated only in the presence of endogenous ATP generated by PK. Indeed, only models 3 and 4 (Fig. 1, schemes 3 and 4) and their corresponding simplified versions (3s and 4s) were able to reproduce the data very well. In those models, an additional compartment with ATPase and PK activity (C4) was introduced, and this compartment was quite isolated from the rest of the cell. The exchange coefficient for movement of ATP and ADP into or out of that compartment was found to be <1 nmol/(mM min mg prot). Compared to the exchange constant describing the movement through mitochondrial outer membrane (~1900 nmol/(mM min mg prot)), it is clear that there is almost no significant movement from or to C4 during the steady state. Such a low exchange coefficient is analogous to the exchange coefficient values in the phenomenological models of creatine kinase (CK) and adenine nucleotide translocase (ANT) coupling (21). As in the case with CK-ANT models, the model of C4 presented here should be considered only as a phenomenological description of the coupling between the glycolytic system represented by PK and some of the ATPases. For a mechanistic description, full kinetic analysis should be done, and several mechanisms of the coupling should be considered, as has been done for CK-ANT (22). Only after such analysis, when the mechanism of the coupling is identified, can meaningful exchange coefficients be derived. Right now, the values obtained by models 3, 3s, 4, and 4s should be considered only as a strong indication of functional coupling between PK and ATPases in permeabilized rat cardiomyocytes.

Until it becomes clear which ATPases are not active in cardiomyocytes without ATP supplied by PK, and why there is a difference between ATP-stimulated respiration rates recorded in fibers and cardiomyocytes, it will be hard to estimate the extent of diffusion restrictions in the cell. Indeed, the models that include functional coupling between PK and ATPases (C4 in models 3, 3s, 4, and 4s) predict relatively modest diffusion restriction for ATP and ADP induced by intracellular structures. However, in our experiments, a large fraction of ATPases was active only in the presence of an active PK system. In experiments performed on fibers, on the other hand, the situation is different. As discussed

above, respiration rate was activated by ATP much more in fibers than in the cardiomyocyte preparations in this study. This suggests that in fibers, most of ATPases are active without PK-supplied ATP, whereas this is not the case for cardiomyocytes. Alternatively, fibers could have higher ATPase activity than cardiomyocytes. As a result, diffusion is predicted to be relatively restricted when the fiber data are analyzed (12–14). In this work, we predict larger diffusion restrictions only in the models that do not include functional coupling between PK and ATPase (models 2 and 2s). Thus, the extent of diffusion restriction predicted by models depends on the fraction of ATPases activated in the cells and on the coupling between PK and ATPases. For accurate estimation of diffusion restrictions, the discrepancy between results for cardiomyocytes and those for fibers has to be resolved.

We do not know at this stage which ATPases are active in cardiomyocytes with PK-supplied ATP, i.e., which ATPases are functionally coupled to PK. One possibility is the SR calcium ATPase (SERCA). Specifically, it is known that PK is functionally coupled to SERCA and is localized next to it in the SR vesicles from heart and skeletal muscle (23,24), but other ATPases can also be coupled to PK. For example, the Na-K-ATPase is preferentially fueled by ATP from glycolysis (25). In general, glycolysis tends to support sarcolemmal function, whereas mitochondrial respiration supports contractile function (1). However, it has been shown that glycolytic energy buffering can affect contractile function in a manner similar to that observed with CK (26). Thus, it is also possible that PK, which binds to the I-band of the sarcomeres (27), is coupled to myosin ATPase. It should be noticed, though, that in the experiments presented here, the concentration of Ca^{2+} in the intracellular medium is not higher than that in the resting cell, and thus, most of the ATPases involved in excitation-contraction coupling were not fully activated. Further experiments will address which ATPases are represented by C4 in our model and exhibit this strong coupling to PK.

All the models in this study predicted similar exchange coefficients for diffusion through the mitochondrial outer membrane (Table 2). Let us illustrate the meaning of the obtained exchange coefficient value. For example, in the measurements performed with the concentration of exogenous ADP equal to the apparent Km(ADP) value (~0.3 mM), the respiration rate is ~50 nmol O_2/(min mg prot), or ADP consumption is 300 nmol/(min mg prot) (assuming $P/O_2 = 6$). To sustain such a flux through the mitochondrial outer membrane, the ADP gradient has to be 300 nmol/(min mg prot)/1900 nmol/(mM min mg prot) = 0.16 mM. This value is close to our estimate obtained using a 3D mathematical model of intracellular diffusion in the fiber (14). That model took into account the intracellular distribution of mitochondria (28) as well as sarcoplasmic reticulum (29). According to our simulations, the gradient of ADP in similar conditions would be ≤ 0.15 mM (14).

In both models, the ADP and ATP gradients induced by mitochondrial outer membrane depend on the respiration rate, with gradients up to ~0.3 mM expected at rates close to the maximal respiration rate. The estimate of apparent Km(ADP) obtained in this work is somewhat smaller than that obtained by others for isolated brain and heart mitochondria after addition of tubulin (30,31). In those experiments, two populations of mitochondria were identified with one of them (Km(ADP) = ~0.3 mM), presumably corresponding to the situation in the intracellular environment. Thus, although our results show that there is a significant diffusion restriction induced by the mitochondrial outer membrane in permeabilized cardiomyocytes, we predict that it is somewhat smaller than the diffusion restriction found in experiments on isolated mitochondria with tubulin in solution.

The finding that intracellular PK is tightly coupled to some ATPases supports the view of metabolism as a highly developed compartmentalized network (1). With the intracellular diffusion restricted (12,16) and anisotropic (15) in rat cardiomyocytes, formation of microdomains with local ATP consumption and production is possible. As one of the ATPases that can be coupled tightly to PK, SERCA is one of several critical systems that are functionally coupled to local ATP regeneration via glycolysis, glycogenolysis, or CK (32–35). A similar trend has been identified in mitochondria, with the evidence that the respiratory chain is organized in supercomplexes (36). To understand the behavior of such compartmentalized and coupled systems, mathematical models describing the interaction between molecules have to be developed and integrated into cell models. Such integrated models, when fully developed, will help us to understand the metabolic pathways in normal conditions and the effects of metabolic remodeling of the failing heart, and thereby to identify treatment protocols for patients based on modulation of the metabolic pathways (37,38).

In conclusion, we have generated a solid data set that we used to analyze intracellular diffusion restrictions in rat cardiomyocytes. On the basis of our analysis, we have confirmed previous findings of a significant restriction by the outer mitochondrial membrane. Also, we have confirmed a functional coupling between mitochondria and a fraction of ATPases in the cell. The new finding in this study is that a large fraction of ATPases seems to be tightly coupled to PK. This highlights the importance of glycolysis in energy production for cardiac function. To determine the intracellular diffusion restrictions that are expected to group ATP-consuming and -producing systems, we need to explain why there is a discrepancy between ATPase stimulation of respiration in cardiomyocytes and that in fibers, and which ATPases are coupled to mitochondria and PK.

SUPPORTING MATERIAL

Additional text is available at http://www.biophysj.org/biophysj/supplemental/S0006-3495(10)00357-7.

Publication I

REFERENCES

1. Weiss, J. N., L. Yang, and Z. Qu. 2006. Systems biology approaches to metabolic and cardiovascular disorders: network perspectives of cardiovascular metabolism. *J. Lipid Res.* 47:2355–2366.

2. Saks, V., P. Dzeja, …, T. Wallimann. 2006. Cardiac system bioenergetics: metabolic basis of the Frank-Starling law. *J. Physiol.* 571:253–273.

3. Hoerter, J. A., A. Kuznetsov, and R. Ventura-Clapier. 1991. Functional development of the creatine kinase system in perinatal rabbit heart. *Circ. Res.* 69:665–676.

4. Kay, L., V. A. Saks, and A. Rossi. 1997. Early alteration of the control of mitochondrial function in myocardial ischemia. *J. Mol. Cell. Cardiol.* 29:3399–3411.

5. Sokolova, N., M. Vendelin, and R. Birkedal. 2009. Intracellular diffusion restrictions in isolated cardiomyocytes from rainbow trout. *BMC Cell Biol.* 10:90.

6. Birkedal, R., and H. Gesser. 2004. Effects of hibernation on mitochondrial regulation and metabolic capacities in myocardium of painted turtle (*Chrysemys picta*). *Comp. Biochem. Physiol. A Mol. Integr. Physiol.* 139:285–291.

7. Anmann, T., R. Guzun, …, V. Saks. 2006. Different kinetics of the regulation of respiration in permeabilized cardiomyocytes and in HL-1 cardiac cells. Importance of cell structure/organization for respiration regulation. *Biochim. Biophys. Acta.* 1757:1597–1606.

8. Birkedal, R., and H. Gesser. 2006. Intracellular compartmentation of cardiac fibres from rainbow trout and Atlantic cod—a general design of heart cells. *Biochim. Biophys. Acta.* 1757:764–772.

9. Kümmel, L. 1988. Ca, Mg-ATPase activity of permeabilised rat heart cells and its functional coupling to oxidative phosphorylation of the cells. *Cardiovasc. Res.* 22:359–367.

10. Kay, L., K. Nicolay, …, T. Wallimann. 2000. Direct evidence for the control of mitochondrial respiration by mitochondrial creatine kinase in oxidative muscle cells in situ. *J. Biol. Chem.* 275:6937–6944.

11. Seppet, E. K., T. Kaambre, …, V. A. Saks. 2001. Functional complexes of mitochondria with Ca,MgATPases of myofibrils and sarcoplasmic reticulum in muscle cells. *Biochim. Biophys. Acta.* 1504:379–395.

12. Saks, V., A. Kuznetsov, …, M. Vendelin. 2003. Heterogeneity of ADP diffusion and regulation of respiration in cardiac cells. *Biophys. J.* 84:3436–3456.

13. Vendelin, M., M. Eimre, …, V. A. Saks. 2004. Intracellular diffusion of adenosine phosphates is locally restricted in cardiac muscle. *Mol. Cell. Biochem.* 256–257:229–241.

14. Ramay, H. R., and M. Vendelin. 2009. Diffusion restrictions surrounding mitochondria: a mathematical model of heart muscle fibers. *Biophys. J.* 97:443–452.

15. Vendelin, M., and R. Birkedal. 2008. Anisotropic diffusion of fluorescently labeled ATP in rat cardiomyocytes determined by raster image correlation spectroscopy. *Am. J. Physiol. Cell Physiol.* 295:C1302–C1315.

16. Kaasik, A., V. Veksler, …, R. Ventura-Clapier. 2001. Energetic crosstalk between organelles: architectural integration of energy production and utilization. *Circ. Res.* 89:153–159.

17. Guzun, R., N. Timohhina, …, V. Saks. 2009. Regulation of respiration controlled by mitochondrial creatine kinase in permeabilized cardiac cells in situ. Importance of system level properties. *Biochim. Biophys. Acta.* 1787:1089–1105.

18. Monge, C., N. Beraud, …, E. Seppet. 2009. Comparative analysis of the bioenergetics of adult cardiomyocytes and nonbeating HL-1 cells: respiratory chain activities, glycolytic enzyme profiles, and metabolic fluxes. *Can. J. Physiol. Pharmacol.* 87:318–326.

19. Rasmussen, H. N., and U. F. Rasmussen. 2003. Oxygen solubilities of media used in electrochemical respiration measurements. *Anal. Biochem.* 319:105–113.

20. Sikk, P., T. Kaambre, …, V. Saks. 2009. Ultra performance liquid chromatographic analysis of adenine nucleotides and creatine derivatives for kinetic studies. *Proc. Eston. Acad. Sci.* 58:122–131.

21. Vendelin, M., O. Kongas, and V. Saks. 2000. Regulation of mitochondrial respiration in heart cells analyzed by reaction-diffusion model of energy transfer. *Am. J. Physiol. Cell Physiol.* 278:C747–C764.

22. Vendelin, M., M. Lemba, and V. A. Saks. 2004. Analysis of functional coupling: mitochondrial creatine kinase and adenine nucleotide translocase. *Biophys. J.* 87:696–713.

23. Xu, K. Y., J. L. Zweier, and L. C. Becker. 1995. Functional coupling between glycolysis and sarcoplasmic reticulum Ca^{2+} transport. *Circ. Res.* 77:88–97.

24. Xu, K. Y., and L. C. Becker. 1998. Ultrastructural localization of glycolytic enzymes on sarcoplasmic reticulum vesicles. *J. Histochem. Cytochem.* 46:419–427.

25. Dizon, J., D. Burkhoff, …, J. Katz. 1998. Metabolic inhibition in the perfused rat heart: evidence for glycolytic requirement for normal sodium homeostasis. *Am. J. Physiol.* 274:H1082–H1089.

26. Harrison, G. J., M. H. van Wijhe, …, J. H. van Beek. 2003. Glycolytic buffering affects cardiac bioenergetic signaling and contractile reserve similar to creatine kinase. *Am. J. Physiol. Heart Circ. Physiol.* 285:H883–H890.

27. Kraft, T., M. Messerli, …, B. Brenner. 1995. Equilibration and exchange of fluorescently labeled molecules in skinned skeletal muscle fibers visualized by confocal microscopy. *Biophys. J.* 69:1246–1258.

28. Birkedal, R., H. A. Shiels, and M. Vendelin. 2006. Three-dimensional mitochondrial arrangement in ventricular myocytes: from chaos to order. *Am. J. Physiol. Cell Physiol.* 291:C1148–C1158.

29. Segretain, D., A. Rambourg, and Y. Clermont. 1981. Three dimensional arrangement of mitochondria and endoplasmic reticulum in the heart muscle fiber of the rat. *Anat. Rec.* 200:139–151.

30. Monge, C., N. Beraud, …, V. A. Saks. 2008. Regulation of respiration in brain mitochondria and synaptosomes: restrictions of ADP diffusion in situ, roles of tubulin, and mitochondrial creatine kinase. *Mol. Cell. Biochem.* 318:147–165.

31. Rostovtseva, T. K., K. L. Sheldon, …, D. L. Sackett. 2008. Tubulin binding blocks mitochondrial voltage-dependent anion channel and regulates respiration. *Proc. Natl. Acad. Sci. USA.* 105:18746–18751.

32. Korge, P., S. K. Byrd, and K. B. Campbell. 1993. Functional coupling between sarcoplasmic-reticulum-bound creatine kinase and Ca^{2+}-ATPase. *Eur. J. Biochem.* 213:973–980.

33. Minajeva, A., R. Ventura-Clapier, and V. Veksler. 1996. Ca2+ uptake by cardiac sarcoplasmic reticulum ATPase in situ strongly depends on bound creatine kinase. *Pflugers Arch.* 432:904–912.

34. Weiss, J. N., and S. T. Lamp. 1989. Cardiac ATP-sensitive K^+ channels. Evidence for preferential regulation by glycolysis. *J. Gen. Physiol.* 94:911–935.

35. Dhar-Chowdhury, P., M. D. Harrell, …, W. A. Coetzee. 2005. The glycolytic enzymes, glyceraldehyde-3-phosphate dehydrogenase, triose-phosphate isomerase, and pyruvate kinase are components of the K^{ATP} channel macromolecular complex and regulate its function. *J. Biol. Chem.* 280:38464–38470.

36. Lenaz, G., and M. L. Genova. 2007. Kinetics of integrated electron transfer in the mitochondrial respiratory chain: random collisions vs. solid state electron channeling. *Am. J. Physiol. Cell Physiol.* 292:C1221–C1239.

37. van Bilsen, M., F. A. van Nieuwenhoven, and G. J. van der Vusse. 2009. Metabolic remodelling of the failing heart: beneficial or detrimental? *Cardiovasc. Res.* 81:420–428.

38. Neubauer, S. 2007. The failing heart—an engine out of fuel. *N. Engl. J. Med.* 356:1140–1151.

Biophysical Journal, Volume 98

Supporting Material

ADP compartmentation analysis reveals coupling between pyruvate kinase and ATPases in heart muscle

Mervi Sepp, Marko Vendelin, Heiki Vija, and Rikke Birkedal

Supporting material

ADP compartmentation analysis reveals coupling between pyruvate kinase and ATPases in heart muscle *Mervi Sepp, Marko Vendelin, Heiki Vija, and Rikke Birkedal*

Here, we give the description of cardiomyocyte isolation and numerical methods used to solve the mathematical models.

Experimental procedures: Isolation of cardiomyocytes and solutions

Isolation of cardiomyocytes. Cardiomyocytes were isolated following the method described previously (1) but with some modifications. The animals received an i.p. injection of 2500 U heparin and were anesthetized with 260 mg/kg sodium pentobarbital (Dorminal^{TM}). The excised heart was swiftly placed in ice-cold wash solution (see composition below) to minimize ischemic damage. The heart was Langendorff perfused with wash solution at constant pressure of 80 cm H_2O for 5 minutes before the perfusate was changed to digestion solution containing 0.75 - 1 mg/ml of collagenase A (Roche; see composition below). This solution was recirculated with a rate of 5.1 ml/min until the pressure was 0 mm Hg (approx. 40 min). After this, the ventricle was cut into four pieces and transferred into 10 ml digestion solution. It was incubated with gentle shaking in waterbath at 37°C for additional 10-20 minutes. This last step turned out to be crucial to obtain calcium tolerant cells that contracted upon electrical field stimulation indicating a proper cell isolation. When the ventricular tissue pieces began to disassemble, they were transferred to sedimentation solution (see composition below), cut a few times with a scissor and the cells were suspended with a pipette. The cell suspension was passed through a nylon mesh and viable cells separated by sedimentation. Calcium concentration in the cell suspension was increased gradually to 1 mM with repeated wash-sedimentation cycles after which the cells were washed three times with large volumes of Ca^{2+}-free solution. The cells were stored in this solution at room temperature until use. The isolated cells were checked under the microscope during each wash to make sure that the suspension contained at least 75 % healthy, rod-shaped cells. They were also controlled after oxygraphy measurements to make sure that Ca^{2+} had been adequately washed out during the final three washes: if Ca^{2+} had not been washed out of the extracellular medium in which the cells were stored, the cells would have contracted upon permeabilization, but this was never observed.

Solutions. Wash solution (mM): NaCl 117, KCl 5.7, NaHCO$_3$ 4.4, MgCl$_2$ 1.7, KH$_2$PO$_4$ 1.5, sucrose 120, BES 21, taurine 20, glucose 11.7 and creatine 10. pH was adjusted to 7.1 with NaOH at 25°.

Digestion solution (mM): NaCl 117, KCl 5.7, NaHCO$_3$ 4.4, MgCl$_2$ 1.7, KH$_2$PO$_4$ 1.5, HEPES 21.1, taurine 20, glucose 11.7, creatine 11, phoshocreatine 10, pyruvate 2, 2 mg/ml BSA and 0.75-1 mg/ml collagenase A (Roche). pH was adjusted to 7.1 with NaOH at 25°.

Sedimentation solution contained the same compounds as digestion solution except that collagenase A was replaced by 20μM CaCl$_2$, 10μM leupeptin and 2μM soybean trypsin inhibitor.

Mitomed solution (mM): KH$_2$PO$_4$ 3, MgCl$_2$ 3, sucrose 110, K-lactobionate 60, taurine 20, HEPES 20, EGTA 0.5, DTT 0.5, malate 2, glutamate 5 and 5mg/ml BSA. pH was adjusted to 7.1 with KOH at 25°. In all experiments, the isolated cardiomyocytes were permeabilized with 20μg/ml of saponin.

Mathematical model

We used four different model versions to reproduce the experimental data. The model solution was obtained in the form of concentration distributions within the different compartments in the cell.

1

Each model gives an estimation of the overall diffusion restriction between intracellular environment and extracellular solution as well as restrictions between ATPases and mitochondria according to the model architecture. It is assumed that the diffusion restrictions imposed on ADP and ATP are the same. The solution volumes in the models were taken from the experimental setup, changing between different experiment types: 2 ml for oxygraph and spectrophotometric measurements; 5 ml for HPLC measurements.

The experiments reflect cell population behavior. In the models, we describe the distribution of metabolites in one representative cell. In order to estimate the volumes of different compartments within a cell, we first assumed that the combined cell volumes take up 15% of the cell suspension added in the experiments (10-20 and 80 μL suspension added to 2 or 5 ml, respectively). The used value for combined cell volumes is speculative as it is difficult to assess it in the cell suspension. We checked how changing of the combined cell volumes affects modeling results to assess its influence on the model solution. Decreasing it 10 or 100 times did not change the conclusions drawn from the modeling results. The volume of mitochondrial matrix was assumed to be 33% of the cell volume, mitochondrial intermembrane space (IMS) was 1% of the cell volume, and the volume of cytosolic compartment was the rest.

In the model setup we considered eight types of experiments: 1) mitochondrial respiration stimulated by ADP, 2) mitochondrial respiration stimulated by ATP, 3) ATP stimulated respiration inhibited by PEP, 4) ATP stimulated respiration inhibited by PK + PEP, 5) ATPase activity without OxPhos, 6) endogenous PK activity, 7) concentration of ADP released into solution as a function of time in presence of OxPhos, and 8) concentration of ADP released into solution as a function of time in the absence of OxPhos. To relate ATP synthesis to OxPhos, P/O$_2$ ratio equal to 6 was assumed.

Model 1. The simplest model has three compartments - solution, cytosol and IMS (Fig. 1, scheme 1). The fluxes of metabolites induced by diffusion between those compartments are

$$
\begin{array}{rcl}
J_{ATP} & = & C_{sol-cyt}(ATP_{sol} - ATP_{cyto}) \\
J_{2\,ATP} & = & C_{MoM}(ATP_{cyto} - ATP_{IMS}) \\
J_{ADP} & = & C_{sol-cyt}(ADP_{sol} - ADP_{cyto}) \\
J_{2\,ADP} & = & C_{MoM}(ADP_{cyto} - ADP_{IMS}),
\end{array}
\tag{1}
$$

where $C_{sol-cyt}$ is the exchange coefficients between solution and cytosol and and C_{MoM} between cytosol and IMS.

As it is shown in Fig 1 (scheme 1), the following processes are included in model 1 in addition to diffusion between compartments: ATP synthesis in IMS by oxidative phosphorylation (rate V_{ATPsyn}); ATP consumption by ATPases in cytosol (rate V_{ATPase}); and synthesis of ATP by pyruvate kinase (PK) reaction in solution (rate V_{PK}). For simplicity, the rates are given using a phenomenological description. ATP synthesis rate is

$$
V_{ATPsyn} = \frac{V_{maxATPsyn} \cdot ADP_{IMS}}{ADP_{IMS} + K_{mATPsyn}},
\tag{2}
$$

where the $K_{mATPsyn}$ was taken equal to 0.015 mM (2) in this and all other models. For ATPase, a competitive inhibition by ADP is assumed:

$$
V_{ATPase} = \frac{V_{maxATPase} \cdot ATP_{cyto}}{ATP_{cyto} + K_{mATPase}\left(1 + \frac{ADP_{cyto}}{K_{iATPase}}\right)}.
\tag{3}
$$

Exogenous PK reaction is assumed to depend only on ADP:

$$
V_{PK} = \frac{V_{maxPK} \cdot ADP_{sol}}{ADP_{sol} + K_{PK}}.
\tag{4}
$$

2

Here, dependence of PK rate on PEP is not taken into account explicitly since PEP level is assumed to be same in all compartments. Since the PEP concentration used in experiments (5 mM) is considerably larger than the concentration of ADP, the influence of PEP concentration gradients on the kinetics is assumed to be minor. Apparent kinetic constant K_{PK} was taken equal to 0.3 mM in all models.

The kinetic equations for metabolite concentrations in each compartment are as follows:

$$
\begin{aligned}
dATP_{sol}/dt &= (-J_{ATP} + V_{PK})/W_{sol} \\
dADP_{sol}/dt &= (-J_{ADP} - V_{PK})/W_{sol} \\
dATP_{cyto}/dt &= (-V_{ATPase} + J_{ATP} - J_{2\,ATP})/W_{cyto} \\
dADP_{cyto}/dt &= (V_{ATPase} + J_{ADP} - J_{2\,ADP})/W_{cyto} \\
dATP_{IMS}/dt &= (J_{2\,ATP} + V_{ATPsyn})/W_{IMS} \\
dADP_{IMS}/dt &= (J_{2\,ADP} - V_{ATPsyn})/W_{IMS},
\end{aligned}
\tag{5}
$$

where W_{sol} is the volume of solution, W_{cyto} is the volume of cytosol and W_{IMS} is the volume of IMS.

The optimized parameters were: $V_{maxATPsyn}$, $C_{sol-cyt}$, C_{MoM}, $V_{maxATPase}$, $K_{mATPase}$, and $K_{iATPase}$.

Model 2. Model 2 (Fig. 1, scheme 2) is based on model 1 with ATPase activity split into two fractions (ATPase1 and ATPase2) with different apparent kinetic constants and addition of endogenous PK activity (PKend). Model 2 has the same number of compartments as model 1 with the diffusion between compartments described by Eq. 1. Activity of endogenous PK is given by

$$
V_{PKend1} = \frac{V_{maxPKend1} \cdot ADP_{cyto}}{ADP_{cyto} + K_{PKend}}.
\tag{6}
$$

Rates for ATPase fractions are

$$
V_{ATPase1} = \frac{V_{maxATPase1} \cdot ATP_{cyto}}{ATP_{cyto} + K_{mATPase1}\left(1 + \frac{ADP_{cyto}}{K_{iATPase1}}\right)},
\tag{7}
$$

$$
V_{ATPase2} = \frac{V_{maxATPase2} \cdot ATP_{cyto}}{ATP_{cyto} + K_{mATPase2}\left(1 + \frac{ADP_{cyto}}{K_{iATPase2}}\right)}.
\tag{8}
$$

For model 2, the kinetic equations for metabolites are as follows:

$$
\begin{aligned}
dATP_{sol}/dt &= (-J_{ATP} + V_{PK})/W_{sol} \\
dADP_{sol}/dt &= (-J_{ADP} - V_{PK})/W_{sol} \\
dATP_{cyto}/dt &= \\
&\quad (-V_{ATPase1} - V_{ATPase_2} + J_{ATP} - J_{2\,ATP} + V_{PKend1})/W_{cyto} \\
dADP_{cyto}/dt &= \\
&\quad (V_{ATPase1} + V_{ATPase_2} + J_{ADP} - J_{2\,ADP} - V_{PKend1})/W_{cyto} \\
dATP_{IMS}/dt &= (J_{2\,ATP} + V_{ATPsyn})/W_{IMS} \\
dADP_{IMS}/dt &= (J_{2\,ADP} - V_{ATPsyn})/W_{IMS},
\end{aligned}
\tag{9}
$$

The optimized parameters for model 2 were: $V_{maxATPsyn}$, $C_{sol-cyt}$, C_{MoM}, $V_{maxATPase1}$, $V_{maxATPase2}$, $K_{mATPase1}$, $K_{mATPase2}$, $K_{iATPase1}$, $K_{iATPase2}$, $V_{maxPKend}$, and K_{PKend}.

Model 3. In model 3 (Fig. 1, scheme 3), we introduced an additional intracellular compartment (compartment 4, C4) with volume (W_{C4}) equal to 10% of cytosolic volume to test whether some of ATPases are coupled to endogenous PK. Part of endogenous PK and ATPase activities are located in

3

C4. In this model, C4 is connected to cytosol. As a result, fluxes of metabolites induced by diffusion between compartments in model 3 are as follows:

$$
\begin{aligned}
J_{ATP} &= C_{sol-cyt}(ATP_{sol} - ATP_{cyto}) \\
J_{2\,ATP} &= C_{MoM}(ATP_{cyto} - ATP_{IMS}) \\
J_{3\,ATP} &= C_{cyt-C4}(ATP_{cyto} - ATP_{C4})
\end{aligned}
$$

$$
\begin{aligned}
J_{ADP} &= C_{sol-cyt}(ADP_{sol} - ADP_{cyto}) \\
J_{2\,ADP} &= C_{MoM}(ADP_{cyto} - ADP_{IMS}) \\
J_{3\,ADP} &= C_{cyt-C4}(ADP_{cyto} - ADP_{C4}).
\end{aligned}
\tag{10}
$$

As in model 2, ATP synthase is described in IMS by Eq. 2, PK reaction in solution is described by Eq. 4, and, in cytosol, endogenous PK and ATPase reactions are described by Eq. 6 and Eq. 7, respectively. Reaction rates of ATPase and endogenous PK in C4 are given by

$$
V_{ATPase2} = \frac{V_{maxATPase2} \cdot ATP_{C4}}{ATP_{C4} + K_{mATPase2}\left(1 + \frac{ADP_{C4}}{K_{iATPase2}}\right)}
\tag{11}
$$

and

$$
V_{PKend2} = \frac{V_{maxPKend2} \cdot ADP_{C4}}{ADP_{C4} + K_{PKend}}.
\tag{12}
$$

The kinetic equations for the metabolites in different compartments are:

$$
\begin{aligned}
dATP_{sol}/dt &= (-J_{ATP} + V_{PK})/W_{sol} \\
dADP_{sol}/dt &= (-J_{ADP} - V_{PK})/W_{sol} \\
dATP_{cyto}/dt &= \\
&\quad (-V_{ATPase} + J_{ATP} - J_{2\,ATP} + V_{PKend1})/W_{cyto} \\
dADP_{cyto}/dt &= \\
&\quad (V_{ATPase} + J_{ADP} - J_{2\,ADP} - V_{PKend1})/W_{cyto} \\
dATP_{C4}/dt &= \\
&\quad (-V_{ATPase1} + J_{ATP} - J_{2\,ATP} - J_{3\,ATP} + V_{PKend2})/W_{C4} \\
dADP_{C4}/dt &= \\
&\quad (V_{ATPase} + J_{ADP} - J_{2\,ADP} - J_{3\,ADP} - V_{PKend2})/W_{C4} \\
dATP_{IMS}/dt &= (J_{2\,ATP} + V_{ATPsyn})/W_{IMS} \\
dADP_{IMS}/dt &= (J_{2\,ADP} - V_{ATPsyn})/W_{IMS}
\end{aligned}
\tag{13}
$$

The optimized parameters were: $V_{maxATPsyn}$, $C_{sol-cyt}$, C_{MoM}, C_{cyt-C4}, $V_{maxATPase1}$, $V_{maxATPase2}$, $K_{mATPase1}$, $K_{mATPase2}$, $K_{iATPase1}$, $K_{iATPase2}$, $V_{maxPKend1}$, $V_{maxPKend2}$, K_{PKend} (this constant was the same for the endogenous PK located in cytosol and C4).

Model 4. Model 4 (Fig. 1, scheme 4) is a modification of model 3 with the only difference being the connection of C4 to the rest of the cell. In model 4, C4 is in direct contact with IMS instead of cytosol. All the expressions describing reactions in the compartments are the same as in model 3. The difference between the models is in the fluxes of metabolites induced by diffusion. For model 4, those fluxes are

$$
\begin{aligned}
J_{ATP} &= C_{sol-cyt}(ATP_{sol} - ATP_{cyto}) \\
J_{2\,ATP} &= C_{MoM}(ATP_{cyto} - ATP_{IMS}) \\
J_{4\,ATP} &= C_{IMS-C4}(ATP_{IMS} - ATP_{C4})
\end{aligned}
$$

$$
\begin{aligned}
J_{ADP} &= C_{sol-cyt}(ADP_{sol} - ADP_{cyto}) \\
J_{2\,ADP} &= C_{MoM}(ADP_{cyto} - ADP_{IMS}) \\
J_{4\,ADP} &= C_{IMS-C4}(ADP_{IMS} - ADP_{C4}).
\end{aligned}
\tag{14}
$$

4

The kinetic equations are:

$$dATP_{sol}/dt = (-J_{ATP} + V_{PK})/W_{sol}$$
$$dADP_{sol}/dt = (-J_{ADP} - V_{PK})/W_{sol}$$
$$dATP_{cyto}/dt =$$
$$\quad (-V_{ATPase} + J_{ATP} - J_{2\,ATP} + V_{PKend1})/W_{cyto}$$
$$dADP_{cyto}/dt =$$
$$\quad (V_{ATPase} + J_{ADP} - J_{2\,ADP} - V_{PKend1})/W_{cyto}$$
$$dATP_{C4}/dt =$$
$$\quad (-V_{ATPase1} + J_{ATP} - J_{2\,ATP} - J_{4\,ATP} + V_{PKend2})/W_{C4}$$
$$dADP_{C4}/dt =$$
$$\quad (V_{ATPase} + J_{ADP} - J_{2\,ADP} - J_{4\,ADP} - V_{PKend2})/W_{C4}$$
$$dATP_{IMS}/dt = (J_{2\,ATP} + V_{ATPsyn})/W_{IMS}$$
$$dADP_{IMS}/dt = (J_{2\,ADP} - V_{ATPsyn})/W_{IMS}$$

$$(15)$$

The optimized parameters were $V_{maxATPsyn}$, $C_{sol-cyt}$, C_{MoM}, C_{IMS-C4}, $V_{maxATPase1}$, $V_{maxATPase2}$, $K_{mATPase1}$, $K_{mATPase2}$, $K_{iATPase1}$, $K_{iATPase2}$, $V_{maxPKend1}$, $V_{maxPKend2}$, K_{PKend}.

Simplified versions of models 2, 3 and 4. In addition to these four models we also constructed simplified versions of models 2, 3 and 4 (2s, 3s, and 4s, respectively). In simplified models, we assumed that the apparent kinetic constants for ATPases are the same in all compartments:

$$K_{mATPase1} = K_{mATPase2}$$
$$K_{iATPase1} = K_{iATPase2}.$$

$$(16)$$

Fitting. To find the optimal model parameters, we performed fitting of the model solution to the measured data using the least squares method. The minimized error function was

$$\varepsilon = \sum_k^N \left[\sum_i \left(\frac{v_{ki}^{calc} - v_{ki}^{expr}}{\sigma_{ki}^{expr}} \right)^2 \right],$$

$$(17)$$

where index k runs through experiment types ($N = 8$ experiment types considered) and i through points in an experiment, v_{ki}^{calc} is the rate or ADP concentration (depending on the type of experiment k) calculated by the model and v_{ki}^{expr} the corresponding measured value, σ_{ki}^{expr} is the standard deviation of an experimental value.

To avoid non-physiological solutions during optimization, we limited the range of the parameters as follows: apparent Michaelis-Menten (K_m) and inhibition (K_i) constants for ATPases were limited from 0.05 to 10 mM; apparent K_m for endogenous PK was limited from 0.01 to 10 mM; apparent V_{max} for endogenous PK was lower than $7200 \frac{nmol}{min \cdot mg\ prot}$. In addition, exchange coefficients between cytosol and solution ($C_{sol-cyt}$) and cytosol and compartment 4 (C_{cyt-C4}) were limited to $10^6 \frac{1}{mM} \frac{nmol}{min \cdot mg\ prot}$. At such high values, the diffusion between compartments was not limiting and the model solution was not influenced if the exchange coefficient was increased further.

Statistical analysis of the modeling results. The fits obtained by different models were analyzed using several tests.

First, the sensitivity of each model parameter was assessed by estimating confidence intervals. For that, all model parameters were fixed at the found optimal values except one parameter that was either increased or reduced. As a result, the model fit became worse than with the optimal model parameters. As soon as the fit became so much worse than the p-value was 0.05 according to extra sum-of-squares F-test (F-test) when compared with an optimal fit, the value of the model parameter was recorded as

5

a value corresponding to the minimum or maximum of the confidence interval. This procedure was repeated with all model parameters.

Second, the fits obtained by different models were compared to evaluate whether the fits obtained by more complicated models were significantly better. For that, an F-test to compare the nested models was used. In addition, corrected Akaike information criterion and Bayesian information criterion were computed to compare the fits of the different models.

Numerical methods. The system of ordinary differential equations was numerically solved by an integrator that is able to automatically switch between stiff (backward differentiation formula) and non-stiff (Adams) integration routines, depending on the characteristics of the solution, and adapts the time-step to achieve a desired level of solution accuracy, which was in turn tested by varying the tolerance of the ordinary differential equation solver (3). The optimization was performed using the Levenberg-Marquardt algorithm (4).

References

1. Sikk, P., T. Kaambre, H. Vija, K. Tepp, T. Tiivel, A. Nutt, and V. Saks, 2009. Ultra performance liquid chromatographic analysis of adenine nucleotides and creatine derivatives for kinetic studies. *Proceedings of the Estonian Academy of Sciences* 58:122–131.

2. Saks, V. A., Z. A. Khuchua, E. V. Vasilyeva, Y. O. Belikova, and A. V. Kuznetsov, 1994. Metabolic compartmentation and substrate channelling in muscle cells. Role of coupled creatine kinases in in vivo regulation of cellular respiration–a synthesis. *Mol Cell Biochem* 133-134:155–192.

3. Hindmarsh, A. C., 1983. ODEPACK, A Systematized Collection of ODE Solvers. *Scientific Computing* 1:55–64.

4. Moré, J. J., D. C. Sorensen, K. E. Hillstrom, and B. S. Garbow, 1984. The MINPACK Project. *In* W. J. Cowell, editor, Sources and Development of Mathematical Software, Prentice-Hall.

6

Jepihhina N, Beraud N, Sepp M, Birkedal R, Vendelin M

Permeabilized rat cardiomyocyte response demonstrates intracellular origin of diffusion obstacles.

Permeabilized Rat Cardiomyocyte Response Demonstrates Intracellular Origin of Diffusion Obstacles

Natalja Jepihhina, Nathalie Beraud, Mervi Sepp, Rikke Birkedal, and Marko Vendelin*
Laboratory of Systems Biology, Institute of Cybernetics, Tallinn University of Technology, Tallinn, Estonia

ABSTRACT   Intracellular diffusion restrictions for ADP and other molecules have been predicted earlier based on experiments on permeabilized fibers or cardiomyocytes. However, it is possible that the effective diffusion distance is larger than the cell dimensions due to clumping of cells and incomplete separation of cells in fiber preparations. The aim of this work was to check whether diffusion restrictions exist inside rat cardiomyocytes or are caused by large effective diffusion distance. For that, we determined the response of oxidative phosphorylation (OxPhos) to exogenous ADP and ATP stimulation in permeabilized rat cardiomyocytes using fluorescence microscopy. The state of OxPhos was monitored via NADH and flavoprotein autofluorescence. By varying the ADP or ATP concentration in flow chamber, we determined that OxPhos has a low affinity in cardiomyocytes. The experiments were repeated in a fluorometer on cardiomyocyte suspensions leading to similar autofluorescence changes induced by ADP as recorded under the microscope. ATP stimulated OxPhos more in a fluorometer than under the microscope, which was attributed to accumulation of ADP in fluorometer chamber. By calculating the flow profile around the cell in the microscope chamber and comparing model solutions to measured data, we demonstrate that intracellular structures impose significant diffusion obstacles in rat cardiomyocytes.

INTRODUCTION

When mitochondrial oxygen consumption is stimulated by exogenous ADP, mitochondria in situ in permeabilized fibers and cells from cardiac muscle have an affinity that is much lower than that of isolated mitochondria (1–3). The cause of this is still uncertain. Usually, the low affinity is attributed to intracellular diffusion restrictions that limit diffusion between the solution surrounding the cell and the mitochondrial inner membrane. As possible diffusion obstacles, limitation of permeability of voltage-dependent anion channel in mitochondrial outer membrane by tubulin (4) and intracellular structures such as sarcoplasmic reticulum and proteins associated with them (3,5–7) have been proposed. From two- and three-dimensional analysis of mitochondrial arrangement, it is clear that rat cardiomyocytes have a very high degree of order (8,9). In such ordered environment, intracellular diffusion obstacles associated with sarcoplasmic reticulum can be responsible for anisotropy in diffusion that was shown by extended raster image correlation spectroscopy (6).

As an alternative explanation, Kongas et al. (10) proposed that low affinity to ADP in permeabilized fibers and cells can be attributed to long diffusion pathways in the experiments: unstirred layers surrounding the cells and fibers may provide a significant restriction of ADP-diffusion rela-

tive to metabolism; fibers and cells in the oxygraph may form clumps, where outer cells restrict diffusion to the inner cells. Although analysis of the data in light of intracellular diffusion restrictions has been commonly used, the alternative explanation of the data by long diffusion distances in the experimental setup has not been tested. Our recent data from rainbow trout approached the long diffusion distance hypothesis (unstirred layers and clumping of cells). The data argued against diffusion restriction by unstirred layers (11). However, they did suggest that trout cardiac fibers were not completely separated and/or were clumping during oxygraph experiments, because the affinity (quantified by apparent K_M for exogenous ADP) of fibers was much lower (apparent K_M higher) than that of isolated cardiomyocytes (11). Note that apparent K_M for ADP was still larger in trout cardiomyocytes than in isolated mitochondria, indicating the existence of intracellular diffusion restrictions in trout cells.

The difference in the affinity of permeabilized trout cells and fibers is opposite to what has been reported for rat heart preparations, where the apparent K_M of permeabilized fibers is similar to that of cardiomyocytes (12). We have never observed cell aggregation in the oxygraph during experiments on rat cardiomyocytes, or under the microscope after experiments. However, it cannot be ruled out that temporary microscopic cell aggregates are formed, so that the diffusion distance from the medium to the mitochondria inside the cells is effectively much larger than the radius of a single cardiomyocyte (10). As a result, formation of aggregates in isolated cardiomyocyte preparation in solution cannot be ruled out based on observation of similar affinities to ADP of permeabilized rat cardiomyocytes and fibers.

This study was designed to check whether permeabilized rat cardiomyocytes exhibit low affinity to exogenous ADP at single cell level. We took advantage of the fact that changes in the autofluorescence of reduced nicotinamide adenine dinucleotide (NADH) and oxidized flavoproteins (FPs) reflect the redox state of the cell (13,14). NADH and FP autofluorescence has been used extensively to characterize the state of respiratory chain: for example, response of isolated mitochondria (13,15) or permeabilized fibers (16,17) to ADP stimulation; response of isolated cardiomyocytes to drugs (18,19); or monitoring mitochondrial function in vivo (20).

NADH autofluorescence is mainly of mitochondrial origin (21,22). FP autofluorescence comes from three groups of flavoproteins: α-lipoamide dehydrogenase, electron transfer flavoprotein, and a third group, which is likely to be acyl-CoA dehydrogenases (23–25). α-Lipoamide dehydrogenase is the catalytic subunit of pyruvate dehydrogenase, α-ketoglutarate dehydrogenase in the citric acid cycle, and the branched chain α-keto acid dehydrogenase complex involved in amino-acid metabolism. As NADH is a cofactor for these dehydrogenases, the redox state of the flavin moiety of α-lipoamide dehydrogenase is in equilibrium with that of mitochondrial $NAD^+/NADH$.

In this study, we recorded the autofluorescence of NADH and FP from single, permeabilized rat cardiomyocytes perfused with solution containing increasing concentrations of ADP and ATP. For comparison, the same experiment was performed on populations of permeabilized cardiomyocytes in a spectrofluorometer to mimic respiration kinetics experiments that have shown low affinity of mitochondrial respiration to exogenous ADP. From the analysis of the measured data by mathematical models, we demonstrate that the low affinity of mitochondrial respiration to exogenous ADP comes, in part, from intracellular diffusion obstacles in rat heart muscle cells.

MATERIALS AND METHODS

Adult outbred Wistar rats of both sexes weighing 300–500 g were used in the experiments. Animal procedures were approved by the Estonian National Committee for Ethics in Animal Experimentation (Estonian Ministry of Agriculture).

Before the experiments, animals were anesthetized with 0.5 mg/kg ketamine (Bioketan, Vetoquinol Biowet, Gorzów Wielkopolski, Poland) and 125 mg/kg dexmedetomidine (Dexdomitor; Orion, Espoo, Finland).

Isolation of cardiomyocytes

Calcium-tolerant cardiomyocytes were isolated as described in Sepp et al. (3). During isolation of cardiomyocytes, we used solutions from Sepp et al. (3) with slight modifications. Solutions are listed in the Supporting Material.

Fluorescence microscopy

Microscope experiments were performed on an inverted Nikon Eclipse Ti-U microscope (Nikon, Tokyo, Japan), described in the Supporting Mate-

rial. Immediately before each experiment, a new batch of cells were permeabilized for 5 min with gentle mixing in an Eppendorf tube with Mitomed solution (see the Supporting Material) containing 25 μg/mL saponin and 50 μM ADP. A fraction of the permeabilized cells was put into a diamond-shaped fast-exchange chamber (15 × 6 mm, RC-24N; Warner Instruments, Harvard Apparatus, March-Hugstetten, Germany) on the microscope. They were allowed to sediment for 5–10 min before starting the superfusion with Mitomed solution containing different concentrations of ADP. Only those cells located in the middle of the chamber were used for measurements. According to the manufacturer, the geometry of the chamber provided laminar flow of solutions during experiments at the used flow rate of ~0.5 mL/min. The ADP concentration was increased stepwise from 50 to 100, 300, 500, 1000, and 2000 μM and the cells were superfused for at least 4.5 min at each step. The same experiment was done with ATP instead of ADP.

Spectrofluorometer recordings

Autofluorescence measurements on population level were performed in 4 mL plastic cuvettes (four-faced transparent cuvettes; Deltalab, Rubí, Spain) on a spectrofluorophotometer (Shimadzu RF-5301; Shimadzu Scientific Instruments, Kyoto, Japan). Autofluorescence spectra of flavoproteins and NADH were recorded using excitation and emission wavelengths similar to those used for microscope single cell studies: for NADH excitation was 340 nm, emission range 400–550 nm; for flavoproteins, excitation was 465 nm, emission range 500–600 nm. All spectra were taken three times to make sure that steady state was reached. The cell suspension was continuously stirred with magnetic stirrer bars (VWR, Wien, Austria) and before each measurement resuspended with a pipette to provide an homogeneous mixture. Autofluorescence of permeabilized cardiomyocytes was first recorded in substrate-free Mitomed solution in presence of 50 μM ADP or ATP, then substrates were added and cells were exposed to increasing concentrations of ADP or ATP, respectively. At the end of each titration, oligomycin and sodium cyanide were added to obtain the signal under fully reduced conditions. Spectra of cell suspension autofluorescence in substrate-free solution and in presence of oligomycin and cyanide were then used to normalize data of titration, as described below.

Analysis of fluorescence signal

Detailed description of analysis of fluorescence signal is given in the Supporting Material.

Statistics

The raw data were analyzed using homemade software. All results are shown as mean $\pm$ SD.

Mathematical models

The experimental data were analyzed by several mathematical models. Description of the models is given in the Supporting Material.
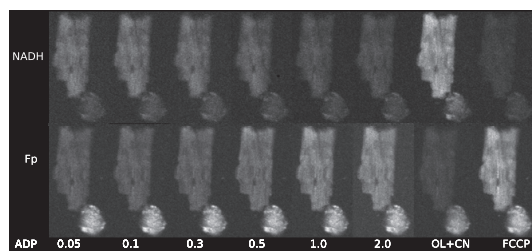
RESULTS

Experimental results

The response of the permeabilized rat cardiomyocytes to changes in the surrounding solution was followed in fluorescence microscope. Two fluorescence signals were recorded from the same cell with the recorded signals corresponding to NADH and flavoproteins (FPs) fluorescence. In the

beginning of the experiment, the cells were permeabilized by saponin. After that, the solution in the imaging chamber was varied and the fluorescence of cells was observed. Representative fluorescence images of the cells are shown on Fig. 1. Note how increase of exogenous ADP leads to reduction in NADH fluorescence and increase of FP fluorescence.

To get the extremes in the levels of fluorescence, we subjected the cells to solutions that inhibit oxidative phosphorylation (solution containing oligomycin and cyanide, OL+CN) or an uncoupled mitochondrial respiratory chain by using the solution containing FCCP (Fig. 1). As it is demonstrated in Fig. 1, NADH fluorescence of nonrod-shaped cardiomyocytes was quite small (*right bottom corner* of images). The same was not true for FP fluorescence, with relatively high FP fluorescence observed in nonrod-shaped cardiomyocytes. Such level of autofluorescence in nonrod-shaped cells is consistent with earlier reports (21). For these cells, FP fluorescence either stayed relatively constant through the whole experiment or changed with the variation of ADP or ATP in solution similar to rod-shaped cardiomyocytes (results not shown).

We quantified the response of the cells to different solutions by calculating the average fluorescence of a cell and using the fluorescence levels recorded in presence of OL+CN and FCCP to normalize the data (see the Supporting Material). Representative traces with average fluorescence changes in a single cell during an experiment are shown in Fig. 2. As shown in Fig. 2, stimulation of respiration by exogenous ADP leads to a larger range of fluorescence changes in the cell than stimulation by exogenous ATP. When adding exogenous ATP, respiration is stimulated due to the hydrolysis of ATP by endogenous ATPases. Note that there is always a significant delay between the time-
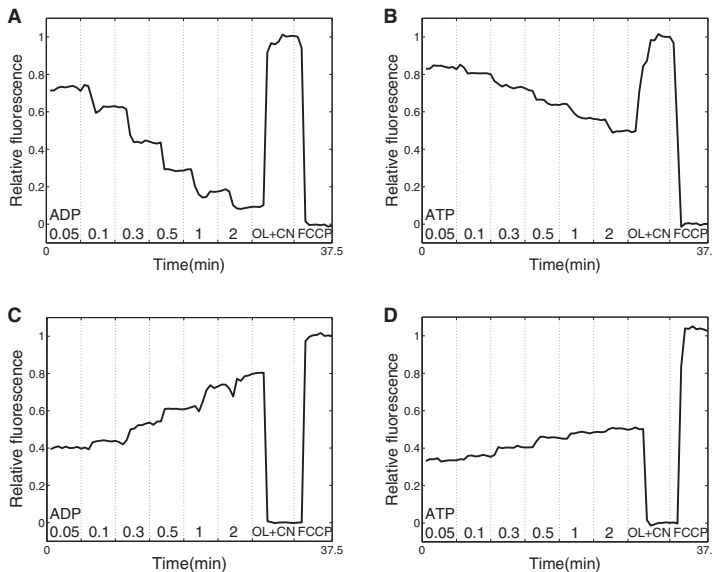
moment at which the new solution started to enter the microscope imaging chamber (*dashed vertical lines* in Fig. 2) and the response of the cell. However, after a few images, the fluorescence of the cell is stable until the next change of solution.

To compare the single cell response to the response of a cell population, the experiments were repeated in a fluorometer. Rat cardiomyocyte suspension was added to the fluorometer cuvette and after permeabilization, increasing amounts of ADP or ATP was added. Fluorescence spectra were recorded to determine the level of NADH and FP fluorescence. As explained in the Supporting Material, we had to avoid use of FCCP in the experiments in the fluorometer due to significant absorbance. For normalization of the fluorescence signal, the fluorescence of permeabilized cells was recorded before addition of substrates (but in the presence of low ADP or ATP). Sample spectra are shown in Fig. S1 in the Supporting Material.

A comparison of fluorescence levels recorded in a microscope ($n = 8$–13) and a fluorometer ($n = 6$) are shown in Fig. 3. As it is evident from Fig. 3, *A* and *C*, NADH and FP fluorescence changes similarly on single cell and population level when exogenous ADP is varied. When respiration is stimulated by ATP, the autofluorescence response is larger in the fluorometer than in the microscope (Fig. 3, *B* and *D*). This difference is induced by the differences in response at lower ATP concentrations. At higher ATP concentrations, NADH and FP fluorescence measured in a fluorometer does not change significantly (compare fluorescence at ATP concentrations of 1 mM and 2 mM, Fig. 3, *B* and *D*). This saturation effect has not been observed in the single cell measurements. The difference in recorded fluorescence response to changes in ADP and ATP are demonstrated in Fig. 3, *E* and *F*. Note how the curve corresponding to NADH fluorescence response to exogenous ATP stimulation is shifted to the right from the curve corresponding to exogenous ADP stimulation. For FP, the corresponding shift is to the left.

Because fluorometer measurements were performed on populations of cardiomyocytes, we could relate changes in NADH and FP fluorescence to changes in respiration rate (VO_2). For that, VO_2 measured on populations of rat cardiomyocytes under similar conditions were used (data taken from Sepp et al. (3)). The relationship between fluorescence and VO_2 is shown in Fig. 4. Because VO_2 was not measured at all ADP and ATP concentrations used in this study, we had to omit several fluorescence measurements in Fig. 4. Note that the relationship between fluorescence and VO_2 is close to linear. This indicates that fluorescence changes follow similar kinetics as VO_2. In addition, we observed that the fluorescence changes induced by exogenous ATP were larger than expected from VO_2 measurements. As a result, the relationship between NADH (or FP) fluorescence and VO_2 is not unique, but depends on the way the respiration is stimulated (Fig. 4, *A* and *B*).

FIGURE 1 Example of the response of permeabilized cardiomyocytes to changes in solution. For demonstration, rod-shaped and nonrod-shaped cells are shown. Autofluorescence of the cells was recorded by fluorescence microscope with the fluorescence induced by 340 nm (*top row*) or 465 nm (*bottom row*) excitation. Note how gradual increase of ADP (concentration in mM shown below images) leads to changes in fluorescence with the maximal and minimal levels of fluorescence induced by oligomycin/ cyanide (OL+CN) and FCCP. As it is clearly visible on the figure, fluorescence of nonrod-shaped cells (*bottom right corner* on all images) is relatively small in recordings of NADH fluorescence. However, the opposite was frequently true for recordings of fluorescence corresponding to flavoprotein (FP) signal.

FIGURE 2   Average fluorescence of a single permeabilized cell exposed to the changes in solution denoted at the bottom. Fluorescence was recorded with excitation light of 340 nm (*top row*) or 465 nm (*bottom row*). The fluorescence was normalized by using the signal recorded in solutions OL+CN and FCCP as extreme values corresponding to relative fluorescence equal to 0 and 1 (see figure). The moment at which the change of solution was started by the experimenter is indicated (*dashed vertical line*). Note how stimulation of respiration by exogenous ADP (*A* and *C*) is able to change the fluorescence in a larger range than stimulation by exogenous ATP (*B* and *D*).

Differences in fluorometer and microscope measurements analyzed by compartmentalized model of a cardiomyocyte

We have shown that the fluorescence response to variation in exogenous ATP concentration was different in fluorometer and microscope (Fig. 3, *B* and *D*). To understand the cause of this difference, respiration stimulation by exogenous ATP can be analyzed by mathematical model of permeabilized rat cardiomyocytes (3). Because, in our experiments, 3 mM inorganic phosphate was present in solution, effects induced by phosphate supply to the cell should be negligible. Thus, we can focus in our analysis on ATP and ADP. When respiration is stimulated by exogenous ATP, endogenous ATPases hydrolyze it to the ADP that would stimulate respiration in mitochondria. In addition, ADP produced by endogenous ATPases can also leave the cell in solution if the concentration of ADP in solution is smaller than in the cell. In the fluorometer cuvette, solution is not exchanged and reaches the steady state relatively fast, as measured by HPLC in similar configuration (3).

In the microscope chamber, the solution is exchanged and ADP produced by upstream cells can be washed out. To track the ADP concentration in the microscope chamber, we have to distinguish between ADP present in prepared ATP solution and ADP produced by ATPases in the microscope chamber. In our conditions, ADP concentration was 1.5% of ATP concentration in prepared solution, as determined earlier by HPLC in solution without cells (3). To estimate ADP produced by all cells in the microscope chamber, we assumed that the ATPase rate can be described by the Michaelis-Menten equation with apparent $K_{m(ATP)}$ of

0.38 mM (3). Maximal ATPase activity of a cell (4.2 fmol/s) can be estimated from activity of ATP synthase (0.54 mM/s, see description of reaction-diffusion-convection model in the Supporting Material); stimulation of respiration by exogenous ATP relative to stimulation by ADP (25% (3)); and the volume of a cell (cylinder with 20-μm diameter and 100-μm length).

Taking into account the cell counts after isolation and series of dilutions made, we had ~1000 cells in a microscope chamber during experiments leading to 4 pmol/s maximal ATPase activity. When checked at all used concentrations of ATP by calculating ATPase rate using the Michaelis-Menten equation, the ADP concentration would increase by 8.1% (at 50 μM ATP in solution) and 5.1% (300 μM ATP) when compared with ADP contained in solution at a flow rate of 0.5 ml/min. Because a significant fraction of the cells is washed out at the beginning of the experiment, the effect of intracellular ATPases on the ADP concentration in the chamber is even smaller. Thus, in the microscope chamber, ADP produced by cells in the chamber has a minor effect and ADP in solution is mainly determined by ADP present in solution before entering the chamber.

To test further whether such differences in the solution surrounding the cells could cause the different fluorescence responses seen in Fig. 3 *B*, we calculated VO$_2$. For comparison, a case with zero ADP in solution surrounding the cells is shown in Fig. 5. Note that in the case of zero ADP, there is still ATPase activity in the cell and some of the produced ADP stimulates respiration. As it is clear from the simulation results, ADP buildup during the measurements in the closed chamber configuration contributes significantly to VO$_2$. From these simulation results, we conclude that the
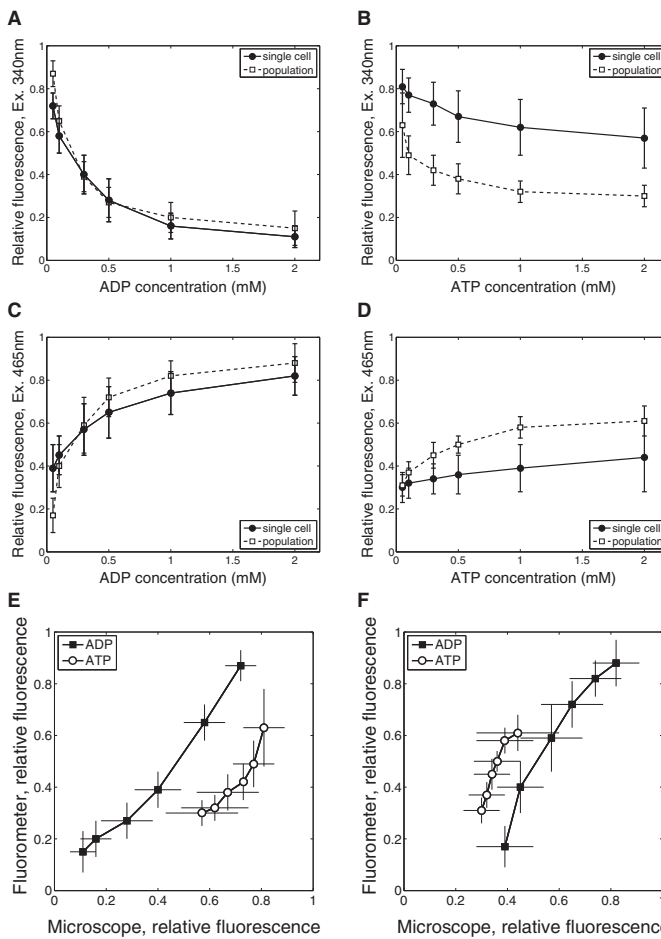
FIGURE 3 Comparison of fluorescence recordings performed on single cell level using fluorescence microscope with recordings on cell population level using fluorometer. The average fluorescence at different levels of exogenous ADP (*A* and *C*) and ATP (*B* and *D*) is shown for single cell and cell population recordings. Finally, average fluorescence recorded on single cell and population level is plotted against each other with fluorescence excited by 340 nm and 465 nm in *E* and *F*, respectively.

differences in NADH and FP fluorescence response to stimulation by endogenously generated ADP in fluorometer and microscope are caused by differences in the design of the corresponding measurement chambers.

Influence of unstirred water layers on the measurements

The low affinity of respiration, as evidenced by NADH and FP to changes in extracellular ADP, suggest significant intracellular diffusion restrictions. However, such low affinity can be also induced by large unstirred water layers surrounding the cells in the fluorometer or microscope chambers. Although analysis of unstirred water layers in the fluorometer chamber is not trivial due to the stirring and mixing of the cells in the experiments, the situation in the microscope chamber can be analyzed in detail. In our conditions, the flow in the chamber is laminar. By approximating the micro-

scope chamber by simplified geometry, we calculated the flow profile of the solution in the chamber (Fig. 6 *A*). The flow velocity was fastest near the inflow and outflow. In the center of the chamber, where the measurements were performed, the flow velocity reached ~3100 μm/s at the surface of the solution. Near the cell, next to the cover glass, the flow is considerably slower. However, even 20 μm from the glass, the flow was >100 μm/s in the central region of the chamber. Assuming that there is no flow of solution through the cell, the corrected flow profile in the cell surroundings was calculated. In those simulations, the flow profile in the middle of microscope chamber was taken into account. The flow in the cell surroundings is shown in Fig. 6 *B* by streamlines and arrows.

The calculated flow profile in the cell surroundings was used to analyze the influence of unstirred water layers on the measurements. For that, a reaction-diffusion-convection model was composed and we calculated the distribution of
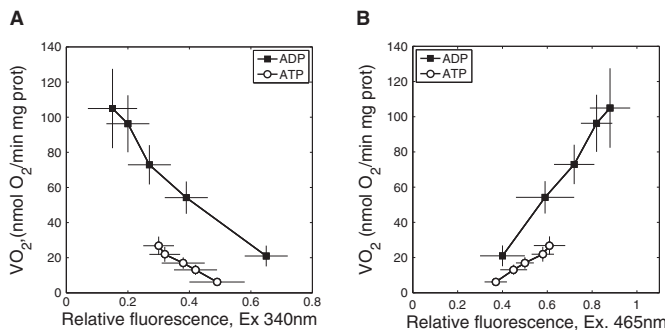
FIGURE 4 Relationship between fluorescence recorded in fluorometer (excitation 340 nm and 465 nm on *A* and *B*, respectively) and respiration rate. Note that the relationship is different for ADP and ATP stimulation.

ADP in solution and inside the cell taking into account mitochondrial respiration, diffusion, and convection of ADP. When 1 mM ADP is used in the solution entering the chamber, the model predicts significant diffusion gradients between the solution and parts of the cell next to the cover glass with the lowest ADP concentration equal to 0.67 mM (Fig. 6 *B*). In those simulations, it was assumed that apparent $K_{m(ADP)}$ of respiration was 0.015 mM, i.e., the same as for isolated mitochondria. To analyze how the supply of ADP influences VO_2 of the isolated cardiomyocyte, we calculated VO_2 of the cell in different conditions. Assuming that apparent $K_{m(ADP)}$ of mitochondria is 0.015 mM, we could see a large difference on calculated VO_2 when ADP was supplied by infinitely fast diffusion, diffusion as in water, and with the diffusion assisted by flow of solution (Fig. 6 *C*).

Note that when we take into account the flow surrounding the cell, the apparent affinity of VO_2 to ADP is considerably higher than the measured one (*solid line* in Fig. 6 *C*). Here,

the VO_2 measured in an oxygraphy chamber for cell suspension (data from Sepp et al. (3)) is shown for comparison. Assuming that NADH and FP fluorescence is linearly related to VO_2 we estimated the relative VO_2 of a single cell from fluorescence measurements (Fig. 3, *A* and *C*). For that, fluorescence at zero ADP was taken into account in estimation of VO_2 by subtracting it. The fluorescence at zero ADP was found by fitting fluorescence measurements with a Michaelis-Menten-type relationship with the shift corresponding to fluorescence level at zero ADP. As it is clear from Fig. 6 *C*, to reproduce the experimental data, the affinity of mitochondrial respiration to ADP has to be reduced significantly by increasing apparent $K_{m(ADP)}$ of respiration to 0.15–0.45 mM. This demonstrates that low affinity of respiration is induced, in part, by intracellular diffusion restrictions.

DISCUSSION

According to our results, the fluorescence response to exogenous ADP and ATP stimulation was similar on single cell and population levels if we take into account the differences in experimental setups. On both studied levels, NADH and FP fluorescence varied when ADP was changed up to the millimolar range indicating a low affinity of mitochondrial oxidative phosphorylation to exogenous ADP. From the mathematical analysis of the measurements in microscope chamber, we demonstrated that low affinity of the respiration to exogenous ADP is in part induced by intracellular diffusion restrictions. To our knowledge, this is the first time the existence of intracellular diffusion restrictions for ADP has been demonstrated from experiments on single cells.

To study the autofluorescence of cardiomyocytes, we used a wide-field fluorescence microscope equipped with a sensitive camera. By using such setup and following a single isolated cardiomyocyte, we avoided complications that can occur in tissue preparations and in confocal imaging. In the studies on tissue or organ level, one has to compensate for organ motion, inhomogeneity of the cells, and absorption and scattering of excitation light and fluorescence by tissue.
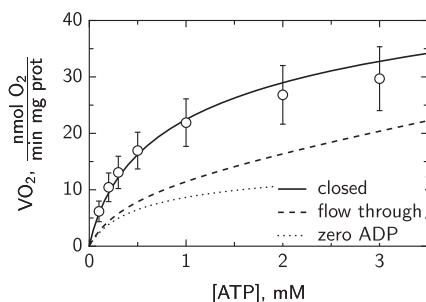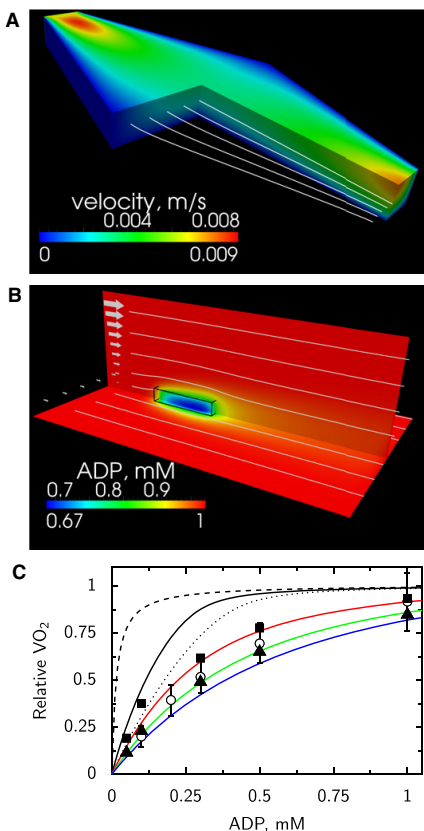

FIGURE 5 Calculated respiration rate VO_2 stimulated by exogenous ATP in permeabilized cardiomyocytes in the surroundings that mimic the situation in fluorometer (*solid line*) or microscope imaging chamber (*dashed line*). In fluorometer, measurements are performed in closed chamber whereas in microscope the solution is changed as it flows through the imaging chamber. As a result, ADP in solution can either accumulate (closed chamber) or will stay relatively low (flow through chamber). In simulations, flow through chamber had ADP concentration proportional to added ATP, in agreement with small ATP contamination by ADP. For comparison, VO_2 calculated with zero ADP concentration in solution surrounding the cell is shown (*dotted line*).

FIGURE 6   Analysis of single cell respiration in the microscope fast exchange chamber. (*A*) Flow profile in the microscope chamber found by the mathematical model. The flow profile is described by velocity magnitude (shown by *color*) and streamlines (*white lines*). At inflow (*top left*), the velocity is higher than at outflow (*bottom right*) due to the larger opening of the chamber at outflow. (*B*) Distribution of ADP (shown by *color*) predicted by the mathematical model around a cell situated in the middle of a chamber, attached to the glass. The location of the cell is outlined (*black wire-frame*) on the image. The flow in the box was calculated on basis of the flow distribution in the chamber taking into account the flow around the cell. The flow is indicated by the arrows (*left*) and streamlines (*white lines*). Note how flow of solution leads to asymmetric distribution of ADP next to the cell. (*C*) Influence of ADP mixing mechanisms on respiration rate of a cell in microscope chamber. Assuming that there are no intracellular diffusion restrictions, the calculated affinity of respiration to ADP is very high in the case of infinitely fast diffusion (*dashed black line*). If ADP is supplied just by diffusion, the affinity drops significantly (*dotted black line*). Taking into account flow distribution in the chamber, the predicted affinity of respiration to ADP (*solid black line*) is significantly higher that the one determined from experiments. For comparison, respiration rate dependency determined on the cell suspension in respiration chamber is shown (*open dots*) as well as respiration rate estimated from NADH (*solid squares*) and FP (*solid triangles*). Only by assuming significant intracellular diffusion restrictions modeled by increasing an apparent $K_{m(ADP)}$ of mitochondrial respiration to 0.15 mM (*red line*), 0.3 mM (*green line*), or 0.45 mM (*blue line*), is it possible to reproduce the measurements if the flow in the chamber is taken into account.

When confocal microscopy is used, small movement of the cell could lead to changes in focal plane that have to be taken into account. Due to the nature of the fluorescence microscope point-spread function, the signal is integrated through the whole thickness of the cell (point-spread function of our microscope has been published earlier in Laasmaa et al. (26)). As a result, small movements of the cell induced by changes in solution flow do not alter the measurements if the signal is averaged over the whole cell. In addition, use of a highly sensitive camera allowed us to reduce bleaching by attenuating the excitation light.

According to our results, changes in NADH and FP autofluorescence were linearly related to respiration rate (Fig. 4). Similar linear relationships were observed when respiration rates were varied by changes in substrates at different calcium levels (27). In our work, calcium, substrate, and inorganic phosphate levels were kept the same. As a result, regulation of respiration was rather simple and carried out by ADP in the vicinity of mitochondria. Such simple control probably resulted in the simple relationship between respiration rate, and NADH and FP autofluorescence.

The main result of this work is the demonstration of low ADP-affinity of mitochondrial respiration in single permeabilized cardiomyocytes. From the similar response of autofluorescence to stimulation of respiration by ADP and ATP on single cell and population level, we conclude that the analysis of intracellular diffusion on population of permeabilized cardiomyocytes is adequate and does not suffer from clumping of the cells in measurement solution. The differences in response of autofluorescence to stimulation by ATP (Fig. 3, *B* and *D*) were attributed to accumulation of ADP during measurements in the fluorometer chamber. As we have demonstrated earlier in similar setup by HPLC measurements (3), the ADP concentration increases from ~0.03 mM to ~0.06 mM during stimulation of respiration with 2 mM ATP. When oxidative phosphorylation is active, the ADP level stabilizes at 0.06 mM level. Note that the initial ADP was present as a small fraction in the injected ATP. This buildup of ADP in the surrounding solution leads to larger respiration rate, as demonstrated in Fig. 5 and can explain the larger autofluorescence response in fluorometer to stimulation of ATP compared to the measurements in microscope (Fig. 3, *B* and *D*).

Because single cell and cell populations results are similar, one can take advantage of both preparations in the studies. When larger population is used, it is possible to use macroscopical methods, such as following respiration rate by measuring oxygen concentration changes in solution, HPLC to determine dynamics of metabolite changes, and absorbance spectroscopy. Those methods have been applied in numerous studies (1,11,28), with our recent study applying a large set of them to analyze ADP compartmentation in permeabilized cardiomyocytes (3). Although macroscopical approaches are not possible on a single-cell level, there are clear advantages of using a single-cell preparation.

The main advantage is the ability to select a particular cell. As it is shown in Fig. 1, the response of a viable rod-shaped cardiomyocyte could be different from that of a contracted nonrod-shaped cell. In the microscope, we could choose the cells on the basis of their shape and response to external stimuli. This is not possible on a population level, because in population-level studies there is always a fraction of the cells that have been damaged during isolation. In addition, the single cell preparation allows us to study intracellular heterogeneity of the metabolism, such as metabolic oscillations (29–31). For regional analysis, confocal microscopy can be used (17) or image deconvolution algorithms to enhance fluorescence images. For deconvolution, several options exist with several open source deconvolution packages made available recently including end-user software packages or programming libraries (see Laasmaa et al. (32) and references within).

Although there are clear advantages in the use of single cell preparations, there is an important complication. Namely, to study the response of permeabilized cardiomyocytes to external stimuli, we are mainly limited to fluorescence-based methods. As we have done in this study, the response of mitochondrial oxidative phosphorylation was analyzed through autofluorescence of mitochondria. Unfortunately, we cannot yet relate that autofluorescence to respiration rate directly. In this work, we assumed that the linear relationships among VO_2 and NADH and FP fluorescence (Fig. 4) holds for the measurements in the microscope chamber as well. This is a phenomenological relationship and may not hold in all conditions.

As a part of the solution to the problem of relating VO_2 to fluorescence, mathematical models of oxidative phosphorylation can be used. Several detailed models are available that, with the proper calibration, could be applied to extract rates of the processes on the basis of fluorescence measurements. For example, mitochondrial respiration models developed by several groups (33–40) can be used as a starting point for development and calibration of the model that would be able to relate fluorescence measurements to respiration rate. Although all the details of regulation of oxidative phosphorylation are, to our knowledge, not yet known, and, consequently, none of the existing models is perfect, it should be possible to find a set of parameters that would reproduce the simpler experiments. For example, in our experiments, only ATP and ADP were varied and there was no variation of calcium, phosphate, and substrates leading to simple relationship between VO_2 and fluorescence (Fig. 4).

As one of the advantages of using single cell preparation, the influence of the unstirred water layer surrounding the cell can be quantified. Here, by using several mathematical models, we found the flow profile in the chamber and in the vicinity of the cell (Fig. 6, A and B). Knowing the flow profile, it is possible to find the influence of ADP or ATP supply from the solution in the cell and separate diffusion gradients induced by intracellular structures from overall diffusion gradients in the system (Fig. 6, B and C). As it is clear from our simulations, intracellular diffusion restrictions are significant (compare *black* and *colored solid lines* in Fig. 6 C). In addition to intracellular diffusion restrictions, diffusion gradients induced by ADP supply in the chamber play a significant role as well (compare *dashed* and *solid lines* in Fig. 6 C). In our simulations, the cell was positioned along the flow.

We repeated the simulations with the cell positioned perpendicular to the flow and found that computed VO_2-ADP relationships at different $K_{m(ADP)}$ were very close to the relationships found with the cell oriented along the flow (results not shown). This suggests that orientation of the cell positioned on the cover glass does not play a major role on the experimental outcome. However, on the basis of our analysis, we can recommend imaging the cell in the part of the chamber with the higher flow velocity (Fig. 6 A). This would reduce contribution of ADP supply in the overall gradients.

The demonstration that the diffusion restrictions are not induced by clumping of the cells in an oxygraph has important physiological consequences. As we have shown in this work, single permeabilized rat cardiomyocytes have a low affinity to exogenous ADP. From this, we conclude that there are significant diffusion restrictions between the solution surrounding the cell and the mitochondrial inner membrane. As we have shown earlier, on the basis of mathematical analysis of measurements performed on permeabilized rat heart muscle fibers and isolated cardiomyocytes, the mitochondrial outer membrane should lead to a diffusion gradient that is ≤ 0.16 mM (3,7) at half-maximal respiration rate with the rest of the gradient induced by some other intracellular structures. Those structures are not distributed uniformly, but are probably localized in certain areas of the cell, as demonstrated in analysis of respiration response kinetics to stimulation by ATP (5). When assuming that the rest of the diffusion gradient is induced by sarcoplasmic reticulum and proteins in its neighborhood, a very significant diffusion obstacle on that level was predicted by a three-dimensional reaction-diffusion model of rat heart muscle fiber (7).

The physiological role of such diffusion restrictions is still not clear, and is a subject of further studies. At present, we have not yet identified which intracellular structures are responsible for diffusion restrictions. As a result, we cannot predict whether those diffusion restrictions would influence intracellular energy fluxes in the heart leading to modulation of energy transfer depending on the workload (41). In addition, signaling, or response to pathological conditions can be influenced as well. However, what we have demonstrated in this work is that the diffusion restrictions that lower the affinity of mitochondrial respiration to exogenous ADP are localized within permeabilized rat cardiomyocytes.

Publication II

SUPPORTING MATERIAL

REFERENCES

1. Kümmel, L. 1988. Ca, Mg-ATPase activity of permeabilized rat heart cells and its functional coupling to oxidative phosphorylation of the cells. *Cardiovasc. Res.* 22:359–367.

2. Veksler, V. I., A. V. Kuznetsov, …, V. A. Saks. 1987. Mitochondrial respiratory parameters in cardiac tissue: a novel method of assessment by using saponin-skinned fibers. *Biochim. Biophys. Acta.* 892:191–196.

3. Sepp, M., M. Vendelin, …, R. Birkedal. 2010. ADP compartmentation analysis reveals coupling between pyruvate kinase and ATPases in heart muscle. *Biophys. J.* 98:2785–2793.

4. Rostovtseva, T. K., K. L. Sheldon, …, D. L. Sackett. 2008. Tubulin binding blocks mitochondrial voltage-dependent anion channel and regulates respiration. *Proc. Natl. Acad. Sci. USA.* 105:18746–18751.

5. Vendelin, M., M. Eimre, …, V. A. Saks. 2004. Intracellular diffusion of adenosine phosphates is locally restricted in cardiac muscle. *Mol. Cell. Biochem.* 256–257:229–241.

6. Vendelin, M., and R. Birkedal. 2008. Anisotropic diffusion of fluorescently labeled ATP in rat cardiomyocytes determined by raster image correlation spectroscopy. *Am. J. Physiol. Cell Physiol.* 295:C1302–C1315.

7. Ramay, H. R., and M. Vendelin. 2009. Diffusion restrictions surrounding mitochondria: a mathematical model of heart muscle fibers. *Biophys. J.* 97:443–452.

8. Vendelin, M., N. Béraud, …, V. A. Saks. 2005. Mitochondrial regular arrangement in muscle cells: a "crystal-like" pattern. *Am. J. Physiol. Cell Physiol.* 288:C757–C767.

9. Birkedal, R., H. A. Shiels, and M. Vendelin. 2006. Three-dimensional mitochondrial arrangement in ventricular myocytes: from chaos to order. *Am. J. Physiol. Cell Physiol.* 291:C1148–C1158.

10. Kongas, O., T. L. Yuen, …, K. Krab. 2002. High K_m of oxidative phosphorylation for ADP in skinned muscle fibers: where does it stem from? *Am. J. Physiol. Cell Physiol.* 283:C743–C751.

11. Sokolova, N., M. Vendelin, and R. Birkedal. 2009. Intracellular diffusion restrictions in isolated cardiomyocytes from rainbow trout. *BMC Cell Biol.* 10:90.

12. Appaix, F., A. V. Kuznetsov, …, V. Saks. 2003. Possible role of cytoskeleton in intracellular arrangement and regulation of mitochondria. *Exp. Physiol.* 88:175–190.

13. Chance, B., and G. R. Williams. 1955. Respiratory enzymes in oxidative phosphorylation. III. The steady state. *J. Biol. Chem.* 217:409–427.

14. Chance, B., B. Schoener, …, Y. Nakase. 1979. Oxidation-reduction ratio studies of mitochondria in freeze-trapped samples. NADH and flavoprotein fluorescence signals. *J. Biol. Chem.* 254:4764–4771.

15. Chance, B., and M. Baltscheffsky. 1958. Spectroscopic effects of adenosine diphosphate upon the respiratory pigments of rat-heart-muscle sarcosomes. *Biochem. J.* 68:283–295.

16. Winkler, K., A. V. Kuznetsov, …, W. S. Kunz. 1995. Laser-excited fluorescence studies of mitochondrial function in saponin-skinned skeletal muscle fibers of patients with chronic progressive external ophthalmoplegia. *Biochim. Biophys. Acta.* 1272:181–184.

17. Kuznetsov, A. V., O. Mayboroda, …, W. S. Kunz. 1998. Functional imaging of mitochondria in saponin-permeabilized mice muscle fibers. *J. Cell Biol.* 140:1091–1099.

18. Huang, S., A. A. Heikal, and W. W. Webb. 2002. Two-photon fluorescence spectroscopy and microscopy of NAD(P)H and flavoprotein. *Biophys. J.* 82:2811–2825.

19. Sedlic, F., D. Pravdic, …, M. Bienengraeber. 2010. Monitoring mitochondrial electron fluxes using NAD(P)H-flavoprotein fluorometry reveals complex action of isoflurane on cardiomyocytes. *Biochim. Biophys. Acta.* 1797:1749–1758.

20. Mayevsky, A., and E. Barbiro-Michaely. 2009. Use of NADH fluorescence to determine mitochondrial function in vivo. *Int. J. Biochem. Cell Biol.* 41:1977–1988.

21. Eng, J., R. M. Lynch, and R. S. Balaban. 1989. Nicotinamide adenine dinucleotide fluorescence spectroscopy and imaging of isolated cardiac myocytes. *Biophys. J.* 55:621–630.

22. Mayevsky, A., and G. G. Rogatsky. 2007. Mitochondrial function in vivo evaluated by NADH fluorescence: from animal models to human studies. *Am. J. Physiol. Cell Physiol.* 292:C615–C640.

23. Kunz, W. S. 1986. Spectral properties of fluorescent flavoproteins of isolated rat liver mitochondria. *FEBS Lett.* 195:92–96.

24. Kunz, W. S., and F. N. Gellerich. 1993. Quantification of the content of fluorescent flavoproteins in mitochondria from liver, kidney cortex, skeletal muscle, and brain. *Biochem. Med. Metab. Biol.* 50:103–110.

25. Chorvat, Jr., D., J. Kirchnerova, …, A. Chorvatova. 2005. Spectral unmixing of flavin autofluorescence components in cardiac myocytes. *Biophys. J.* 89:L55–L57.

26. Laasmaa, M., M. Vendelin, and P. Peterson. 2011. Application of regularized Richardson-Lucy algorithm for deconvolution of confocal microscopy images. *J. Microsc.* 243:124–140.

27. Territo, P. R., V. K. Mootha, …, R. S. Balaban. 2000. Ca^{2+} activation of heart mitochondrial oxidative phosphorylation: role of the F_0/F_1-ATPase. *Am. J. Physiol. Cell Physiol.* 278:C423–C435.

28. Saks, V. A., Y. O. Belikova, and A. V. Kuznetsov. 1991. In vivo regulation of mitochondrial respiration in cardiomyocytes: specific restrictions for intracellular diffusion of ADP. *Biochim. Biophys. Acta.* 1074:302–311.

29. Romashko, D. N., E. Marban, and B. O'Rourke. 1998. Subcellular metabolic transients and mitochondrial redox waves in heart cells. *Proc. Natl. Acad. Sci. USA.* 95:1618–1623.

30. Aon, M. A., S. Cortassa, and B. O'Rourke. 2004. Percolation and criticality in a mitochondrial network. *Proc. Natl. Acad. Sci. USA.* 101:4447–4452.

31. Kurz, F. T., M. A. Aon, …, A. A. Armoundas. 2010. Spatio-temporal oscillations of individual mitochondria in cardiac myocytes reveal modulation of synchronized mitochondrial clusters. *Proc. Natl. Acad. Sci. USA.* 107:14315–14320.

32. Laasmaa, M., M. Vendelin, and P. Peterson. 2011. Application of regularized Richardson-Lucy algorithm for deconvolution of confocal microscopy images. *J. Microsc.* 243:124–140.

33. Jafri, M. S., S. J. Dudycha, and B. O'Rourke. 2001. Cardiac energy metabolism: models of cellular respiration. *Annu. Rev. Biomed. Eng.* 3:57–81.

34. Korzeniewski, B. 1998. Regulation of ATP supply during muscle contraction: theoretical studies. *Biochem. J.* 330:1189–1195.

35. Vendelin, M., O. Kongas, and V. Saks. 2000. Regulation of mitochondrial respiration in heart cells analyzed by reaction-diffusion model of energy transfer. *Am. J. Physiol. Cell Physiol.* 278:C747–C764.

Publication II

36. Beard, D. A. 2005. A biophysical model of the mitochondrial respiratory system and oxidative phosphorylation. *PLOS Comput. Biol.* 1:e36.

37. Wu, F., F. Yang, …, D. A. Beard. 2007. Computer modeling of mitochondrial tricarboxylic acid cycle, oxidative phosphorylation, metabolite transport, and electrophysiology. *J. Biol. Chem.* 282:24525–24537.

38. Nguyen, M.-H. T., S. J. Dudycha, and M. S. Jafri. 2007. Effect of Ca^{2+} on cardiac mitochondrial energy production is modulated by Na^+ and H^+ dynamics. *Am. J. Physiol. Cell Physiol.* 292:C2004–C2020.

39. Cortassa, S., M. A. Aon, …, R. L. Winslow. 2006. A computational model integrating electrophysiology, contraction, and mitochondrial bioenergetics in the ventricular myocyte. *Biophys. J.* 91:1564–1589.

40. Bazil, J. N., G. T. Buzzard, and A. E. Rundell. 2010. Modeling mitochondrial bioenergetics with integrated volume dynamics. *PLOS Comput. Biol.* 6:e1000632.

41. Vendelin, M., J. A. Hoerter, …, J. L. Mazet. 2010. Modulation of energy transfer pathways between mitochondria and myofibrils by changes in performance of perfused heart. *J. Biol. Chem.* 285:37240–37250.

42. Kushmerick, M. J., and R. J. Podolsky. 1969. Ionic mobility in muscle cells. *Science.* 166:1297–1298.

43. Bangerth, W., R. Hartmann, and G. Kanschat. 2007. Deal.II—a general purpose object oriented finite element library. *ACM Trans. Math. Softw.* 33:24.

PUBLICATION III

Illaste A, Kalda M, Schryer DW, Sepp M **Life of mice - development of cardiac energetics**.

JOURNAL CLUB

Life of mice – development of cardiac energetics

Ardo Illaste, Mari Kalda, David W. Schryer and Mervi Sepp

Laboratory of Systems Biology, Institute of Cybernetics at Tallinn University of Technology, Akadeemia tee 21, 12618, Tallinn, Estonia

Email: ardo@sysbio.ioc.ee

Production and transfer of metabolites like ATP and phosphocreatine within cardiomyocytes is crucial for the robust availability of mechanical work. In mammalian cardiomyocytes, mitochondria, the main suppliers of usable chemical energy in the form of ATP, are situated adjacent to both the ATPases near the mechanical apparatus, and the sarco(endo)plasmic reticulum Ca^{2+}-ATPase (SERCA) calcium pumps. Operation of these ATPases requires a high ATP/ADP ratio, which is maintained by two parallel energy transfer systems – creatine kinase (CK) and direct adenine nucleotide channelling (DANC). Compartmentation of energy metabolites works to lessen the impact of dynamic changes in the availability of usable energy on the operation of these ATPases, and allows for a higher phosphorylation potential where it is required most.

The operational mechanism, structure and development of the barriers responsible for energetic compartmentation within cardiomyocytes have yet to be elucidated despite intensive research in this area. A recent article in *The Journal of Physiology* by Piquereau *et al.* (2010) is an extensive investigation into how the structural and energetic properties of mouse heart muscle change during postnatal development. It includes observations on structural changes and cellular morphology using electron microscopy, quantification of mitochondrial, myofibrillar and SR proteins, assessment of organelle functionality, and the quantification of the energy flux in both the CK and DANC transfer systems. SERCA function was measured via calcium mediated tension generation, while myosin ATPase function was quantified by measuring rigor tension development. Total activity of CK and mitochondrial CK (mi-CK) were estimated.

The article by Piquereau *et al.* builds upon a strong research tradition at Inserm U769, Univ. Paris-Sud, which focuses on studying how cardiac mechanisms function in response to both pathological and physiological stimuli. This includes work on contractile, sarcoplasmic reticulum (SR), and mitochondrial proteins, membrane receptors, ion channels and signalling. Their work has inspired new areas of inquiry into the function of energy compartmentation in the heart with various implications for therapeutic targets to improve both function and clinical outcomes.

As main results of their recent publication, Piquereau *et al.* concluded that the formation of energetic microdomains occurs very early in postnatal development, and that the maturation of cellular architecture plays an important role in achieving maximal flexibility in regulation of ATP production by mitochondria. They found that the development of regulatory energetic pathways does not happen simultaneously. Throughput of energy transfer between mitochondria and myosin ATPases is correlated with the changes in the cytoarchitecture in contrast to the CK supported energy transfer which seems to depend on specific localization and expression of CK. Development between days 3 and 7 is crucial in increasing the capacity of energy transfer and involves major remodelling of the contacts between organelles. The density of intracellular organelles increases at the expense of free cytosolic space. Contacts between mitochondria and longitudinally oriented myofibrils and between SR and mitochondria are established to form an effective intracellular energetic unit. After the first week (*post natum*), a different phase of hypertrophy occurs without major structural changes to the contacts between organelles. After 3 weeks, the respiratory capacity of mitochondria increases, whereas heart weight to body weight ratio decreases. The main results of the article are summarized in Fig. 1.

Considerable effort has been invested by Piquereau *et al.* in determining various changes during cardiomyocyte maturation. Several questions arise, however, when comparing the publication with previous studies. Firstly, in 3-day-old cells, based on results from electron microscopy and SR protein expression experiments, the authors deduce SR not to be present in quantities high enough to enable SR Ca^{2+} content measurement. However, volume measurements from electron microscopy are known to be very sensitive to sample preparation procedures, especially as dimensions of different organelles can change in different ratios as a result of fixation. The low level of SR protein expression in 3-day-old cells could be explained by results obtained in embryonic mouse cardiomyocytes (Takeshima *et al.* 1998), where SR Ca^{2+} release channels do not play a major role in excitation–contraction (EC) coupling but, instead, are required for cellular Ca^{2+} homoestasis. Full SR function develops rapidly in neonates, possibly explaining both the dramatic increase in SR Ca^{2+} content between day 3 and day 7 fibres, and the difficulty the authors had in conducting the experiment with fibres from 3-day-old mice.

Secondly, the authors concluded that the functional coupling of adenine nucleotide translocase (ANT) and mi-CK ('functional activity' in Piquereau *et al.* 2010) was considerably higher in adult myocytes. This conclusion, however, seems to be based on misinterpreting the K_{mADP}/K_{Cr} ratio graph (article Fig. 5*F*). As is evident from the K_m plots in the article (article Fig. 5E), K_{mCr} is constant throughout the ageing process, whereas K_{mADP} increases notably in older fibres. The increase in K_{mADP}/K_{Cr} ratio stems from the increase of K_{mADP} and is not, in this case, indicating increases in mi-CK–ANT coupling nor mi-CK activity. Rather, it can be interpreted as indication of an increase in diffusion restrictions to adenine nucleotides in the cytosol caused by changes in either mitochondrial outer membrane or myofibrillar and other cytosolic structures, or both (Vendelin & Birkedal, 2008; Sepp *et al.* 2010). In order to measure the coupling between mi-CK and ANT, different experimental techniques need to be employed, such as measuring changes in respiration in response to ATP titration.

Two observations can be made from further analysing SR calcium uptake and rigor tension sensitivity results from the article (article Figs 2 and 4). By looking at ratios of values obtained during different

conditions, it is possible to eliminate auxiliary effects and focus on how the role of energy supply pathways change in relation to one another as the cell matures. Two examples are given in Fig. 1 (bottom row). Firstly, from the difference in rigor tension levels (ΔpMgATP$_{50}$) supported by CK and ATP energy supply systems (Fig. 1, line b), it is evident that myosin ATPase activity supported by CK is consistently higher than exogenous ATP throughout the growing process. On the other hand, the capacity of the CK system to load the SR increases $\sim$2 times by day 61 (Fig. 1, line d). We suggest that this is further evidence of the role of SR transitioning from maintaining Ca^{2+} homeostasis (Takeshima *et al.* 1998) to playing an essential role in EC coupling. A possible explanation for this could be activation of SR-bound CK by day 21, whereas myo-

fibril bound CK is already active from day three. Secondly, pMgATP$_{50}$(DANC) – pMgATP$_{50}$(ATP) (Fig. 1, line a) indicates that after an initial increase caused by changes in mitochondrial positioning, myofibrils stay constantly more sensitive to stimulation via direct channelling compared to exogenous ATP. At the same time, however, direct channelling is able to maintain an increasingly higher SR load than exogenous ATP (Fig. 1, line c). This can be explained by structural changes in the cell, whereby SR becomes more closely situated with respect to mitochondria (article Fig. 8*D*). Clearly, these interpretations should be verified through further experiments and modelling.

Building on results obtained by Piquereau *et al.* some directions could be explored in the future. One matter of interest would be how the role of glycolysis changes during maturation. It has been shown that embryonic mouse heart responds in a similar manner to inhibition of either glycolysis or oxidative phosphorylation and that in early stages of postnatal development, ATP consumed by ion pumps is preferentially supplied through glycolysis (Chen *et al.* 2007). Additionally, in 1-day-old rabbit, 44% of consumed ATP comes from glycolysis, whereas by day 7 this goes down to 7% (Lopaschuk *et al.* 1992). In the paper under discussion, the possible contribution of glycolysis to ATP supply was not directly addressed. Especially in young mouse cells, the effect from this could be considerable and might impact some of the conclusions of the article.

Another possible area to explore in the future could be to analyse these results with the aid of a computational model.
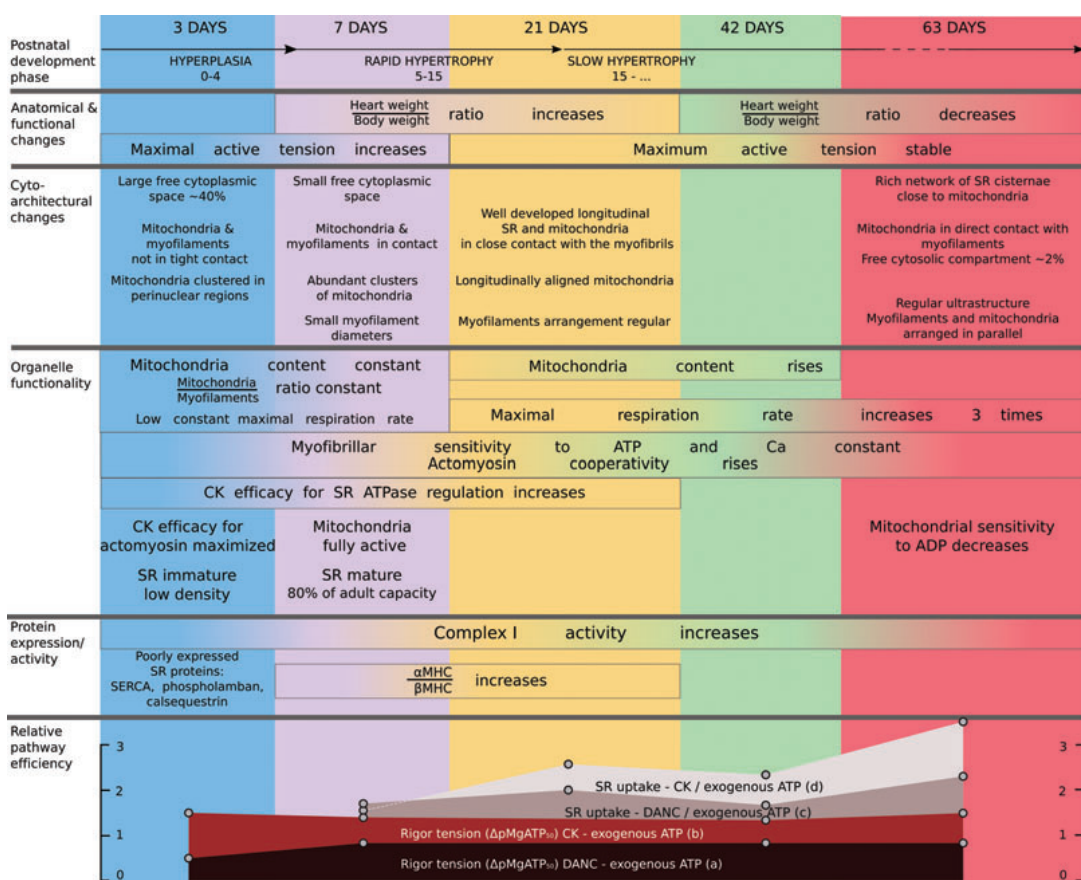

Figure 1. Summary of results from the article by Piquereau *et al*.

Publication III

This would help in further unravelling the interplay between different factors during cell maturation, especially in questions where experimental methods fail to yield clear results. Different mathematical models could be compared with statistical methods in order to determine the role of various pathways and the existence of metabolite pools or spatial compartmentation in the developing cell (Sepp *et al.* 2010).

In summary, the extensive experimental work performed in the work by Piquereau *et al.* covers various aspects of energy metabolism and morphological changes in the cell during maturation. The work provides new information on postnatal development of heart energetics in mice – a popular animal model used for studying the effects of genetic manipulation.

References

Chen F, De Diego C, Xie L, Yang J, Klitzner T & Weiss J (2007). Effects of metabolic inhibition on conduction, Ca transients, and arrhythmia vulnerability in embryonic mouse hearts. *Am J Physiol Heart Circ Physiol* **293**, H2472–2478.

Lopaschuk G, Collins-Nakai R & Itoi T (1992). Developmental changes in energy substrate use by the heart. *Cardiovasc Res* **26**, 1172–1180.

Piquereau J, Novotova M, Fortin D, Garnier A, Ventura-Clapier R, Veksler V & Joubert F (2010). Postnatal development of mouse heart: formation of energetic microdomains. *J Physiol* **588**, 2443–2454.

Sepp M, Vendelin M, Vija H & Birkedal R (2010). ADP Compartmentation analysis reveals coupling between pyruvate kinase and ATPases in heart muscle. *Biophys J* **98**, 2785–2793.

Vendelin M & Birkedal R (2008). Anisotropic diffusion of fluorescently labeled ATP in rat cardiomyocytes determined by raster image correlation spectroscopy. *Am J Physiol Cell Physiol* **295**, C1302–C1315.

Takeshima H, Komazaki S, Hirose K, Nishi M, Noda T & Iino M (1998). Embryonic lethality and abnormal cardiac myocytes in mice lacking ryanodine receptor type 2. *EMBO J* **17**, 3309–3316.

Branovets J, Sepp M, Kotlyarova S, Jepihhina N, Sokolova N, Aksentijevic D, Lygate C. A, Neubauer S, Vendelin M, Birkedal R

Creatine deficient GAMT-/- mice show no adaptational changes in mitochondrial organization or compartmentation in permeabilized cardiomyocytes.

AJP–Heart and Circulatory Physiology, 2013, *in press*

The rules of the publisher prevent reprint of this manuscript prior to final publication. Official committe members and opponents will be given a copy of the submitted manuscript to enable them to carry out a judicious review of this disseratation.

Sepp M, Kotlyarova S, Sokolova N, Vendelin M

Glycolysis-coupled Na$^+$/K$^+$ ATPase has high activity in permeabilized rat cardiomyocytes.

submitted, 2013

The rules of the publisher prevent publication of the manuscript of Publication IV prior to acceptance. Official committe members and opponents will be given a copy of the submitted manuscript to enable them to carry out a judicious review of this disseratation.

DISSERTATIONS DEFENDED
AT TALLINN UNIVERSITY OF TECHNOLOGY
ON NATURAL AND EXACT SCIENCES

1. **Olav Kongas**. *Nonlinear Dynamics in Modeling Cardiac Arrhytmias.* 1998.
2. **Kalju Vanatalu**. *Optimization of Processes of Microbial Biosynthesis of Isotopically Labeled Biomolecules and Their Complexes.* 1999.
3. **Ahto Buldas**. *An Algebraic Approach to the Structure of Graphs.* 1999.
4. **Monika Drews**. *A Metabolic Study of Insect Cells in Batch and Continuous Culture: Application of Chemostat and Turbidostat to the Production of Recombinant Proteins.* 1999.
5. **Eola Valdre**. *Endothelial-Specific Regulation of Vessel Formation: Role of Receptor Tyrosine Kinases.* 2000.
6. **Kalju Lott**. *Doping and Defect Thermodynamic Equilibrium in ZnS.* 2000.
7. **Reet Koljak**. *Novel Fatty Acid Dioxygenases from the Corals Plexaura homomalla and Gersemia fruticosa.* 2001.
8. **Anne Paju**. *Asymmetric oxidation of Prochiral and Racemic Ketones by Using Sharpless Catalyst.* 2001.
9. **Marko Vendelin**. *Cardiac Mechanoenergetics in silico.* 2001.
10. **Pearu Peterson**. *Multi-Soliton Interactions and the Inverse Problem of Wave Crest.* 2001.
11. **Anne Menert**. *Microcalorimetry of Anaerobic Digestion.* 2001.
12. **Toomas Tiivel**. *The Role of the Mitochondrial Outer Membrane in in vivo Regulation of Respiration in Normal Heart and Skeletal Muscle Cell.* 2002.
13. **Olle Hints**. *Ordovician Scolecodonts of Estonia and Neighbouring Areas: Taxonomy, Distribution, Palaeoecology, and Application.* 2002.
14. **Jaak Nõlvak**. *Chitinozoan Biostratigrapy in the Ordovician of Baltoscandia.* 2002.
15. **Liivi Kluge**. *On Algebraic Structure of Pre-Operad.* 2002.
16. **Jaanus Lass**. *Biosignal Interpretation: Study of Cardiac Arrhytmias and Electromagnetic Field Effects on Human Nervous System.* 2002.
17. **Janek Peterson**. *Synthesis, Structural Characterization and Modification of PAMAM Dendrimers.* 2002.
18. **Merike Vaher**. *Room Temperature Ionic Liquids as Background Electrolyte Additives in Capillary Electrophoresis.* 2002.
19. **Valdek Mikli**. *Electron Microscopy and Image Analysis Study of Powdered Hardmetal Materials and Optoelectronic Thin Films.* 2003.
20. **Mart Viljus**. *The Microstructure and Properties of Fine-Grained Cermets.* 2003.
21. **Signe Kask**. *Identification and Characterization of Dairy-Related Lactobacillus.* 2003
22. **Tiiu-Mai Laht**. *Influence of Microstructure of the Curd on Enzymatic and Microbiological Processes in Swiss-Type Cheese.* 2003.
23. **Anne Kuusksalu**. *2−5A Synthetase in the Marine Sponge Geodia cydonium.* 2003.
24. **Sergei Bereznev**. *Solar Cells Based on Polycristalline Copper-Indium Chalcogenides and Conductive Polymers.* 2003.
25. **Kadri Kriis**. *Asymmetric Synthesis of C2-Symmetric Bimorpholines and Their Application as Chiral Ligands in the Transfer Hydrogenation of Aromatic Ketones.* 2004.
26. **Jekaterina Reut**. *Polypyrrole Coatings on Conducting and Insulating Substracts.* 2004.
27. **Sven Nõmm**. *Realization and Identification of Discrete-Time Nonlinear Systems.* 2004.
28. **Olga Kijatkina**. *Deposition of Copper Indium Disulphide Films by Chemical Spray Pyrolysis.* 2004.
29. **Gert Tamberg**. *On Sampling Operators Defined by Rogosinski, Hann and Blackman Windows.* 2004.
30. **Monika Übner**. *Interaction of Humic Substances with Metal Cations.* 2004.
31. **Kaarel Adamberg**. *Growth Characteristics of Non-Starter Lactic Acid Bacteria from Cheese.* 2004.
32. **Imre Vallikivi**. *Lipase-Catalysed Reactions of Prostaglandins.* 2004.
33. **Merike Peld**. *Substituted Apatites as Sorbents for Heavy Metals.* 2005.
34. **Vitali Syritski**. *Study of Synthesis and Redox Switching of Polypyrrole and Poly(3,4-ethylenedioxythiophene) by Using in-situ Techniques.* 2004.
35. **Lee Põllumaa**. *Evaluation of Ecotoxicological Effects Related to Oil Shale Industry.* 2004.
36. **Riina Aav**. *Synthesis of 9,11-Secosterols Intermediates.* 2005.
37. **Andres Braunbrück**. *Wave Interaction in Weakly Inhomogeneous Materials.* 2005.

38. **Robert Kitt**. *Generalised Scale-Invariance in Financial Time Series.* 2005.
39. **Juss Pavelson**. *Mesoscale Physical Processes and the Related Impact on the Summer Nutrient Fields and Phytoplankton Blooms in the Western Gulf of Finland.* 2005.
40. **Olari Ilison**. *Solitons and Solitary Waves in Media with Higher Order Dispersive and Nonlinear Effects.* 2005.
41. **Maksim Säkki**. *Intermittency and Long-Range Structurization of Heart Rate.* 2005.
42. **Enli Kiipli**. *Modelling Seawater Chemistry of the East Baltic Basin in the Late Ordovician–Early Silurian.* 2005.
43. **Igor Golovtsov**. *Modification of Conductive Properties and Processability of Polyparaphenylene, Polypyrrole and polyaniline.* 2005.
44. **Katrin Laos**. *Interaction Between Furcellaran and the Globular Proteins (Bovine Serum Albumin β-Lactoglobulin).* 2005.
45. **Arvo Mere**. *Structural and Electrical Properties of Spray Deposited Copper Indium Disulphide Films for Solar Cells.* 2006.
46. **Sille Ehala**. *Development and Application of Various On- and Off-Line Analytical Methods for the Analysis of Bioactive Compounds.* 2006.
47. **Maria Kulp**. *Capillary Electrophoretic Monitoring of Biochemical Reaction Kinetics.* 2006.
48. **Anu Aaspõllu**. *Proteinases from Vipera lebetina Snake Venom Affecting Hemostasis.* 2006.
49. **Lyudmila Chekulayeva**. *Photosensitized Inactivation of Tumor Cells by Porphyrins and Chlorins.* 2006.
50. **Merle Uudsemaa**. *Quantum-Chemical Modeling of Solvated First Row Transition Metal Ions.* 2006.
51. **Tagli Pitsi**. *Nutrition Situation of Pre-School Children in Estonia from 1995 to 2004.* 2006.
52. **Angela Ivask**. *Luminescent Recombinant Sensor Bacteria for the Analysis of Bioavailable Heavy Metals.* 2006.
53. **Tiina Lõugas**. *Study on Physico-Chemical Properties and Some Bioactive Compounds of Sea Buckthorn (Hippophae rhamnoides L.).* 2006.
54. **Kaja Kasemets**. *Effect of Changing Environmental Conditions on the Fermentative Growth of Saccharomyces cerevisae S288C: Auxo-accelerostat Study.* 2006.
55. **Ildar Nisamedtinov**. *Application of 13C and Fluorescence Labeling in Metabolic Studies of Saccharomyces spp.* 2006.
56. **Alar Leibak**. *On Additive Generalisation of Voronoï's Theory of Perfect Forms over Algebraic Number Fields.* 2006.
57. **Andri Jagomägi**. *Photoluminescence of Chalcopyrite Tellurides.* 2006.
58. **Tõnu Martma**. *Application of Carbon Isotopes to the Study of the Ordovician and Silurian of the Baltic.* 2006.
59. **Marit Kauk**. *Chemical Composition of CuInSe 2 Monograin Powders for Solar Cell Application.* 2006.
60. **Julia Kois**. *Electrochemical Deposition of CuInSe2 Thin Films for Photovoltaic Applications.* 2006.
61. **Ilona Oja Açik**. *Sol-Gel Deposition of Titanium Dioxide Films.* 2007.
62. **Tiia Anmann**. *Integrated and Organized Cellular Bioenergetic Systems in Heart and Brain.* 2007.
63. **Katrin Trummal**. *Purification, Characterization and Specificity Studies of Metalloproteinases from Vipera lebetina Snake Venom.* 2007.
64. **Gennadi Lessin**. *Biochemical Definition of Coastal Zone Using Numerical Modeling and Measurement Data.* 2007.
65. **Enno Pais**. *Inverse problems to determine non-homogeneous degenerate memory kernels in heat flow.* 2007.
66. **Maria Borissova**. *Capillary Electrophoresis on Alkylimidazolium Salts.* 2007.
67. **Karin Valmsen**. *Prostaglandin Synthesis in the Coral Plexaura homomalla: Control of Prostaglandin Stereochemistry at Carbon 15 by Cyclooxygenases.* 2007.
68. **Kristjan Piirimäe**. *Long-Term Changes of Nutrient Fluxes in the Drainage Basin of the Gulf of Finland – Application of the PolFlow Model.* 2007.
69. **Tatjana Dedova**. *Chemical Spray Pyrolysis Deposition of Zinc Sulfide Thin Films and Zinc Oxide Nanostructured Layers.* 2007.
70. **Katrin Tomson**. *Production of Labelled Recombinant Proteins in Fed-Batch Systems in Escherichia coli.* 2007.
71. **Cecilia Sarmiento**. *Suppressors of RNA Silencing in Plants.* 2008.
72. **Vilja Mardla**. *Inhibition of Platelet Aggregation with Combination of Antiplatelet Agents.* 2008.
73. **Maie Bachmann**. *Effect of Modulated Microwave Radiation on Human Resting Electroencephalographic Signal.* 2008.
74. **Dan Hüvonen**. *Terahertz Spectroscopy of Low-Dimensional Spin Systems.* 2008.
75. **Ly Villo**. *Stereoselective Chemoenzymatic Synthesis of Deoxy Sugar Esters Involving Candida antarctica Lipase B.* 2008.
76. **Johan Anton**. *Technology of Integrated Photoelasticity for Residual Stress Measurement in Glass Articles of Axisymmetric Shape.* 2008.

77. **Olga Volobujeva**. *SEM Study of Selenization of Different Thin Metallic Films.* 2008.
78. **Artur Jõgi**. *Synthesis of 4'-Substituted 2,3'-dideoxynucleoside Analogues.* 2008.
79. **Mario Kadastik**. *Doubly Charged Higgs Boson Decays and Implications on Neutrino Physics.* 2008.
80. **Fernando Pérez-Caballero**. *Carbon Aerogels from 5-Methylresorcinol-Formaldehyde Gels.* 2008.
81. **Sirje Vaask**. *The Comparability, Reproducibility and Validity of Estonian Food Consumption Surveys.* 2008.
82. **Anna Menaker**. *Electrosynthesized Conducting Polymers, Polypyrrole and Poly(3,4-ethylenedioxythiophene), for Molecular Imprinting.* 2009.
83. **Lauri Ilison**. *Solitons and Solitary Waves in Hierarchical Korteweg-de Vries Type Systems.* 2009.
84. **Kaia Ernits**. *Study of In2S3 and ZnS Thin Films Deposited by Ultrasonic Spray Pyrolysis and Chemical Deposition.* 2009.
85. **Veljo Sinivee**. *Portable Spectrometer for Ionizing Radiation* "*Gammamapper*". 2009.
86. **Jüri Virkepu**. *On Lagrange Formalism for Lie Theory and Operadic Harmonic Oscillator in Low Dimensions.* 2009.
87. **Marko Piirsoo**. *Deciphering Molecular Basis of Schwann Cell Development.* 2009.
88. **Kati Helmja**. *Determination of Phenolic Compounds and Their Antioxidative Capability in Plant Extracts.* 2010.
89. **Merike Sõmera**. *Sobemoviruses: Genomic Organization, Potential for Recombination and Necessity of P1 in Systemic Infection.* 2010.
90. **Kristjan Laes**. *Preparation and Impedance Spectroscopy of Hybrid Structures Based on CuIn3Se5 Photoabsorber.* 2010.
91. **Kristin Lippur**. *Asymmetric Synthesis of 2,2'-Bimorpholine and its 5,5'-Substituted Derivatives.* 2010.
92. **Merike Luman**. *Dialysis Dose and Nutrition Assessment by an Optical Method.* 2010.
93. **Mihhail Berezovski**. *Numerical Simulation of Wave Propagation in Heterogeneous and Microstructured Materials.* 2010.
94. **Tamara Aid-Pavlidis**. *Structure and Regulation of BDNF Gene.* 2010.
95. **Olga Bragina**. *The Role of Sonic Hedgehog Pathway in Neuro- and Tumorigenesis.* 2010.
96. **Merle Randrüüt**. *Wave Propagation in Microstructured Solids: Solitary and Periodic Waves.* 2010.
97. **Marju Laars**. *Asymmetric Organocatalytic Michael and Aldol Reactions Mediated by Cyclic Amines.* 2010.
98. **Maarja Grossberg**. *Optical Properties of Multinary Semiconductor Compounds for Photovoltaic Applications.* 2010.
99. **Alla Maloverjan**. *Vertebrate Homologues of Drosophila Fused Kinase and Their Role in Sonic Hedgehog Signalling Pathway.* 2010.
100. **Priit Pruunsild**. *Neuronal Activity-Dependent Transcription Factors and Regulation of Human BDNF Gene.* 2010.
101. **Tatjana Knjazeva**. *New Approaches in Capillary Electrophoresis for Separation and Study of Proteins.* 2011.
102. **Atanas Katerski**. *Chemical Composition of Sprayed Copper Indium Disulfide Films for Nanostructured Solar Cells.* 2011.
103. **Kristi Timmo**. *Formation of Properties of CuInSe2 and Cu2ZnSn(S,Se)4 Monograin Powders Synthesized in Molten KI.* 2011.
104. **Kert Tamm**. *Wave Propagation and Interaction in Mindlin-Type Microstructured Solids: Numerical Simulation.* 2011.
105. **Adrian Popp**. *Ordovician Proetid Trilobites in Baltoscandia and Germany.* 2011.
106. **Ove Pärn**. *Sea Ice Deformation Events in the Gulf of Finland and This Impact on Shipping.* 2011.
107. **Germo Väli**. *Numerical Experiments on Matter Transport in the Baltic Sea.* 2011.
108. **Andrus Seiman**. *Point-of-Care Analyser Based on Capillary Electrophoresis.* 2011.
109. **Olga Katargina**. *Tick-Borne Pathogens Circulating in Estonia (Tick-Borne Encephalitis Virus, Anaplasma phagocytophilum, Babesia Species): Their Prevalence and Genetic Characterization.* 2011.
110. **Ingrid Sumeri**. *The Study of Probiotic Bacteria in Human Gastrointestinal Tract Simulator.* 2011.
111. **Kairit Zovo**. *Functional Characterization of Cellular Copper Proteome.* 2011.
112. **Natalja Makarytsheva**. *Analysis of Organic Species in Sediments and Soil by High Performance Separation Methods.* 2011.
113. **Monika Mortimer**. *Evaluation of the Biological Effects of Engineered Nanoparticles on Unicellular Pro- and Eukaryotic Organisms.* 2011.
114. **Kersti Tepp**. *Molecular System Bioenergetics of Cardiac Cells: Quantitative Analysis of Structure-Function Relationship.* 2011.
115. **Anna-Liisa Peikolainen**. *Organic Aerogels Based on 5-Methylresorcinol.* 2011.

116. **Leeli Amon**. *Palaeoecological Reconstruction of Late-Glacial Vegetation Dynamics in Eastern Baltic Area: A View Based on Plant Macrofossil Analysis.* 2011.
117. **Tanel Peets**. *Dispersion Analysis of Wave Motion in Microstructured Solids.* 2011.
118. **Liina Kaupmees**. *Selenization of Molybdenum as Contact Material in Solar Cells.* 2011.
119. **Allan Olspert**. *Properties of VPg and Coat Protein of Sobemoviruses.* 2011.
120. **Kadri Koppel**. *Food Category Appraisal Using Sensory Methods.* 2011.
121. **Jelena Gorbatšova**. *Development of Methods for CE Analysis of Plant Phenolics and Vitamins.* 2011.
122. **Karin Viipsi**. *Impact of EDTA and Humic Substances on the Removal of Cd and Zn from Aqueous Solutions by Apatite.* 2012.
123. **David W. Schryer**. *Metabolic Flux Analysis of Compartmentalized Systems using Dynamic Isotopologue Modeling.* 2012
124. **Ardo Illaste**. *Analysis of Molecular Movements in Cardiac Myocytes.* 2012
125. **Indrek Reile**. *3-Alkylcyclopentane-1,2-Diones in Asymmetric Oxidation and Alkylation Reactions.* 2012.
126. **Tatjana Tamberg**. *Some Classes of Finite 2-Groups and Their Endomorphism Semigroups.* 2012.
127. **Taavi Liblik**. *Variability of Thermohaline Structure in the Gulf of Finland in Summer.* 2012.
128. **Priidik Lagemaa**. *Operational Forecasting in Estonian Marine Waters.* 2012.
129. **Andrei Errapart**. *Photoelastic Tomography in Linear and Non-linear Approximation.* 2012.
130. **Külliki Krabbi**. *Biochemical Diagnosis of Classical Galactosemia and Mucopolysaccharidoses in Estonia.* 2012.
131. **Kristel Kaseleht**. *Identification of Aroma Compounds in Food using SPME-GC/MS and GC-Olfactometry.* 2012.
132. **Kristel Kodar**. *Immunoglobulin G Glycosylation Profiling in Patients with Gastric Cancer.* 2012.
133. **Kai Rosin**. *Solar Radiation and Wind as Agents of the Formation of the Radiation Regime in Water Bodies.* 2012.
134. **Ann Tiiman**. *Interactions of Alzheimer's Amyloid-Beta Peptides with Zn(II) and Cu(II) Ions.* 2012.
135. **Olga Gavrilova**. *Application and Elaboration of Accounting Approaches for Sustainable Development.* 2012.
136. **Olesja Bondarenko**. *Development of Bacterial Biosensors and Human Stem Cell-Based In Vitro Assays for the Toxicological Profiling of Synthetic Nanoparticles.* 2012.
137. **Katri Muska**. *Study of Composition and Thermal Treatments of Quaternary Compounds for Monograin Layer Solar Cells.* 2012.
138. **Ranno Nahku**. *Validation of Critical Factors for the Quantitative Characterization of Bacterial Physiology in Accelerostat Cultures.* 2012.
139. **Petri-Jaan Lahtvee**. *Quantitative Omics-level Analysis of Growth Rate Dependent Energy Metabolism in Lactococcus lactis.* 2012.
140. **Kerti Orumets**. *Molecular Mechanisms Controlling Intracellular Glutathione Levels in Baker's Yeast Saccharomyces cerevisiae and its Random Mutagenized Gluthatione Over-Accumulating Isolate.* 2012.
141. **Loreida Timberg**. *Spice-Cured Sprats Ripening, Sensory Parameters Development, and Quality Indicators.* 2012.
142. **Anna Mihhalevski**. *Rye Sourdough Fermentation and Bread Stability.* 2012.
143. **Liisa Arike**. *Quantitative Proteomics of Escherichia coli: From Relative to Absolute Scale.* 2012.
144. **Kairi Otto**. *Deposition of In2S3 Thin Films by Chemical Spray Pyrolysis.* 2012.
145. **Mari Sepp**. *Functions of the Basic Helix-Loop-Helix Transcription Factor TCF4 in Health and Disease.* 2012.
146. **Anna Suhhova**. *Detection of the Effect of Weak Stressors on Human Resting Electroencephalographic Signal.* 2012.
147. **Aram Kazarjan**. *Development and Production of Extruded Food and Feed Products Containing Probiotic Microorganisms.* 2012.
148. **Rivo Uiboupin**. *Application of Remote Sensing Methods for the Investigation of Spatio-Temporal Variability of Sea Surfa ce Temperature and Chlorophyll Fields in the Gulf of Finland.* 2013.
149. **Tiina Kriščiunaite**. *A Study of Milk Coagulability.* 2013.
150. **Tuuli Levandi**. *Comparative Study of Cereal Varieties by Analytical Separation Methods and Chemometrics.* 2013.
151. **Natalja Kabanova**. *Development of a Microcalorimetric Method for the Study of Fermentation Processes.* 2013.
152. **Himani Khanduri**. *Magnetic Properties of Functional Oxides.* 2013.